

~~CONFIDENTIAL~~

RM A55G19

NACA RM A55G19



RESEARCH MEMORANDUM

A STUDY OF CONICAL CAMBER FOR TRIANGULAR
AND SWEEPBACK WINGS

By John W. Boyd, Eugene Migotsky,
and Benton E. Wetzel

Ames Aeronautical Laboratory
Moffett Field, Calif.

FOR REFERENCE LIBRARY COPY

NOV 22 1955

NOT TO BE TAKEN FROM THIS ROOM

LANGLEY AERONAUTICAL LABORATORY
LIBRARY, NACA
LANGLEY FIELD, VIRGINIA

CLASSIFIED DOCUMENT

This material contains information affecting the National Defense of the United States within the meaning of the espionage laws, Title 18, U.S.C., Secs. 793 and 794, the transmission or revelation of which in any manner to an unauthorized person is prohibited by law.

NATIONAL ADVISORY COMMITTEE FOR AERONAUTICS

WASHINGTON
November 18, 1955

CLASSIFICATION CHANGED
UNCLASSIFIED

By authority of AF-129... Eff. 7/17/58

~~CONFIDENTIAL~~

UNCLASSIFIED

ERRATA

NACA RM A55G19

A STUDY OF CONICAL CAMBER FOR TRIANGULAR
AND SWEEPBACK WINGS

By John W. Boyd, Eugene Migotsky,
and Benton E. Wetzell

November 18, 1955

Figure 1(b):

The ordinate of figure 1(b) is incorrect. The numerical values of $\left(\frac{dz}{dx}\right)_{\text{mod}} \frac{m}{C_{Ld}}$ as read from the figure should be multiplied by a factor of 25.

CLASSIFIED DOCUMENT

This material contains information affecting the National Defense of the United States within the meaning of the espionage laws, TITLE 18, U.S.C., Secs. 793 and 794, the transmission or revelation of which in any manner to an unauthorized person is prohibited by law.

[REDACTED]
NATIONAL ADVISORY COMMITTEE FOR AERONAUTICSRESEARCH MEMORANDUMA STUDY OF CONICAL CAMBER FOR TRIANGULAR
AND SWEEPBACK WINGSBy John W. Boyd, Eugene Migotsky,
and Benton E. Wetzell

SUMMARY

A theoretical and experimental study has been made to determine the effectiveness of camber in reducing the drag due to lift resulting from pressure forces acting on low-aspect-ratio triangular and sweptback wings. The wings investigated were derived by lifting-surface theory for sonic and supersonic speeds, and the theoretical surface shapes were modified to provide airplane surfaces which could be manufactured without undue difficulty. Design charts are included which aid in the selection of camber for various sweepback angles and Mach numbers. Experimental data obtained for certain wings designed from these charts are presented as a measure of the adequacy of the theory.

The experimental results for the triangular and sweptback wings showed that, at high subsonic speeds, the use of a moderate amount of camber resulted in significant reductions in the drag coefficient above a lift coefficient of approximately 0.10. Further, the penalties in the drag coefficient at zero lift were small at supersonic speeds. For the sweptback wing the data showed that, at low speeds ($M = 0.22$), an increase in the amount of camber increased the lift coefficients at which the break in the drag polar occurred. At high subsonic speeds, however, the improvements in the drag characteristics resulting from camber were seriously reduced when the sections were too highly cambered. Moreover, large increases in the minimum drag coefficient at supersonic speeds were incurred.

A comparison of the experimental drag polars with those computed from the linear lifting-surface theory shows that for the moderately cambered wings the theory closely predicts the drag coefficients at the lift coefficient for which the camber was designed. Above the design lift coefficient the experimental drag coefficients were essentially those predicted from a theory wherein no leading-edge suction was assumed. Below the design lift coefficient the experimental values fell between the full-suction polar curve and that for no leading-edge suction.

[REDACTED]

The experimental results also show that at subsonic and supersonic speeds, the use of conical camber for the triangular wing did not significantly affect the lift and moment characteristics except for a small positive increment in pitching moment at zero lift. The data for the swept wings showed that, at subsonic speeds, the camber delayed to higher lift coefficients the reduction in longitudinal stability observed for the uncambered wing.

INTRODUCTION

The total resistance of an airfoil may be considered as being composed of two separate components, the drag at zero lift and the drag associated with the production of lift. In the cruising condition the latter component can become a significant portion of the total drag of an airplane and, therefore, of considerable importance with regard to range.

The drag resulting from the development of lift may also be divided into two components, one associated with the viscous forces, that is, the skin-friction drag, and the other resulting from the pressure forces acting on the wing. The change in skin-friction drag with a change in lift results primarily from a movement of the boundary-layer transition point. This movement is, of course, caused by the pressure gradients acting over the lifting surface. On aircraft at full scale the boundary layer is often turbulent over essentially the entire airplane surface; hence, the change in skin-friction drag with a change in lift coefficient is negligible. This component must, therefore, be removed in wind-tunnel tests in order that proper estimates of the drag-due-to-lift characteristics can be made for full-scale aircraft. The other component of the drag due to lift, that due to pressure forces, may be estimated by thin-airfoil theory. Linear theory, however, predicts very large suction pressures at the leading edges of planar wings which give rise to a force in the thrust direction. Since these pressures cannot be fully developed in a real fluid, a question arises as to how much of the leading-edge thrust can be obtained. Previous experimental investigations (refs. 1, 2, and 3) have indicated that at transonic and supersonic speeds it is difficult to develop a significant portion of this leading-edge thrust for plane triangular wings of small thickness (3 to 5 percent thick).

A theoretical study by Jones in reference 4 indicated that one way to attain an equivalent leading-edge thrust would be to camber the wing leading edge. In this manner the suction pressures would be distributed over a relatively large area of the wing rather than concentrated at the airfoil leading edge. Thus, the magnitude of the pressures necessary to achieve the equivalent of full leading-edge suction would be physically possible.

The initial results of a study directed at determining a cambered surface for triangular wings which would provide an equivalent leading-edge thrust were presented in reference 1. The study showed that incorporation of a conical type of camber in an aspect-ratio-2 triangular wing resulted in substantial reductions in drag due to lift in the cruise lift-coefficient range at transonic speeds.

It is the purpose of the present report to elaborate on the analytical method for deriving conical camber for transonic and supersonic speeds for wings of triangular and sweptback plan form. The report also contains experimental data showing the effects of conical camber on the lift, drag, and pitching-moment characteristics of low-aspect-ratio triangular and sweptback wings at subsonic and supersonic speeds. Comparison of measured drag polars with those computed from lifting-surface theory are made to determine the effectiveness of the design methods.

NOTATION

A	$\frac{\text{slope of any ray from wing apex}}{\text{slope of wing leading edge}}, \frac{a}{m}$
a	slope of any ray from the wing apex, $\cot \phi$
b	wing span
C_D	drag coefficient, $\frac{\text{drag}}{qS}$
C_{D_0}	drag coefficient of uncambered wing at zero lift
ΔC_D	increment in drag coefficient above that for zero lift for plane wing, $C_D - C_{D_0}$
C_{D_s}	drag coefficient resulting from leading-edge suction
C_L	lift coefficient, $\frac{\text{lift}}{qS}$
C_{L_d}	design lift coefficient
C_m	pitching-moment coefficient, $\frac{\text{pitching moment}}{qS\bar{c}}$, referred to the quarter point of the mean aerodynamic chord
$\frac{\Delta C_D}{C_L^2}$	drag-due-to-lift factor of plane wing

- c local chord
- \bar{c} mean aerodynamic chord, $\frac{\int_0^{b/2} c^2 dy}{\int_0^{b/2} c dy}$
- c_r root chord
- c_l section lift coefficient, $\frac{\text{section lift}}{qc}$
- $\frac{dz}{dx}$ slope of the lifting surface, with respect to the xy plane
- $E(k)$ complete elliptic function of the second kind with modulus k
- M free-stream Mach number
- m slope of wing leading edge, $\cot \Lambda$
- n arbitrary positive integer
- Δp pressure difference between upper and lower surface
- q free-stream dynamic pressure
- R Reynolds number, based on the mean aerodynamic chord
- S wing area, formed by extending the leading and trailing edges to the plane of symmetry
- x, y, z Cartesian coordinates in streamwise, spanwise, and vertical directions, respectively
(The origin is at the wing apex for dimensions referring to the wing, except in tables I through VI where x is the distance from the leading edge along the chord, in percent chord, and z is the perpendicular distance from the chord, in percent chord. For dimensions referring to the body the origin is at the nose of the body.)
- α angle of attack of wing root chord, deg
- α_d angle of attack at design lift coefficient, deg
- β $\sqrt{M^2 - 1}$
- η slope of leading edge of superposed uniformly loaded sector
(see sketch (a))
- Λ angle of sweepback of wing leading edge, deg

ϕ angle of sweepback of a ray from the wing apex

Subscripts

a solution for summation of superposed sectors

c theoretical cambered surface

mod modified cambered surface

u constant-load solution for entire wing

α quantities associated with angle of attack

THEORETICAL DEVELOPMENT

General Considerations

The theoretical drag due to lift of a wing may be separated into two components, the vortex drag which depends only on the spanwise load distribution, and the wave drag due to lift, which exists only at supersonic speeds and is a complicated function of both spanwise and chordwise loading over the wing. At transonic and low supersonic speeds, however, the drag due to lift appears primarily as vortex drag which is a minimum when the span loading is elliptical. This condition is fulfilled by the theoretical angle-of-attack loading of plane wings of triangular plan form.

Comparison of experimental and theoretical drag characteristics of thin triangular wings indicates, however, that the low values of drag due to lift predicted theoretically are not obtained because the streamwise force on the wing leading edge due to the high velocity flow around the edge is not fully realized. Jones, in reference 4, suggested that the equivalent of this leading-edge thrust could be developed if the wings were cambered. In this way, physically realizable pressures could be spread over a finite area, and such a wing should more nearly attain its theoretical drag due to lift. Merely requiring that the pressures over the wing be physically realizable, however, is not sufficient to insure low values of drag due to lift. For example, it can be shown that a triangular wing which is cambered to give a uniform loading, and thereby develops the equivalent leading-edge thrust, has a significantly higher theoretical drag due to lift than that of a corresponding plane triangular wing with full leading-edge suction because the span load distribution is triangular instead of elliptical. It is evident, therefore, that in order to attain low values of drag due to lift at transonic and low supersonic speeds two requirements must be satisfied, namely, that the span load

distribution approximate an ellipse and that the pressures over the wing be physically realizable. It should be noted that in the following development no attempt is made to minimize the wave drag due to lift by the proper distribution of the chordwise loading.

A study was undertaken to determine a surface shape that could satisfy the two conditions on the loading. The initial results of this study, presented in reference 1, showed that a conical camber could be derived for a triangular wing which met these requirements. In the following sections the essential features of the derivation of this conical camber are presented. Also included are design charts, with a discussion of their application to triangular and sweptback plan forms. In addition, an approximate method, based on linear theory, is developed for the computation of the drag polars of wings incorporating conical camber.

Derivation of Cambered Surface

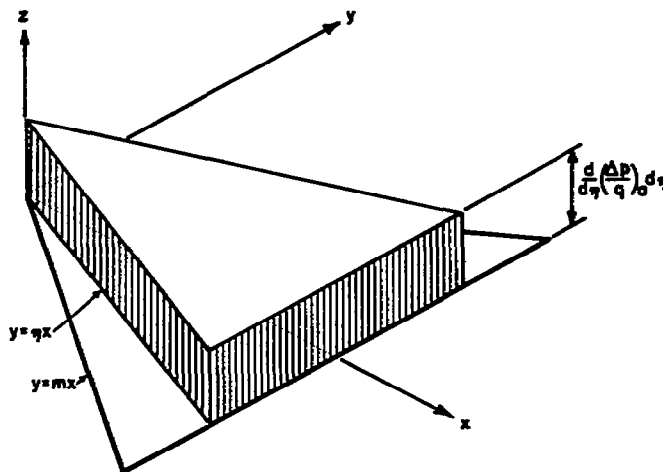
It is convenient in the derivation of the cambered surface to use as a starting point the slope of the surface required for a uniform load distribution and to determine the desired camber by superposition of solutions. In addition, it is convenient to do the major portion of the analysis for the case of $M = \sqrt{2}$. The final results, however, will be generalized for any Mach number greater than or equal to unity.

The slope of the surface for a uniformly loaded triangular wing at $M = \sqrt{2}$ may be obtained from reference 4 and can be written as

$$\left(\frac{dz}{dx}\right)_u = \frac{(\Delta p/q)_u}{4\pi} \left[\frac{\sqrt{1-m^2}}{m} \left(\cosh^{-1} \frac{x-my}{|y-mx|} + \cosh^{-1} \frac{x+my}{|y+mx|} \right) - \frac{2}{m} \cosh^{-1} \frac{x}{|y|} \right] \quad (1)$$

As pointed out in reference 1,¹ it is possible to superpose an infinite number of uniform-load sectors, each with strength $\frac{d(\Delta p/q)_a}{d\eta} d\eta$ and leading-edge slope η , (see sketch (a)) to derive the wing surface corresponding to the loading $(\Delta p/q)_a$.

¹The notation of the present report differs from that of reference 1 in that η and m as used herein correspond, respectively, to m and m_0 of reference 1.



Sketch (a)

Thus,

$$\left(\frac{dz}{dx}\right)_a = \frac{1}{4\pi} \int_0^m \frac{d\left(\frac{\Delta p}{q}\right)_a}{d\eta} \left[\frac{\sqrt{1-\eta^2}}{\eta} \left(\cosh^{-1} \frac{x-\eta y}{|y-\eta x|} + \cosh^{-1} \frac{x+\eta y}{|y+\eta x|} \right) - \frac{2}{\eta} \cosh^{-1} \frac{x}{|y|} \right] d\eta \quad (2)$$

It will be noted that, in general, singularities in the slope will exist at the root and at the leading edge of the wing surface defined by equation (2). The singularity in $(dz/dx)_a$ at the root which arises from the last term of equation (2) leads to a singularity in z which cannot be realized physically. It can be seen from equation (1) that the uniformly loaded wing has a similar singularity at the root. Thus, by superposing equations (1) and (2) the singularity at the root can be removed if the relationship between $(\Delta p/q)_a$ and $(\Delta p/q)_u$ is

$$\frac{d}{d\eta} \left(\frac{\Delta p}{q}\right)_a = - \frac{n \left(\frac{\Delta p}{q}\right)_u}{m^{n+1}} \eta^n \quad (3)$$

where $n > 0$. Integration of equation (3) between the limits of a and m gives the additional loading required along any ray a

$$\left(\frac{\Delta p}{q}\right)_a = - \frac{n}{n+1} \left(\frac{\Delta p}{q}\right)_u \left(1 - A^{n+1}\right) \quad (4)$$

Hence, for a cambered surface which is obtained by superposing the slopes given by equations (1) and (2), the resulting loading may be written, by adding $(\Delta p/q)_u$ to equation (4),

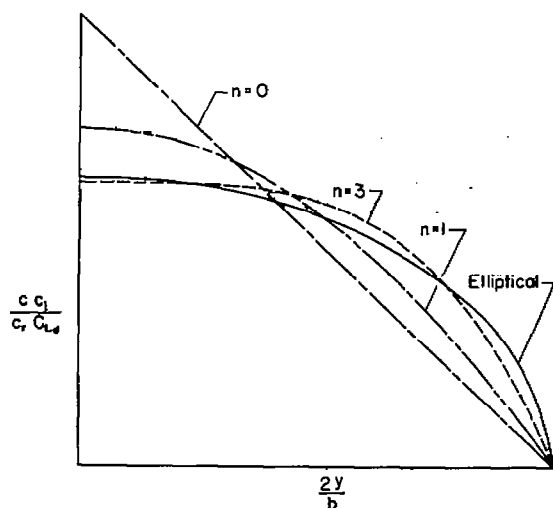
$$\left(\frac{\Delta p}{q}\right)_c = \frac{\left(\frac{\Delta p}{q}\right)_u}{n+1} (1 + nA^{n+1}) \quad (5)$$

The corresponding lift coefficient is denoted the design lift coefficient and is given by

$$C_{L_d} = \frac{2}{n+2} \left(\frac{\Delta p}{q}\right)_u \quad (6)$$

Thus, the design loading on the cambered wing may also be written in the form

$$\left(\frac{\Delta p}{q}\right)_c = \frac{n+2}{2(n+1)} C_{L_d} (1 + nA^{n+1}) \quad (7)$$



Sketch (b)

A comparison of the span load distributions obtained from equation (7) for several values of n showed that for the values of n investigated, $n = 3$ resulted in a span loading that was closest to elliptical (see sketch (b)). Hence, the value of $n = 3$ was chosen to specify the design loading on the cambered wing. The design loading (eq. (7)) then becomes

$$\left(\frac{\Delta p}{q}\right)_c = \frac{5C_{L_d}}{8} (1 + 3A^4) \quad (8)$$

The slope of the cambered wing is obtained by adding equations (1) and (2) and using the design loading to give

$$\left(\frac{dz}{dx}\right)_c = \frac{5C_{Ld}}{8\pi} \left[\frac{\sqrt{1-m^2}}{m} \left(\cosh^{-1} \frac{x-my}{|y-mx|} + \cosh^{-1} \frac{x+my}{|y+mx|} \right) - \frac{3}{m^4} \int_0^m \eta^2 \sqrt{1-\eta^2} \left(\cosh^{-1} \frac{x-\eta y}{|y-\eta x|} + \cosh^{-1} \frac{x+\eta y}{|y+\eta x|} \right) d\eta \right] \quad (9)$$

The integrals in equation (9) were found difficult to evaluate analytically and the following approximation to the square-root term was used:²

$$\sqrt{1-\eta^2} \approx 1 - 0.53 \eta^2 \quad (10)$$

The final expression for the slope of the wing for any Mach number is then obtained by substituting equation (10) into (9), integrating, and applying the Prandtl-Glauert transformation to give

$$\begin{aligned} \left(\frac{dz}{dx}\right)_c = \frac{5C_{Ld}}{8\pi m} & \left\{ \left[\sqrt{1-\beta^2 m^2} - (1-A^3) + 0.318 \beta^2 m^2 (1-A^5) \right] \cosh^{-1} \frac{\left(\frac{1}{\beta m} - \beta mA\right)}{1-A} + \right. \\ & \left[\sqrt{1-\beta^2 m^2} - (1+A^3) + 0.318 \beta^2 m^2 (1+A^5) \right] \cosh^{-1} \frac{\left(\frac{1}{\beta m} + \beta mA\right)}{A+1} + \\ & \left(0.636 \beta^4 m^4 A^4 - 1.682 \beta^2 m^2 A^2 - 0.7615 \right) \frac{\sqrt{1-\beta^2 m^2 A^2}}{\beta^3 m^3} \sin^{-1} \beta m + \\ & \left. \left(0.7615 - 0.159 \beta^2 m^2 - 0.318 \beta^2 m^2 A^2 \right) \frac{\sqrt{(1-\beta^2 m^2 A^2)(1-\beta^2 m^2)}}{\beta^2 m^2} \right\} \quad (11) \end{aligned}$$

²This estimate was obtained by expanding $\sqrt{1-\eta^2}$ in a power series and averaging the contribution of the third term in the series for values of η equal to 0 and 0.6.

The ordinates of the cambered wing, obtained by integrating equation (11), are given by

$$\begin{aligned} \left(\frac{z}{x}\right)_c = \frac{5C_{Ld}}{8\pi m} & \left\{ \left[\left(\sqrt{1 - \beta^2 m^2} - 1 + 0.318 \beta^2 m^2 \right) (1 - A) + \frac{A}{2} (1 - A^2) - \right. \right. \\ & 0.0795 \beta^2 m^2 A (1 - A^4) \left. \right] \cosh^{-1} \left(\frac{\frac{1}{\beta m} - \beta mA}{1 - A} \right) + \left[\left(\sqrt{1 - \beta^2 m^2} - 1 + \right. \right. \\ & 0.318 \beta^2 m^2 \left. \right) (1 + A) - \frac{A}{2} (1 - A^2) + 0.0795 \beta^2 m^2 A (1 - A^4) \left. \right] \cosh^{-1} \left(\frac{\frac{1}{\beta m} + \beta mA}{A + 1} \right) + \\ & \left(0.0795 A^2 + \frac{0.7615}{\beta^2 m^2} - 0.159 \right) \sqrt{(1 - \beta^2 m^2 A^2)(1 - \beta^2 m^2)} + \\ & \left. \left(-\frac{0.7615}{\beta^3 m^3} + \frac{0.9205 A^2}{\beta m} - 0.159 \beta mA^4 \right) \sqrt{1 - \beta^2 m^2 A^2} \sin^{-1} \beta m \right\} \quad (12) \end{aligned}$$

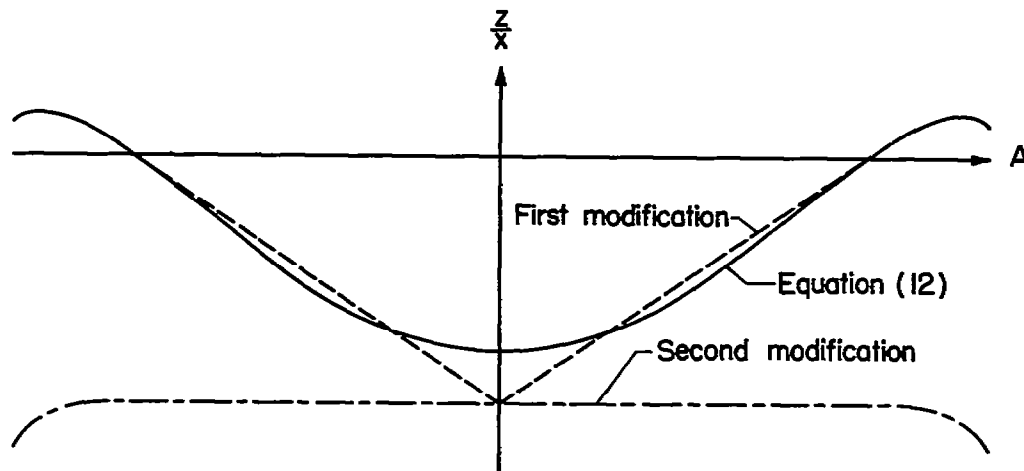
In the limit as Mach number approaches unity, equations (11) and (12) reduce to

$$\left(\frac{dz}{dx}\right)_c = \frac{5C_{Ld}}{8\pi m} \left(A^3 \log \frac{1 + A}{1 - A} - \frac{2}{3} - 2A^2 \right) \quad (13)$$

$$\left(\frac{z}{x}\right)_c = \frac{5C_{Ld}}{8\pi m} \left[\frac{A}{2} (1 - A^2) \log \frac{1 + A}{1 - A} - \frac{2}{3} + A^2 \right] \quad (14)$$

Design Charts for Modified Cambered Surfaces

Triangular wings.- It will be noted that the cambered surface defined by equation (12) has curvature over the entire wing (see sketch (c)). With minor modifications, however, the surface can be made planar over most of the inboard portion of the wing, thereby making it easier to construct. These modifications consist of the following changes: First, the inboard 80 percent of the trace of the cambered surface in a plane normal to the free-stream direction is replaced by a straight line tangent to the trace at the 80-percent-semispan location (sketch (c)). Then, the trace



Sketch (c)

is sheared downward so that the dihedral is removed (second modification, sketch (c)). Finally, a constant value is added to the ordinates in order that the modified-wing ordinates $(z/x)_{\text{mod}}$ be equal to zero over the inboard 80 percent of the wing. This last step is equivalent to reducing the angle of attack of the wing by an amount equal to

$$\frac{\alpha_d}{57.3} = 0.8 \left[\frac{d \left(\frac{z}{x} \right)_c}{dA} \right]_{A=0.8} - \left[\left(\frac{z}{x} \right)_c \right]_{A=0.8}$$

The final equations for the modified cambered wing may then be written

$$\left. \begin{aligned} \left(\frac{dz}{dx} \right)_{\text{mod}} &= 0 && \text{for } 0 \leq A \leq 0.8 \\ \left(\frac{dz}{dx} \right)_{\text{mod}} &= \left(\frac{dz}{dx} \right)_c + 0.8 \left[\frac{d \left(\frac{z}{x} \right)_c}{dA} \right]_{A=0.8} - \left[\left(\frac{z}{x} \right)_c \right]_{A=0.8} && \text{for } 0.8 \leq A \leq 1.0 \end{aligned} \right\} (15)$$

and

$$\left. \begin{aligned} \left(\frac{z}{x}\right)_{\text{mod}} &= 0 && \text{for } 0 \leq A \leq 0.8 \\ \left(\frac{z}{x}\right)_{\text{mod}} &= \left(\frac{z}{x}\right)_c - \left[\left(\frac{z}{x}\right)_c\right]_{A=0.8} - (A - 0.8) \left[\frac{d\left(\frac{z}{x}\right)_c}{dA}\right]_{A=0.8} && \text{for } 0.8 \leq A \leq 1.0 \end{aligned} \right\} (16)$$

The slope of the trace at $A = 0.8$ in the region $0.2 \leq \beta m \leq 0.8$ is

$$\left[\frac{d\left(\frac{z}{x}\right)_c}{dA}\right]_{A=0.8} = \frac{0.298 \beta C_{Ld}}{(\beta m)^{0.961}} \quad (\text{determined graphically})$$

For a Mach number of unity the slope of the trace at $A = 0.80$ is

$$\left[\frac{d\left(\frac{z}{x}\right)_c}{dA}\right] = 0.2765 \frac{C_{Ld}}{m} \quad (\text{determined analytically})$$

The quantities with subscript c are given in equations (11) and (12). The effects of these changes to the wing camber on the span loading are difficult to assess by linear theory. It is believed, however, that they are small.

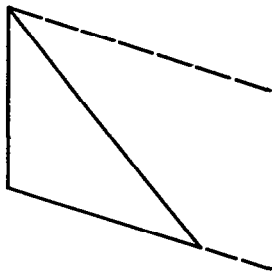
The results of equations (15) and (16) have been summarized in the form of design charts in figure 1 where the quantities $(m/C_{Ld})(dz/dx)_{\text{mod}}$ and $(m/C_{Ld})(z/x)_{\text{mod}}$ are plotted as functions of βm for different values of the parameter, A . For any wing of triangular plan form having a given leading-edge sweep angle, design lift coefficient, and design Mach number, the camber shape can be determined directly from these charts.

Sweptback wings.— The design charts which were derived for triangular wings in the foregoing section can also be applied to determine the camber shape of sweptback wings with straight subsonic leading edges which will have a low value of drag due to lift. The surface shape of the sweptback wing is obtained by calculating the camber shape of a triangular wing with

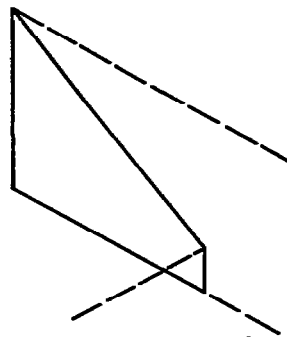
a specified design lift coefficient which circumscribes the sweptback wing. The manner in which the design lift coefficient of the swept wings can be related to the design lift coefficient of the triangular wing will be discussed in a subsequent section.

As has been discussed previously, the camber shape derived for the triangular wings satisfies two important requirements that are conducive to obtaining low values of drag due to lift: (1) that an equivalent leading-edge thrust be developed and (2) that the camber loading be almost elliptical.

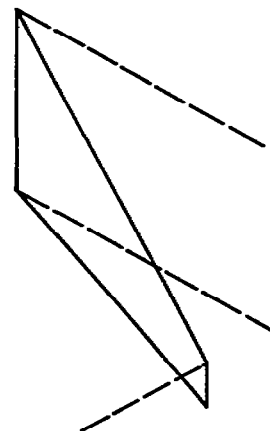
The attainment of the equivalent leading-edge thrust, which is dependent on the magnitude of the pressure acting over the forward portion of the airfoil is realized to essentially the same extent on various sweptback wings (see sketches (d), (e), and (f)) as it is on the triangular wings. Even for the case shown in sketch (f) where the root-trailing-edge Mach line intersects the wing leading edge, the pressures in the



Sketch (d)



Sketch (e)



Sketch (f)

vicinity of the wing leading edge are not greatly affected by the wake effects (see ref. 5) and the equivalent leading-edge thrust is developed. In the regions of the wing affected by the wing tip (sketches (e) and (f)) where, according to the linear theory the lift is essentially zero, some loss in the equivalent leading-edge thrust will occur.

In the application of the camber to the sweptback wings no attempt has been made to satisfy the condition of almost elliptical span loading. However, if the span loading due to camber and the span loading due to angle of attack are not greatly different, as was the case for the triangular wings, the sweptback cambered wings would realize at the design lift coefficient essentially the theoretical drag predicted for a plane wing of the same plan form. The effects of this difference in the loadings on the drag due to lift can be estimated for the cases shown in

sketches (d) and (e). For cases similar to that shown in sketch (f), where the trailing wake affects a large area of the wing, it is more difficult to evaluate the drag due to lift.

Computation of Drag Polars for Cambered Wings

Triangular wings.— The drag of a lifting surface may be obtained by integrating the product of the pressures acting on the surface and the inclination of the surface with respect to the free stream, and evaluating the effect of any singularity in the loading at the leading edge. Since linear thin-airfoil theory is used, the pressures can be superposed and the drag coefficient for the cambered wing may be written

$$C_D = C_{D_0} - \left\{ \frac{c_{r^2}}{S} \int_0^1 \left[\left(\frac{\Delta p}{q} \right)_c + \left(\frac{\Delta p}{q} \right)_\alpha \right] \left[\left(\frac{dz}{dx} \right)_c + \left(\frac{dz}{dx} \right)_\alpha \right] dA \right\} + C_{D_S} \quad (17)$$

At the design Mach number, all the functions needed in this expression, except C_{D_0} , are known from linear theory for the wings which are cambered over the entire span. The camber loading $(\Delta p/q)_c$ is obtained from equation (8); the angle of attack loading $(\Delta p/q)_\alpha$ may be written (see ref. 6)

$$\left(\frac{\Delta p}{q} \right)_\alpha = \frac{2}{\pi \sqrt{1 - A^2}} (C_L - C_{L_d})$$

the slopes of the cambered wing are given in equations (11) and (13); the slope due to angle of attack may be written

$$\left(\frac{dz}{dx} \right)_\alpha = -\Delta\alpha = - \left(\frac{C_L - C_{L_d}}{2\pi m} \right) E \sqrt{1 - \beta^2 m^2}$$

and the leading-edge suction term C_{D_S} , which results from the singularity in the angle-of-attack loading, is given by (ref. 4)

$$C_{D_S} = - \frac{\sqrt{1 - \beta^2 m^2}}{4\pi m} (C_L - C_{L_d})^2$$

For a design Mach number of unity, the preceding integrals can be evaluated analytically. For supersonic speeds, however, the expression for the slope of the cambered surface is unwieldy and the integrals involving $(dz/dx)_c$, in addition to being cumbersome, have singularities at the leading edge. Therefore, the integrals were separated into two parts, one of which contained the singularity and another which was bounded throughout the interval of integration. The singular part was evaluated analytically, and the integrals with bounded functions were determined graphically.

At Mach numbers different from the design Mach number, the camber loading is difficult to obtain by linear theory. Hence, instead of computing the exact linear-theory drag, a method for approximately evaluating the linear-theory drag of the designed wings at off-design Mach numbers was developed. This method is based on the fact that the slopes of cambered surfaces designed for the same lift coefficient but for different values of the parameter β_m , differ primarily in magnitude; the spanwise distributions of slopes are very similar. The magnitudes of the slopes, however, are directly proportional to the design lift coefficient (see eq. (11)). Thus, by proper adjustment of the design lift coefficient, wings with essentially the same cambers were obtained for different values of design Mach number. Hence, the lift-drag polar of a wing designed for a Mach number, M , and lift coefficient, C_{L_d} , was assumed to be, at a Mach number $M' \neq M$, the same as the polar for the equivalent wing designed for M' and C_{L_d}' . The polar for the equivalent wing designed for M' and C_{L_d}' was then computed in the manner described in the preceding paragraphs of this section. For the case of the triangular wing of the present investigation, which was cambered for $C_{L_d} = 0.25$ at $M = 1.53$, it was found that the equivalent design lift coefficients, C_{L_d}' , were 0.215, 0.231, and 0.325 at Mach numbers, M' , equal to 1.0, 1.3, and 1.9, respectively.

It will be noted that, in determining the linear-theory drag of the cambered wings, the leading-edge suction force was included. Since experiments have shown that this suction may not be fully realized, it is of interest to obtain theoretical estimates of the effects of losing leading-edge suction on the drag polars. Hence, theoretical polars were computed by a simple no-suction theory in which it is assumed that the usual linear-theory pressures still act upon the lifting surface but that any singularities in pressure at the leading edge do not give rise to a leading-edge thrust, that is, C_{D_s} is arbitrarily set to zero.

Since it is apparent, however, that the absence of leading-edge suction implies a flow that is basically different from the flow assumed in the usual lifting-surface theory, another method of estimating the drag polar merits consideration. A slender-body solution for a flow where no leading-edge suction exists has been obtained by Brown and Michael in reference 7. In the reference paper the flow over a slender

triangular wing in the presence of leading-edge separation is considered. The angle-of-attack loading obtained in reference 7 was, therefore, used to compute a theoretical drag polar with no leading-edge suction. In this application it is assumed that the angle-of-attack loading is still independent of the camber loading and that the two loadings may be superposed. This assumption may not be valid since the loads on the wing are strongly dependent upon the strength and position of the leading-edge vortices which, in turn, are nonlinear functions of the boundary conditions on the wing.

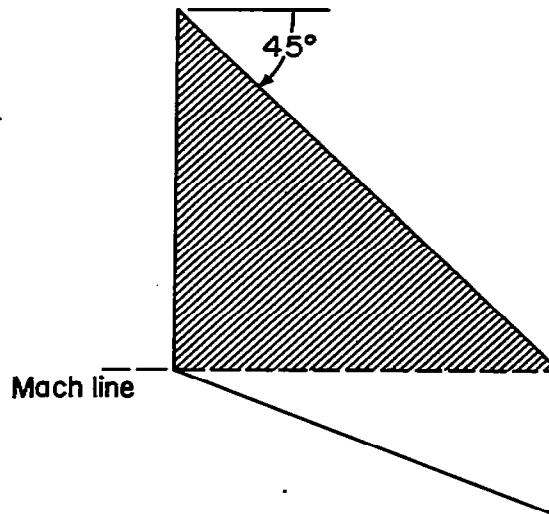
Sweptback wings.- The theoretical drag polar of sweptback wings incorporating conical camber can also be estimated. As noted in the previous section the surface shape of the sweptback wings is determined by specifying the design lift coefficient of the triangular plan form which just circumscribes the sweptback plan form. The question arises, however, as to what to consider as the design lift coefficient of the sweptback wings.

For combinations of plan form and Mach number where there are no trailing-edge or tip effects (see sketch (d)) the design lift coefficient is easily determined. In such a case, the design loading on the sweptback wing is the same as that on the triangular wing and is given by equation (8). It should be noted that the design lift coefficient, C_{L_d} , in equation (8) refers to that of the triangular wing which circumscribes the sweptback wing. Thus, by integration of the loading given by equation (8) over the area of the sweptback plan form, the design lift coefficient of the sweptback wing can be obtained in terms of the design lift coefficient of the triangular wing.

For configurations such as shown in sketch (e), where the camber loading is influenced by the tip effects, the design lift coefficient can be closely approximated. The assumption is made, based on linear-theory considerations that no lift is carried on a lifting surface behind the tip Mach line and, therefore, there is no drag due to lift. Further, the small amount of lift due to camber behind the Mach line from the tip is neglected. The camber loading is then integrated over the wing plan form bounded by the root chord, the leading and trailing edges, and the tip Mach line. For the configurations which are affected both by the trailing wake and by tip effects (see sketch (f)) the determination of the design lift coefficient and, thus, the drag polar is difficult. At present no attempt has been made to compute the drag polar of a sweptback wing incorporating conical camber at Mach numbers where trailing wake effects predominate.

For the sweptback wings of the present investigation the theoretical drag polars have been computed for a Mach number of 1.0. For this computation the assumption has been made that no lift is carried behind the tip Mach line (see sketch (g)). The total lift and drag due to lift experienced by the sweptback wing at a Mach number of 1.0 is, therefore, assumed to be that experienced by the triangular plan form shown in sketch (g).

From the above consideration of equating the total lift of the two plan forms shown in sketch (g), the design lift coefficient of the sweptback wing can be obtained simply by multiplying the design lift coefficient of the triangular wing by the ratio of the area of the triangular wing to the area of the sweptback wing. The drag coefficient can, of course, be obtained in a similar manner. For the sweptback wings presented herein, the equivalent design lift coefficients at a Mach number of 1.0 of the triangular wing from which the surface shape of the sweptback wings were determined were 0.30 and 0.39; the corresponding equivalent design lift coefficients at a Mach number of 1.0 for the sweptback wings as obtained from the above procedure were 0.225 and 0.292, respectively.



Sketch (g)

APPARATUS AND MODELS

Test Facilities

The experimental studies were conducted for the most part in the 6- by 6-foot supersonic wind tunnel, which is a closed-circuit, variable-pressure-type wind tunnel with a Mach number range from 0.6 to 0.9 and from 1.2 to 1.9. A detailed description of the wind tunnel and the characteristics of the air stream at supersonic speeds is available in reference 8. The low-speed ($M = 0.22$) characteristics of some of the models were obtained through additional tests in the 12-foot low-turbulence pressure wind tunnel, which is also a closed-circuit, variable-pressure-type wind tunnel. More detailed information concerning this wind tunnel can be obtained from reference 9.

In both wind tunnels the models were sting-mounted, and the forces and moments measured with an internal, electrical, strain-gage-type balance.

██████████

Selection of Models

The present research program was directed primarily to the investigation of the effects of conical camber on the drag characteristics of wings with sweptback leading edges. For the present investigation two wing plan forms were selected: (1) a triangular wing of aspect ratio 2 and (2) a wing of aspect ratio 3 with 45° sweepback of the leading edge and taper ratio of 0.40. Sketches of the model plan forms are shown in figure 2. The wings were tested with both plane (uncambered) and conically cambered mean surface shapes.

Three uncambered wings were investigated in this program, one of triangular plan form and two of swept plan form. The triangular wing had NACA 0003-63 airfoil sections in streamwise planes. One swept wing, the basic wing, had NACA 64A006 sections perpendicular to the quarter-chord line of swept airfoil sections and the other incorporated the same sections with a leading-edge modification consisting of an increase in the radii of the sections (see fig. 3). The maximum thickness of the sweptback wings was 5 percent in streamwise planes. The coordinates of the airfoil sections used on the uncambered sweptback wings are presented in tables I and II.

Four cambered wings, one of triangular plan form and three of swept plan form, designed according to the procedure described in the section entitled "Theoretical Development" were also investigated. The camber for the triangular wing and a representative sweptback wing is illustrated in figure 4, wherein sketches of airfoil sections at several spanwise stations are presented. The values of the principal design variables for these wings are summarized in the following table:

Plan form	Design β_m	C_{Ld}	Equivalent design lift coefficient at $M = 1.0$	Thickness	Table for coordinates
Triangular	0.577	0.250	0.215	3 percent	III
Sweptback	0	.225	.225	5 percent with modified leading edge ¹	IV
	.577	.330	.292	5 percent	V
	.577	.330	.292	5 percent with modified leading edge ¹	VI

¹See figure 3.

██████████

Also included in the table is the equivalent design lift coefficient at a Mach number of 1.0 (see "Theoretical Development"). Henceforth, the cambered wings will be identified by their equivalent design lift coefficient at a Mach number of 1.0.

In order to determine the effects of Reynolds number on the drag characteristics, tests were also made on a plane triangular wing which had NACA 0005-63 sections.

The body used in conjunction with the wings was that designed to have a minimum wave drag for a given volume (Sears-Haack). In order to accommodate the internal strain-gage balance, the body was cut off as shown in figure 2. The equation of the body is included in figure 2(a). For all models the ratio of the maximum cross-sectional area of the body to the plan-form area of the wing was 0.0509.

TESTS AND PROCEDURES

Range of Test Variables

The experimental portion of the investigation was extended over as wide a range of attitudes and Mach numbers as possible to obtain data which would permit an assessment of the merits or demerits of the wings. In general, angles of attack from -6° to 17° were the limits of the range of this variable, except at transonic speeds where there was a reduction due to choking of the flow. The range of test Mach numbers and Reynolds numbers for the various models is shown in detail in table VII. Also noted in table VII is an index to the tabulated experimental data.

At the low Reynolds numbers (less than 10^7) obtainable in most wind tunnels, extensive regions of laminar flow can exist on the wings when no lift is developed. As lift is developed the pressure gradients acting over the wings change. These changes in pressure gradients cause the boundary-layer transition point to move, thus changing the magnitude of the friction drag. Under such test conditions it would be extremely difficult, if not impossible, to isolate the effect of conical camber on the drag due to lift resulting from the pressure forces. It is evident, therefore, that the change in skin-friction drag with a change in lift must be minimized. In the present investigation this was done by placing roughness strips along rays near the wing leading edge on both upper and lower surfaces to induce transition (see fig. 2). The transition strips were prepared by applying number 60 carborundum onto a thin layer of lacquer. It should be noted further that the drag-due-to-lift results obtained with transition fixed are more representative of flight at much higher Reynolds numbers, wherein fully turbulent flow is to be expected at all angles of attack, than are the transition-free results.

Reduction of Data

The data presented herein have been reduced to standard NACA coefficient form. The pitching-moment coefficient has been referred to the quarter point of the mean aerodynamic chord.

The results obtained in the Ames 6- by 6-foot supersonic wind tunnel have been corrected for the following effects in accordance with the procedures shown in reference 10:

1. The induced effects of the wind-tunnel walls at subsonic speeds resulting from lift on the model.
2. The change in Mach number at subsonic speeds resulting from the constriction of the flow by the wind-tunnel walls.
3. The effect of support interference on the pressure at the base of the model. The base pressure was measured and the drag was adjusted to correspond to that drag which would exist if the base pressure were equal to the free-stream pressure.
4. The effect of stream inclination. Data presented for the swept-back models have been corrected for this effect, the correction being of the order of -0.15° . Sufficient data were not available for the triangular wings to permit a correction for this effect. However, incremental effects such as those due to camber would not be affected by this omission.
5. The longitudinal force on the model due to the streamwise variation of the static pressure as measured in the empty test section. The magnitude of this correction to the drag coefficient was always less than 0.0010.

Data obtained in the 12-foot wind tunnel were corrected for the first four effects. (The stream inclination correction amounted to $+0.10^\circ$ for these data.)

RESULTS AND DISCUSSION

Drag Characteristics

The primary purpose of the present investigation was to evaluate the effectiveness of conical camber in reducing the drag due to lift resulting from the pressure forces acting on triangular and sweptback wings. The theoretical analysis shows that a wing incorporating conical camber should realize a lower value of drag due to lift than a plane wing of the same plan form, if the camber is such that (1) physically realizable pressures exist over the wing (particularly near the leading edge)

and (2) the span loading is nearly elliptical. In order to evaluate experimentally the effects of such camber on the drag characteristics of low-aspect-ratio wings, a triangular wing of aspect ratio 2 and a 45° swept wing of aspect ratio 3 incorporating conical camber were investigated over a wide range of test variables.

The initial results of the investigation, presented in reference 1, indicated that substantial reductions in the drag due to lift could be obtained through the use of conical camber on an aspect-ratio-2 triangular wing. The data presented in reference 1, however, were all obtained with transition free; hence the drag-due-to-lift characteristics include any variations resulting from changes in the skin-friction drag coefficient with lift coefficient. Further, it was found that some of the drag data presented in reference 1 (for the wings cambered to approximate an elliptical span load distribution) were in error.³ Thus, the data in the present report should be used in lieu of the results of reference 1. The experimental data obtained in the present investigation are presented for the complete range of test variables in tables VIII through XV. For the purpose of analysis only certain pertinent data are presented graphically.

Effect of Reynolds number.-- Before evaluating the effectiveness of conical camber on the drag characteristics, it is necessary to determine any changes in viscous forces with changes in lift coefficient and Reynolds number. Changes in viscous forces were believed to occur primarily as a result of a movement of the boundary-layer transition point. To establish the relative importance of the movement of the transition point on the drag characteristics, tests were conducted over a wide Reynolds number range with fixed and free transition. The results of these tests are shown in figure 5 for a 5-percent-thick plane wing for Mach numbers of 0.81, 0.90, and 1.30. These data demonstrate that, as Reynolds number was increased from 2.8×10^6 to 11.3×10^6 , the drag due to lift of the wing with free transition appeared to decrease rapidly (see fig. 5(a)). The results obtained with fixed transition which simulated the fully turbulent boundary layer, characteristic of full-scale Reynolds numbers at transonic and supersonic speeds, showed a considerably smaller reduction in drag due to lift with increasing Reynolds number. Furthermore, as can be seen in figure 5(b), with free transition the drag coefficient at zero lift increased with increasing Reynolds number, while with fixed transition the drag coefficient at zero lift decreased with increasing Reynolds number. These data are strong evidence that a significant part of the apparent change in drag due to lift with Reynolds number for the plane wing with transition free is the result of a movement of the transition point and the associated change in skin-friction drag as Reynolds number and lift coefficient were varied. Thus, in order

³The drag coefficients presented in tables XVII and XVIII of reference 1 are generally in error above a lift coefficient of approximately 0.20.

to eliminate the effect of movement of the transition point on the drag due to lift it is necessary to fix the transition point near the wing leading edge.

The question as to what effects further increases in Reynolds number to full-scale values might have on the drag-due-to-lift characteristics still remains. Sufficient high Reynolds number data are not available at transonic and supersonic speeds to permit a definitive evaluation of this effect. However, in view of the small change in drag due to lift noted over the Reynolds number range tested it seems unlikely that further increases in Reynolds number would result in large reductions in the drag due to lift for plane wings.

From a limited amount of data obtained for a 5-percent-thick cambered wing (fig. 6) it is fairly evident that with free or fixed transition the increment in drag above the zero lift drag, in general, changed only slightly with Reynolds number. This result indicates that the camber may have induced transition naturally near the leading edge of the wing. That the boundary layer was turbulent over most of the cambered wing, with free or fixed transition, is further indicated by the decrease in drag coefficient at zero lift with increasing Reynolds number in both instances. The forward transition of the boundary-layer flow on the cambered wing appears to be consistent with studies presented in references 11 and 12. These studies showed that boundary-layer instability occurred on highly swept wings as a result of the three-dimensional nature of the potential flow which gave rise to a spanwise pressure gradient on the wing. The addition of the camber used herein appears to have resulted in more severe spanwise pressure gradients at zero lift, and thus a more unstable boundary layer, than that of the plane wing.

It will be noted that there is a drag increment associated with the transition strips, as indicated by the highest Reynolds number data for the plane wing (see fig. 5(b)); transition strips must therefore be used on all the wings for proper comparisons. That the high Reynolds number data of the plane wing are indicative of the drag increment associated with the transition strips is further substantiated by the results of the cambered wing (fig. 6) which shows essentially the same drag increment throughout the Reynolds number range. Since the drag increment resulting from the transition strips is essentially the same for both the plane and the cambered wings, a direct comparison of the results with transition fixed is permissible.

Effects of conical camber - triangular wings.- The effectiveness of conical camber derived in the previous sections in reducing the increment of drag resulting from lift is shown in figures 7 and 8. These data show that the use of conical camber results in substantial reductions in drag at lift coefficients above 0.10 at high subsonic speeds ($M=0.81$ and 0.90). At lift coefficients of 0.30 and above, these reductions of drag coefficient amounted to more than 0.0100. Such reductions would greatly improve the performance of aircraft designed to cruise in this lift-coefficient

range at transonic speeds. In addition, the data show that conical camber can be employed without incurring undue penalties in the supersonic drag characteristics, the maximum increase in minimum drag coefficient being about 0.0030 at $M = 1.7$. The beneficial effect of the camber in reducing the drag due to lift was greatest at subsonic speeds; however, as can be seen in figure 8, reductions in drag due to lift with resulting reductions in total drag at lift coefficients of 0.20 and above were also realized at supersonic speeds. Thus, despite the penalty in minimum drag due to camber at supersonic speeds, the maximum lift-drag ratio of the cambered wings, which occurs at a lift coefficient of approximately 0.2, is never lower than that of the plane wing for Mach numbers up to 1.90.

As a means of further demonstrating the effectiveness of the design methods used to improve the drag-due-to-lift characteristics, the measured drag polars for the cambered wing are compared in figure 9 with those computed from linear theory. Experimental data for Mach numbers of 0.90, 1.30, 1.53, and 1.90 are compared, respectively, with computed polars for Mach numbers of 1.0, 1.30, 1.53, and 1.90. Theoretical polars for the cambered wing are presented for the conditions of full leading-edge suction and no leading-edge suction. For a Mach number of 1.0 there are shown two theoretical cambered-wing polars for the case of no leading-edge suction, the derivations of which are discussed in "Theoretical Development." In addition, the ideal drag polar for the plane wing with full leading-edge suction at $M = 1.0$ is shown. Experimental values of C_{D_0} for the plane wing were used in computing the theoretical polars for both the plane and the cambered wing.

It is interesting to note that at a Mach number of unity where no wave drag exists the theoretical polar for the cambered wing closely approximates the theoretical polar for the plane wing, full leading-edge suction being assumed in both cases. This similarity of the two polars is a consequence of the fact that, in the design of the conically cambered wing, the span load distribution resulting from camber was very nearly equal to that due to angle of attack which for triangular wings is elliptical. Had the span loading due to camber been exactly the same as that due to angle of attack the two polars would have been identical.

The calculations for a Mach number of 1.0 show that the no-leading-edge-suction polars as well as the full-suction polar agree with the ideal-plane-wing polar at the design lift coefficient (0.215) but depart as the lift coefficient is increased or decreased from this value. The predicted values of the drag coefficient for no-leading-edge suction based on the solution of reference 7 are somewhat less than those predicted from the simple no-suction polar above or below the design lift coefficient.

A comparison of the experimental data obtained at a Mach number of 0.90 with the theoretical polar for a Mach number of unity shows that conical camber is quite effective near the design lift coefficient, the

increment in drag due to lift⁴ being equal to the minimum drag due to lift increment possible for a wing of this aspect ratio. At lift coefficients less than the design value the experimental drag coefficients lie between the theoretical cambered wing polar for full leading-edge suction and those for no leading-edge suction. It is gratifying to note, however, that only a small penalty in the drag coefficient at zero lift was incurred from the camber, indicating that a significant amount of the leading-edge suction due to the pressure peak in the vicinity of the nose is still being achieved when the lift coefficient is less than the design. Although it might be expected that some leading-edge suction would be realized at small lift coefficients above the design, such is apparently not the case; the experimental drag coefficients are generally somewhat greater than those predicted by the no-leading-edge-suction polars.

At supersonic speeds the agreement between the theoretical full-suction polar and experiment is reasonably good near the design lift coefficient although the experimental drag is generally somewhat higher than the theoretical value. Qualitatively the agreement between theory and experiment at Mach numbers of 1.30 and 1.53 is similar to that shown at a Mach number of 0.90. At a Mach number of 1.90, however, the drag polar calculated for the case of full leading-edge suction predicts closely that obtained experimentally up to a lift coefficient of approximately 0.30.

Effects of conical camber - sweptback wings.- It was shown in the theoretical study presented herein that the conical camber derived for triangular wings should also be effective in reducing the drag due to lift of thin sweptback wings at transonic speeds. Sweptback wings incorporating two different amounts of this conical camber were therefore investigated to determine experimentally the effectiveness of this camber on such plan forms. In addition, to improve the low-speed characteristics ($M < 0.25$) an increase in the nose radius was incorporated on some of the sweptback wings. As shown in figure 10, the effects of this modification to the nose radius were found to be generally small throughout the speed range wherein the data were obtained ($M \geq 0.60$) for both the plane and cambered wings. The exception to this result is the case of the cambered wing at high lift coefficients near a Mach number of 0.60 wherein the wing with the modified nose radius had lower drag coefficients. Unfortunately, data were not available which would permit a direct comparison of the plane and cambered wings with the same nose radius for Mach numbers equal to and greater than 0.60. However, in view of the small effects of the nose radius on the drag characteristics of both the plane and cambered wings, the results presented in figures 11 and 12, in which the data for the plane wing with the normal nose radius are compared with the results

⁴The increment in drag due to lift of the cambered wing is considered to be that increment in drag above the minimum drag coefficient (C_{D_0}) of the plane wing.

for the cambered wing with the modified nose radius (for $M \geq 0.60$), are believed to show primarily the effects of camber. The results presented for a Mach number of 0.22 compare the data of the various wings with the modified nose radius.

Examination of the results of figure 11 shows that at a Mach number of 0.22 the effect of camber on the drag coefficient is small at the lower lift coefficients whereas large improvements are evident at lift coefficients above 0.50. The apparent ineffectiveness of the camber in reducing the drag coefficient at lift coefficients below 0.50 is not surprising in view of the fact that the plane wing realized almost the minimum drag-due-to-lift increment possible for a wing of this aspect ratio, thereby precluding a further reduction in drag. This low drag is associated with the fact that at low speeds the minimum pressure coefficient attainable at the wing leading edge is considerably lower than that at transonic speeds. Thus, the leading-edge suction force necessary for the attainment of low drag due to lift is more likely to be attained.

At the higher lift coefficients at a Mach number of 0.22, considerable reductions in the drag coefficients were obtained through the use of camber. As shown in figure 11 there occurs a break in the drag polar of the plane wing at a lift coefficient of approximately 0.50. The value of the lift coefficient at which the rapid increase in the drag coefficient occurs is increased as the amount of camber is increased. These results indicate that attached flow was maintained on the cambered wings to somewhat higher lift coefficients than on the plane wings. A comparison of the results with data for lower Reynolds numbers, not presented graphically, indicated that increasing the Reynolds number resulted in a similar improvement in the drag characteristics at high lift coefficients for the plane and cambered wings. Thus, increasing the Reynolds number appears to have the same effect as camber in delaying to a higher lift coefficient the onset of flow separation. It is probable that further increases in Reynolds number would result in further improvements in the low-speed characteristics of the plane and cambered wings.

The effects of camber on the drag characteristics at higher subsonic speeds ($M \geq 0.60$) are considerably different from those noted at a Mach number of 0.22. (See figs. 11 and 12.) At subsonic Mach numbers of 0.60 or greater the amount of camber incorporated in the wing was found to have a significant effect on the drag coefficient throughout the lift-coefficient range. Examination of the data shows that cambering the wing for a design lift coefficient of 0.225 resulted in substantial reductions in the drag coefficients at a lift coefficient above 0.10. For lift coefficients less than 0.50, the more highly cambered wing always experienced drag coefficients that were greater than those of the moderately cambered wing. It is evident from these results that, especially at high subsonic speeds ($M \geq 0.8$), the improvements in drag resulting from camber can be seriously reduced if the sections are too highly cambered.

It is likely that the adverse effects of overcambering the wing are due to the effects of compressibility similar to those shown for two-dimensional wings in reference 13. These section data showed that improvements in the drag characteristics accompanying increases in the amount of camber were in evidence at low and moderate Mach numbers but that the advantage of camber disappeared at the higher Mach numbers. The incorporation of a large amount of camber actually resulted in deleterious effects on the drag characteristics at Mach numbers of 0.8 and above.

At supersonic speeds the wing cambered for a lift coefficient of 0.225 showed a small penalty in drag coefficient at zero lift, a maximum increase of approximately 0.0020 occurring; whereas the more highly cambered wing showed a penalty of approximately 0.0045. It should be noted, however, that a small part of the increment in the drag at zero lift experienced by both of the cambered wings is due to the increase in nose radius shown previously (see fig. 10). Further examination of the data shows that the drag due to lift at supersonic speeds was reduced by camber, with the result that no penalty in drag coefficient was incurred for the moderately cambered wing at lift coefficients above 0.10. The drag coefficients of the more highly cambered wing, however, were greater than those of both the plane and the moderately cambered wing at all lift coefficients.

A comparison of the experimental and theoretical polars for the sweptback wing (see fig. 13) is interesting in that it indicates the applicability of the design methods, which were originally derived for triangular plan forms, to sweptback wings. (It should be noted that the experimental data for a Mach number of 0.90 are compared with the theory for a Mach number of 1.0.) Here, as for the triangular wings, the theoretical cambered-wing polars are in close agreement with the ideal polar for the plane wing assuming full leading-edge suction in each case. The cambered-wing polar for no leading-edge suction departs from the ideal polar as the lift coefficient deviates from the design lift coefficient. The results show that, for the wing cambered for a lift coefficient of 0.225, the experimental drag coefficient is in excellent agreement with the predicted value near the design lift coefficient. As the lift coefficient is increased from the design point the experimental drag coefficients are essentially those predicted by the no-suction polar. At lift coefficients less than the design value, the experimental values fall between the full-suction polar and that for no leading-edge suction. The small penalty in the drag at zero lift suggests that a portion of the leading-edge suction is still being realized below the design condition.

For the more highly cambered wing the experimental drag coefficient at the design lift coefficient is somewhat greater than that predicted by the theory. This disagreement between the theory and experiment is believed to be due, in part at least, to the fact that for this amount

of camber the adverse effects of compressibility at $M = 0.9$ result in high experimental drags. Above the design lift the experimental drag is greater than that predicted by theory whereas below the design condition the experimental data are generally between the full-suction and no-suction polars.

The preceding results have shown that large reductions in the drag coefficients can be realized at transonic speeds on a triangular and a 45° sweptback wing by the use of conical camber. However, the results available on the sweptback wing have shown that excessive camber can seriously affect the benefits possible at transonic speeds as well as result in large penalties at supersonic speeds. The results of figure 14 which present the incremental drag coefficient due to camber as a function of design lift coefficient at several Mach numbers are presented as a guide to indicate the amount of conical camber that should be incorporated in an aircraft utilizing a 45° sweptback wing. It is evident from these data that to realize the maximum gains at transonic speeds the camber employed should not exceed that corresponding to a design lift coefficient of approximately 0.22. Moreover, it appears from the limited data available that the use of somewhat less camber might result in essentially the same benefits in drag as obtained in the present experimental investigation. Any reduction in the amount of camber would, of course, result in smaller penalties in the drag near zero lift at supersonic speeds.

Lift and Moment Characteristics

During the investigation, experimental results were also obtained showing the effects of conical camber on the lift and moment characteristics of the triangular and sweptback wings. A brief description of these results is included herein.

Triangular wings.- It is well known that the aerodynamic center and the lift-curve slope near zero lift are primarily functions of wing plan form, and are uninfluenced by the provision of camber. Such a result is shown in figure 15, wherein the lift and pitching-moment curves of the cambered wing are essentially parallel with those of the plane wing but are displaced slightly. The small positive shift in the angle of zero lift, which is due to washout resulting from the camber, is of little significance but the positive shift in pitching moment at zero lift, the magnitude of which decreased with increasing Mach number, would result in a small decrease in the trim drag of an airplane.

Sweptback wings.- Examination of the data of figure 16 shows that throughout the Mach number range investigated, the slope of the lift and pitching-moment curves near zero lift were essentially unaffected by camber but that the curves were slightly displaced. The small negative shift in the pitching moment resulting from camber would result in small increases in the trim drag.

The results for a Mach number of 0.22 show that the range of lift coefficients wherein the lift curve was essentially linear was increased through the use of camber, indicating that attached flow was maintained on the cambered wings to somewhat higher lift coefficients than on the plane wing. These improvements in the flow characteristics resulting from camber were also reflected in improvements in the static longitudinal stability at high lift coefficients at subsonic speeds. The reduction in longitudinal stability for the plane wing at a Mach number of 0.22, which manifested itself as an unstable break in the pitching-moment curve at a lift coefficient of 0.60, was delayed to a lift coefficient of approximately 0.75 and 0.85 on the wings cambered for lift coefficients of 0.225 and 0.292, respectively. The reduction in longitudinal stability for the plane wing at high subsonic speeds was also alleviated to some extent by the camber. At supersonic speeds the lift curve and the longitudinal stability remained essentially unchanged by camber.

CONCLUSIONS

A theoretical and experimental investigation was made to determine primarily the effectiveness of conical camber in reducing the drag due to lift resulting from pressure forces acting on low-aspect-ratio triangular and sweptback wings. The results of this investigation showed:

1. The use of a moderate amount of camber resulted in significant reductions in the drag coefficient above a lift coefficient of 0.10 at high subsonic speeds for both triangular and sweptback wings. Further, the penalties in drag at zero lift were small at supersonic speeds.
2. Increasing the amount of camber on the sweptback wing resulted in some improvements in the drag characteristics at high lift coefficients at low speed, but at high subsonic speeds the improvements in the drag characteristics were seriously reduced. At supersonic speeds increasing the amount of camber resulted in large increases in the drag coefficients.
3. The drag coefficients predicted by lifting-surface theory were in close agreement with experimental results at the lift coefficient for which the camber was designed for the moderately cambered wings. Above the design lift coefficient the experimental drag coefficients were essentially those predicted from a no-suction theory; below the design lift coefficient the experimental values fell between the full-suction polar and that for no leading-edge suction.
4. The lift and moment characteristics of the triangular wing at subsonic and supersonic speeds were not significantly affected by camber.

The reduction in longitudinal stability observed for the uncambered sweptback wing at subsonic speeds was delayed to higher lift coefficients by the use of camber.

Ames Aeronautical Laboratory
National Advisory Committee for Aeronautics
Moffett Field, Calif., July 19, 1955

REFERENCES

1. Hall, Charles F.: Lift, Drag, and Pitching Moment of Low-Aspect-Ratio Wings at Subsonic and Supersonic Speeds. NACA RM A53A30, 1953.
2. Osborne, Robert S., and Kelly, Thomas C.: A Note on the Drag Due to Lift of Delta Wings at Mach Numbers up to 2.0. NACA RM L53A16a, 1953.
3. Polhamus, Edward C.: Drag Due to Lift at Mach Numbers up to 2.0. NACA RM L53I22b, 1953.
4. Jones, Robert T.: Estimated Lift-Drag Ratios at Supersonic Speeds. NACA TN 1350, 1947.
5. Cohen, Doris: Formulas for the Supersonic Loading, Lift and Drag of Flat Swept-Back Wings with Leading Edges Behind the Mach Lines. NACA Rep. 1050, 1951. (Formerly NACA TN's 1555, 1991, and 2093)
6. Stewart, H. J.: Lift of a Delta Wing at Supersonic Speeds. Quart. Appl. Math., vol. IV, no. 3, Oct. 1946, pp. 246-254.
7. Brown, Clinton E., and Michael, William H., Jr.: On Slender Delta Wings with Leading-Edge Separation. NACA TN 3430, 1955.
8. Frick, Charles W., and Olson, Robert N.: Flow Studies in the Asymmetric Adjustable Nozzle of the Ames 6- by 6-Foot Supersonic Wind Tunnel. NACA RM A9E24, 1949.
9. Edwards, George G., and Stephenson, Jack D.: Tests of a Triangular Wing of Aspect Ratio 2 in the Ames 12-Foot Pressure Wind Tunnel. I - The Effect of Reynolds Number and Mach Number on the Aerodynamic Characteristics of the Wing With Flap Undelected. NACA RM A7K05, 1948.
10. Boyd, John W.: Aerodynamic Characteristics of Two 25-Percent Trailing-Edge Flaps on an Aspect-Ratio-2 Triangular Wing at Subsonic and Supersonic Speeds. NACA RM A52D01c, 1952.

11. Stuart, J. T.: The Basic Theory of Stability of Three-dimensional Boundary Layers. British ARC, Fluid Motion Sub-Committee 15,904, FM 1899, May 13, 1953.
12. Owen, P. R., and Randall, D. G.: Boundary-Layer Transition on a Sweptback Wing: A Further Investigation. British R.A.E. Tech Memo No. Aero. 330, Feb. 1953.
13. Summers, James L., and Treon, Stuart L.: The Effects of Amount and Type of Camber on the Variation With Mach Number of the Aerodynamic Characteristics of a 10-Percent Thick NACA 64-A Series Airfoil Section. NACA TN 2096, 1950.

TABLE I.- COORDINATES OF AIRFOIL SECTIONS FOR PLANE WING OF ASPECT RATIO 3 WITH 45° SWEEPBACK, 5 PERCENT THICK WITH NORMAL LEADING EDGE
 [Coordinates are presented for sections parallel to the plane of symmetry.]

2y/b	x percent c	z percent c	x percent c	z percent c	x percent c	z percent c
0-1.00 ^a	0	0	25.200	2.289	71.452	1.709
	.672	.464	30.997	2.429	75.872	1.468
	1.008	.559	36.610	2.511	80.170	1.217
	1.678	.704	42.050	2.541	84.352	0.963
	3.340	.964	47.325	2.522	88.421	.715
	6.623	1.317	52.440	2.438	92.384	.473
	9.850	1.571	57.404	2.304	96.212	.238
	13.023	1.776	62.223	2.132	100.000	.009
	19.213	2.077	66.903	1.931		

^aLeading-edge radius: 0.190 percent chord

TABLE II.- COORDINATES OF AIRFOIL SECTIONS FOR PLANE WING OF ASPECT RATIO 3 WITH 45° SWEEPBACK, 5 PERCENT THICK WITH MODIFIED LEADING EDGE
 [Coordinates are presented for sections parallel to the plane of symmetry.]

2y/b	x percent c	z percent c	x percent c	z percent c	2y/b	x percent c	z percent c	x percent c	z percent c
0 ^a	0	0	47.325	2.522	0.67 ^d	0	0	47.325	2.522
	.672	.464	52.440	2.438		.672	.745	52.440	2.438
	1.008	.559	57.404	2.304		1.008	.842	57.404	2.304
	1.678	.704	62.223	2.132		1.678	.972	62.223	2.132
	3.340	.964	66.903	1.931		3.340	1.242	66.903	1.931
	6.623	1.317	71.452	1.709		6.623	1.609	71.452	1.709
	9.850	1.571	75.872	1.468		9.850	1.847	75.872	1.468
	13.023	1.776	80.170	1.217		13.023	2.030	80.170	1.217
	19.213	2.077	84.352	.963		19.213	2.236	84.352	.963
	25.200	2.289	88.421	.715		25.200	2.354	88.421	.715
	30.997	2.429	92.384	.473		30.997	2.429	92.384	.473
	36.610	2.511	96.212	.238		36.610	2.511	96.212	.238
	42.050	2.541	100.000	.009		42.050	2.541	100.000	.009
0.25 ^b	0	0	47.325	2.522	0.83 ^e	0	0	47.325	2.522
	.672	.572	52.440	2.438		.672	.817	52.440	2.438
	1.008	.663	57.404	2.304		1.008	.920	57.404	2.304
	1.678	.808	62.223	2.132		1.678	1.050	62.223	2.132
	3.340	1.067	66.903	1.931		3.340	1.322	66.903	1.931
	6.623	1.426	71.452	1.709		6.623	1.689	71.452	1.709
	9.850	1.677	75.872	1.468		9.850	1.931	75.872	1.468
	13.023	1.868	80.170	1.217		13.023	2.100	80.170	1.217
	19.213	2.135	84.352	.963		19.213	2.281	84.352	.963
	25.200	2.310	88.421	.715		25.200	2.372	88.421	.715
	30.997	2.429	92.384	.473		30.997	2.429	92.384	.473
	36.610	2.511	96.212	.238		36.610	2.511	96.212	.238
	42.050	2.541	100.000	.009		42.050	2.541	100.000	.009
0.50 ^c	0	0	47.325	2.522	1.00 ^f	0	0	47.325	2.522
	.672	.676	52.440	2.438		.672	.891	52.440	2.438
	1.008	.768	57.404	2.304		1.008	.988	57.404	2.304
	1.678	.907	62.223	2.132		1.678	1.118	62.223	2.132
	3.340	1.176	66.903	1.931		3.340	1.393	66.903	1.931
	6.623	1.528	71.452	1.709		6.623	1.750	71.452	1.709
	9.850	1.778	75.872	1.468		9.850	1.993	75.872	1.468
	13.023	1.963	80.170	1.217		13.023	2.155	80.170	1.217
	19.213	2.194	84.352	.963		19.213	2.317	84.352	.963
	25.200	2.333	88.421	.715		25.200	2.382	88.421	.715
	30.997	2.429	92.384	.473		30.997	2.429	92.384	.473
	36.610	2.511	96.212	.238		36.610	2.511	96.212	.238
	42.050	2.541	100.000	.009		42.050	2.541	100.000	.009

^aLeading-edge radius: 0.190 percent chord
^bLeading-edge radius: 0.236 percent chord
^cLeading-edge radius: 0.370 percent chord
^dLeading-edge radius: 0.520 percent chord
^eLeading-edge radius: 0.713 percent chord
^fLeading-edge radius: 0.924 percent chord

TABLE III.- COORDINATES OF AIRFOIL SECTIONS FOR TRIANGULAR WING OF ASPECT RATIO 2, 3 PERCENT THICK, CONICALLY CAMBERED FOR $C_{L\alpha} = 0.215$ AT $M = 1.0$ [Coordinates are presented for sections parallel to the plane of symmetry.]

$2y/b$	x percent c	z percent c	x percent c	z percent c	x percent c	z percent c
0^a	0	0	20.000	1.435	70.000	.916
	1.250	.473	25.000	1.485	80.000	.656
	2.500	.653	30.000	1.500	90.000	.362
	5.000	.888	35.000	1.488	95.000	.202
	7.500	1.050	40.000	1.450	100.000	.032
	10.000	1.170	50.000	1.323		
	15.000	1.336	60.000	1.141		

$2y/b$	Upper surface		Lower surface		$2y/b$	Upper surface		Lower surface		
	x percent c	z percent c	x percent c	z percent c		x percent c	z percent c	x percent c	z percent c	
0.20^a	0	-.522	0	-.522	0.60^a	29.737	1.434	29.788	-1.574	
	1.154	.224	1.283	-.713		34.760	1.486	34.782	-1.500	
	2.408	.548	2.504	-.772		40.000	1.450	40.000	-1.450	
	4.926	.879	4.963	-.901		50.000	1.323	50.000	-1.323	
	7.500	1.050	7.500	1.050		60.000	1.141	60.000	-1.141	
	10.000	1.170	10.000	1.170		70.000	.916	70.000	-.916	
	15.000	1.336	15.000	1.336		80.000	.656	80.000	-.656	
	20.000	1.435	20.000	1.435		90.000	.362	90.000	-.362	
	25.000	1.485	25.000	1.485		95.000	.202	95.000	-.202	
	30.000	1.500	30.000	1.500		100.000	.032	100.000	-.032	
	35.000	1.488	35.000	1.488		0.80^a	0	-8.354	0	-8.354
	40.000	1.450	40.000	1.450			1.015	-7.472	.794	-8.398
	50.000	1.323	50.000	1.323			2.221	-6.810	2.618	-8.060
	60.000	1.141	60.000	1.141			4.633	-5.854	5.089	-7.575
	70.000	.916	70.000	.916			7.074	-5.054	7.545	-7.089
80.000	.656	80.000	.656	9.545	-4.383		10.016	-6.692		
85.000	.548	85.000	.548	14.502	-3.324	14.943	-5.971			
90.000	.362	90.000	.362	19.503	-2.530	19.885	-5.339			
95.000	.202	95.000	.202	24.489	-1.824	24.842	-4.780			
100.000	.032	100.000	.032	29.504	-1.235	29.798	-4.236			
0.40^a	0	-1.392	0	-1.392	34.505	-.824	34.799	-3.795		
	1.103	-.544	1.313	-1.465	39.550	-.471	39.756	-3.383		
	2.328	-.137	2.539	-1.426	49.595	.059	49.742	-2.618		
	4.818	.422	4.994	-1.343	59.656	.324	59.759	-1.971		
	7.317	.779	7.455	-1.318	67.745	.456	69.804	-1.383		
	9.832	1.034	9.924	-1.304	79.232	.471	79.261	-.838		
	14.856	1.338	14.885	-1.289	89.910	.368	89.910	-.353		
	20.000	1.435	20.000	-1.435	94.955	.221	94.954	-.191		
	25.000	1.485	25.000	-1.485	100.000	.029	100.000	-.029		
	30.000	1.500	30.000	-1.500	0.90^a	0	-19.235	0	-19.235	
	35.000	1.488	35.000	-1.488		.971	-18.206	1.412	-19.059	
	40.000	1.450	40.000	-1.450		2.147	-17.471	2.382	-18.765	
	50.000	1.323	50.000	-1.323		4.588	-16.471	5.176	-18.176	
	60.000	1.141	60.000	-1.141		7.000	-15.558	7.588	-17.441	
	70.000	.916	70.000	.916		14.412	-13.088	15.029	-15.706	
80.000	.656	80.000	.656	19.382	-11.882	20.000	-14.706			
85.000	.548	85.000	.548	24.382	-10.794	24.941	-13.735			
90.000	.362	90.000	.362	29.353	-9.735	29.882	-12.735			
95.000	.202	95.000	.202	34.382	-9.000	34.882	-11.971			
100.000	.032	100.000	.032	39.412	-8.294	39.853	-11.206			
0.60^a	0	-3.133	0	-3.133	49.500	-7.118	49.823	-9.765		
	1.066	-2.221	1.339	-3.126	59.559	-6.068	59.823	-8.382		
	2.265	-1.714	2.574	-2.986	69.676	-5.294	69.853	-7.147		
	4.722	-.971	5.031	-2.721	79.765	-4.529	79.852	-5.853		
	7.193	-.419	7.480	-2.501	89.882	-4.118	89.941	-4.853		
	9.687	-.007	9.944	-2.331	94.941	-3.941	94.970	-4.353		
	14.681	.633	14.879	-2.031	100.000	-3.708	100.000	-3.645		
	19.697	1.030	19.836	-1.831						
	24.713	1.280	24.809	-1.692						

^aLeading-edge radius: 0.100 percent chord

TABLE IV.- COORDINATES OF AIRFOIL SECTIONS FOR WING OF ASPECT RATIO 3 WITH 45° SWEEPBACK, 5 PERCENT THICK WITH MODIFIED LEADING EDGE, CONICALLY CAMBERED FOR $C_{L\alpha} = 0.225$ AT $M = 1.0$
 [Coordinates are presented for sections parallel to the plane of symmetry.]

2y/b	x percent c	x percent c	x percent c	x percent c	x percent c	x percent c	
0 ^a	0 .672 1.008 1.678 3.340 6.623 9.890 13.023 19.213	0 .464 .799 .704 .964 1.317 1.571 1.776 2.077	25.000 30.997 36.610 42.050 47.325 52.440 57.404 62.223 66.903	2.289 2.429 2.511 2.541 2.522 2.438 2.304 2.132 1.931	71.452 75.872 80.170 84.352 88.421 92.384 96.212 100.000	1.709 1.468 1.217 .963 .715 .473 .238 .009	
2y/b	x percent c	x, percent c		2y/b	x percent c	x, percent c	
		Upper surface	Lower surface			Upper surface	Lower surface
0.25 ^b	0 .672 1.008 1.678 3.340 6.623 9.890 13.023 19.213 25.200 30.997 36.610 42.050 47.325 52.440 57.404 62.223 66.903 71.452 75.872 80.170 84.352 88.421 92.384 96.212 100.000	-0.435 .806 .335 .541 .892 1.317 1.571 1.776 2.077 2.289 2.429 2.511 2.541 2.522 2.438 2.304 2.132 1.931 1.709 1.468 1.217 .963 .715 .473 .238 .009	-0.435 -.740 -.793 -.669 -1.037 -1.317 -1.571 -1.776 -2.077 -2.289 -2.429 -2.511 -2.541 -2.522 -2.438 -2.304 -2.132 -1.931 -1.709 -1.468 -1.217 -.963 -.715 -.473 -.238 -.009	0.67	47.325 52.440 57.404 62.223 66.903 71.452 75.872 80.170 84.352 88.421 92.384 96.212 100.000	2.522 2.438 2.304 2.132 1.931 1.709 1.468 1.217 .963 .715 .473 .238 .009	-2.522 -2.438 -2.304 -2.132 -1.931 -1.709 -1.468 -1.217 -.963 -.715 -.473 -.238 -.009
0.50 ^c	0 .672 1.008 1.678 3.340 6.623 9.890 13.023 19.213 25.200 30.997 36.610 42.050 47.325 52.440 57.404 62.223 66.903 71.452 75.872 80.170 84.352 88.421 92.384 96.212 100.000	-1.046 -.961 -.821 -.628 -.491 -1.074 -1.463 -1.685 -1.741 -2.077 -2.289 -2.429 -2.511 -2.541 -2.522 -2.438 -2.304 -2.132 -1.931 -1.709 -1.468 -1.217 -.963 -.715 -.473 -.238 -.009	-1.046 -1.333 -1.352 -1.380 -1.444 -1.595 -1.685 -1.815 -2.077 -2.289 -2.429 -2.511 -2.541 -2.522 -2.438 -2.304 -2.132 -1.931 -1.709 -1.468 -1.217 -.963 -.715 -.473 -.238 -.009	0.83 ^d	0 .672 1.008 1.678 3.340 6.623 9.890 13.023 19.213 25.200 30.997 36.610 42.050	-2.450 -1.478 -2.955 -1.348 -2.929 -1.115 -2.877 -.662 -2.774 -1.04 -2.609 -.635 -2.528 -1.063 -2.302 -1.685 -2.476 -2.100 -2.489 -2.346 -2.515 -2.490 -2.541 -2.541 -2.522 -2.438 -2.304 -2.132 -1.931 -1.709 -1.468 -1.217 -.963 -.715 -.473 -.238 -.009	-2.450 -2.955 -2.929 -2.877 -2.774 -2.609 -2.528 -2.302 -2.476 -2.489 -2.515 -2.541 -2.541 -2.522 -2.438 -2.304 -2.132 -1.931 -1.709 -1.468 -1.217 -.963 -.715 -.473 -.238 -.009
1.00 ^e	0 .672 1.008 1.678 3.340 6.623 9.890 13.023 19.213 25.200 30.997 36.610 42.050 47.325 52.440 57.404 62.223 66.903 71.452 75.872 80.170 84.352 88.421 92.384 96.212 100.000	-1.631 -.821 -.680 -.443 .054 -1.028 -1.466 -1.978 -1.931 -1.998 -2.279 -2.429 -2.511 -2.541	-1.631 -2.009 -2.080 -2.030 -1.998 -1.944 -1.978 -1.970 -2.030 -2.160 -2.300 -2.429 -2.511 -2.541	1.00 ^f	0 .672 1.008 1.678 3.340 6.623 9.890 13.023 19.213 25.200 30.997 36.610 42.050 47.325 52.440 57.404 62.223 66.903 71.452 75.872 80.170 84.352 88.421 92.384 96.212 100.000	-3.678 -2.495 -2.382 -2.171 -1.701 -3.775 -3.308 -3.370 -3.176 -3.046 -2.950 -2.852 -2.711 -2.641 -2.479 -2.317 -2.132 -1.931 -1.709 -1.468 -1.217 -.963 -.715 -.473 -.238 -.009	-3.678 -4.294 -4.310 -4.249 -4.067 -3.775 -3.548 -3.370 -3.176 -3.046 -2.950 -2.852 -2.711 -2.641 -2.479 -2.317 -2.132 -1.931 -1.709 -1.468 -1.217 -.963 -.715 -.473 -.238 -.009
0.67 ^g	0 .672 1.008 1.678 3.340 6.623 9.890 13.023 19.213 25.200 30.997 36.610 42.050	-1.631 -.821 -.680 -.443 .054 -1.028 -1.466 -1.978 -1.931 -1.998 -2.279 -2.429 -2.511 -2.541	-1.631 -2.009 -2.080 -2.030 -1.998 -1.944 -1.978 -1.970 -2.030 -2.160 -2.300 -2.429 -2.511 -2.541	0.67 ^h	0 .672 1.008 1.678 3.340 6.623 9.890 13.023 19.213 25.200 30.997 36.610 42.050	-1.631 -2.009 -2.080 -2.030 -1.998 -1.944 -1.978 -1.970 -2.030 -2.160 -2.300 -2.429 -2.511 -2.541	-1.631 -2.009 -2.080 -2.030 -1.998 -1.944 -1.978 -1.970 -2.030 -2.160 -2.300 -2.429 -2.511 -2.541

^aLeading-edge radius: 0.190 percent chord

^bLeading-edge radius: 0.236 percent chord

^cLeading-edge radius: 0.370 percent chord

^dLeading-edge radius: 0.320 percent chord

^eLeading-edge radius: 0.713 percent chord

^fLeading-edge radius: 0.924 percent chord

TABLE V.- COORDINATES OF AIRFOIL SECTIONS FOR WING OF ASPECT RATIO 3 WITH 45° SWEEPBACK, 5 PERCENT THICK WITH NORMAL LEADING EDGE, CONICALLY CAMBERED FOR $C_{L\alpha} = 0.292$ AT $M = 1.0$
 [Coordinates are presented for sections parallel to the plane of symmetry.]

2y/b	x		x		x		x	
	percent c	percent c	percent c	percent c	percent c	percent c	percent c	percent c
0 ^a	0	0	25.200	2.289	71.452	1.709		
	.672	.464	30.997	2.429	75.872	1.468		
	1.008	.559	36.610	2.511	80.170	1.217		
	1.678	.704	42.050	2.541	84.352	.963		
	3.340	.964	47.325	2.522	88.421	.715		
	6.623	1.317	52.440	2.438	92.384	.473		
	9.950	1.571	57.404	2.304	96.212	.238		
	13.023	1.776	62.223	2.132	100.000	.009		
	19.213	2.077	66.903	1.931				

2y/b	x		x		2y/b	x		x	
	percent c	percent c		percent c		percent c	percent c		
		Upper surface	Lower surface				Upper surface	Lower surface	
0.25 ^a	0	-.579	-.579	0.67	47.325	2.522	-2.522		
	.762	.130	-.069		52.440	2.438	-2.438		
	2.287	.640	-.976		57.404	2.304	-2.304		
	3.812	.938	-1.090		62.223	2.132	-2.132		
	5.337	1.166	-1.204		66.903	1.931	-1.931		
	7.624	1.395	-1.395		71.452	1.709	-1.709		
	9.950	1.570	-1.570		75.872	1.468	-1.468		
	13.023	1.776	-1.776		80.170	1.217	-1.217		
	19.213	2.077	-2.077		84.352	.963	-.963		
	25.200	2.289	-2.289		88.421	.715	-.715		
	30.997	2.429	-2.429		92.384	.473	-.473		
	36.610	2.511	-2.511		96.212	.238	-.238		
	42.050	2.541	-2.541		100.000	.009	-.009		
	47.325	2.522	-2.522						
52.440	2.438	-2.438							
0.50 ^a	0	-1.407	-1.407	0.67 ^a	0	-3.292	-3.292		
	.926	-.565	-1.657		1.037	-2.333	-3.500		
	1.852	-.157	-1.618		1.944	-1.905	-3.461		
	3.703	.389	-1.639		3.240	-1.400	-3.344		
	5.555	.778	-1.657		5.105	-.778	-3.163		
	7.406	1.074	-1.685		7.778	-.156	-3.037		
	11.110	1.528	-1.768		10.369	.311	-2.890		
	14.813	1.842	-1.898		13.554	1.053	-2.748		
	19.213	2.077	-2.077		19.447	1.478	-2.670		
	25.200	2.289	-2.289		25.923	2.009	-2.605		
	30.997	2.429	-2.429		29.812	2.216	-2.579		
	36.610	2.511	-2.511		34.997	2.424	-2.566		
	42.050	2.541	-2.541		42.050	2.541	-2.541		
	47.325	2.522	-2.522		47.325	2.522	-2.522		
52.440	2.438	-2.438		52.440	2.438	-2.438			
0.67 ^a	0	-2.192	-2.192	1.00 ^a	0	-4.942	-4.942		
	.864	-1.350	-2.430		.810	-4.099	-5.152		
	1.620	-.903	-2.479		1.620	-3.645	-5.087		
	3.240	-.410	-2.333		3.240	-2.965	-4.893		
	5.400	.162	-2.246		6.861	-2.306	-4.699		
	7.950	.616	-2.192		6.481	-1.912	-4.537		
	10.800	1.123	-2.149		9.721	-1.118	-4.281		
	15.120	1.588	-2.160		16.202	.069	-3.824		
	20.520	2.020	-2.225		19.442	.470	-3.662		
	24.841	2.246	-2.300		24.303	1.053	-3.467		
	30.997	2.429	-2.429		29.164	1.491	-3.273		
	36.610	2.511	-2.511		35.644	1.912	-3.078		
	42.050	2.541	-2.541		40.505	2.106	-2.949		
					45.366	2.220	-2.819		
				50.226	2.268	-2.697			
				57.404	2.252	-2.333			
				62.216	2.139	-2.139			
				66.903	1.931	-1.931			
				71.452	1.709	-1.709			
				75.872	1.468	-1.468			
				80.170	1.217	-1.217			
				84.352	.963	-.963			
				88.421	.715	-.715			
				92.384	.473	-.473			
				96.212	.238	-.238			
				100.000	.009	-.009			

^aLeading-edge radius: 0.190 percent chord

TABLE VI.- COORDINATES OF AIRFOIL SECTIONS FOR WING OF ASPECT RATIO 3 WITH 45° SWEEPBACK, 5 PERCENT THICK WITH MODIFIED LEADING EDGE, CONICALLY CAMBERED FOR $C_{L\alpha} = 0.292$ AT $M = 1.0$
 [Coordinates are presented for sections parallel to the plane of symmetry.]

2y/b	x		x		x		
	percent c	percent c	percent c	percent c	percent c	percent c	
0 ^a	0	0	25.200	2.289	71.452	1.709	
	.672	.464	30.997	2.429	75.872	1.468	
	1.008	.599	36.610	2.511	80.170	1.217	
	1.678	.704	42.050	2.541	84.352	.963	
	3.340	.964	47.325	2.522	88.421	.715	
	6.623	1.317	52.440	2.438	92.384	.473	
	9.850	1.571	57.404	2.304	96.212	.238	
	13.023	1.776	62.223	2.132	100.000	.009	
	19.213	2.077	66.903	1.931			
2y/b	x percent c	x _s percent c		2y/b	x percent c	x _s percent c	
		Upper surface	Lower surface			Upper surface	Lower surface
0.25 ^b	0	-.379	-.379	0.67	47.325	2.522	-2.522
	.672	-.175	-.945		52.440	2.438	-2.438
	1.008	-.343	-.984		57.404	2.304	-2.304
	1.678	-.572	-1.052		62.223	2.132	-2.132
	3.340	-.968	-1.159		66.903	1.931	-1.931
	6.623	-1.418	-1.418		71.452	1.709	-1.709
	9.850	-1.677	-1.677		75.872	1.468	-1.468
	13.023	-1.868	-1.868		80.170	1.217	-1.217
	19.213	-2.135	-2.135		84.352	.963	-.963
	25.200	-2.310	-2.310		88.421	.715	-.715
	30.997	-2.429	-2.429		92.384	.473	-.473
	36.610	-2.511	-2.511		96.212	.238	-.238
	42.050	-2.541	-2.541		100.000	.009	-.009
	47.325	-2.522	-2.522				
52.440	-2.438	-2.438	0.83 ^c	0	-3.292	-3.292	
57.404	-2.304	-2.304		.672	-2.139	-3.811	
62.223	-2.132	-2.132		1.008	-1.977	-3.849	
66.903	-1.931	-1.931		1.678	-1.646	-3.623	
71.452	-1.709	-1.709		3.340	-.953	-3.681	
75.872	-1.468	-1.468		6.623	-.613	-3.422	
80.170	-1.217	-1.217		9.850	-.266	-3.266	
84.352	-.963	-.963		13.023	1.053	-3.098	
88.421	-.715	-.715		19.213	1.672	-2.851	
92.384	-.473	-.473		25.200	2.035	-2.683	
96.212	-.238	-.238		30.997	2.261	-2.592	
100.000	.009	.009		36.610	2.463	-2.553	
				42.050	2.541	-2.541	
				47.325	2.522	-2.522	
			52.440	2.438	-2.438		
			57.404	2.304	-2.304		
			62.223	2.132	-2.132		
			66.903	1.931	-1.931		
			71.452	1.709	-1.709		
			75.872	1.468	-1.468		
			80.170	1.217	-1.217		
			84.352	.963	-.963		
			88.421	.715	-.715		
			92.384	.473	-.473		
			96.212	.238	-.238		
			100.000	.009	-.009		
0.50 ^c	0	-1.407	-1.407	1.00 ^d	0	-4.942	-4.942
	.672	-.472	-1.833		.672	-3.678	-5.541
	1.008	-.278	-1.892		1.008	-3.516	-5.597
	1.678	0	-1.892		1.678	-3.159	-5.509
	3.340	.509	-1.852		3.340	-2.447	-5.298
	6.623	1.176	-1.870		6.623	-1.442	-4.974
	9.850	1.592	-1.935		9.850	-.648	-4.666
	13.023	1.889	-2.018		13.023	-.055	-4.391
	19.213	2.176	-2.176		19.213	.681	-3.905
	25.200	2.333	-2.333		25.200	1.215	-3.500
	30.997	2.429	-2.429		30.997	1.620	-3.240
	36.610	2.511	-2.511		36.610	1.944	-3.046
	42.050	2.541	-2.541		42.050	2.139	-2.900
	47.325	2.522	-2.522		47.325	2.268	-2.738
52.440	2.438	-2.438	52.440	2.285	-2.544		
57.404	2.304	-2.304	57.404	2.251	-2.333		
62.223	2.132	-2.132	62.223	2.132	-2.132		
66.903	1.931	-1.931	66.903	1.931	-1.931		
71.452	1.709	-1.709	71.452	1.709	-1.709		
75.872	1.468	-1.468	75.872	1.468	-1.468		
80.170	1.217	-1.217	80.170	1.217	-1.217		
84.352	.963	-.963	84.352	.963	-.963		
88.421	.715	-.715	88.421	.715	-.715		
92.384	.473	-.473	92.384	.473	-.473		
96.212	.238	-.238	96.212	.238	-.238		
100.000	.009	-.009	100.000	.009	-.009		
0.67 ^d	0	-2.192	-2.192	1.00 ^e	0	-4.942	-4.942
	.672	-1.134	-2.668		.672	-3.678	-5.541
	1.008	-.961	-2.700		1.008	-3.516	-5.597
	1.678	-.670	-2.689		1.678	-3.159	-5.509
	3.340	-.168	-2.603		3.340	-2.447	-5.298
	6.623	.724	-2.495		6.623	-1.442	-4.974
	9.850	1.296	-2.441		9.850	-.648	-4.666
	13.023	1.631	-2.405		13.023	-.055	-4.391
	19.213	2.084	-2.376		19.213	.681	-3.905
	25.200	2.322	-2.358		25.200	1.215	-3.500
	30.997	2.429	-2.441		30.997	1.620	-3.240
	36.610	2.511	-2.511		36.610	1.944	-3.046
	42.050	2.541	-2.541		42.050	2.139	-2.900
					47.325	2.268	-2.738
			52.440	2.285	-2.544		
			57.404	2.251	-2.333		
			62.223	2.132	-2.132		
			66.903	1.931	-1.931		
			71.452	1.709	-1.709		
			75.872	1.468	-1.468		
			80.170	1.217	-1.217		
			84.352	.963	-.963		
			88.421	.715	-.715		
			92.384	.473	-.473		
			96.212	.238	-.238		
			100.000	.009	-.009		

^aLeading-edge radius: 0.190 percent chord
^bLeading-edge radius: 0.236 percent chord
^cLeading-edge radius: 0.370 percent chord
^dLeading-edge radius: 0.520 percent chord
^eLeading-edge radius: 0.713 percent chord
^fLeading-edge radius: 0.924 percent chord

TABLE VII.- RANGE OF TEST VARIABLES AND INDEX OF TABULATED RESULTS.

Model	Transition	$R \times 10^{-6}$	M	Tabulated results, table
Plane triangular wing, 3 percent thick	Fixed	2.8	0.81, 0.90, 1.30, 1.70, 1.90	VIII(a)
		5.6	0.81, 0.90, 1.30, 1.70, 1.90	
		7.7	1.30	
		8.5	0.81, 0.90	
Plane triangular wing, 3 percent thick	Free	2.8	0.81, 0.90, 1.30, 1.70, 1.90	VIII(b)
		5.6	0.81, 0.90, 1.30, 1.70, 1.90	
		7.7	1.30	
		8.5	0.81, 0.90	
Plane triangular wing, 5 percent thick	Fixed	2.8	0.81, 0.90, 1.30	IX(a)
		5.6	0.81, 0.90, 1.30	
		7.7	1.30	
	Free	8.5	0.81, 0.90	IX(b)
		11.3	0.81, 0.90	
		2.8	0.81, 0.90, 1.30	
Triangular wing, 3 percent thick, cambered for $C_{L_d} = 0.215$ at $M = 1.0$	Fixed	5.6	0.61, 0.81, 0.90, 1.30, 1.70	X(a)
		7.5	1.90	
		11.3	0.81, 0.90	
	Free	5.6	0.61, 0.81, 0.90, 1.30, 1.70	X(b)
		7.5	1.90	
		11.3	0.81, 0.90	
Plane sweptback wing, 5 percent thick, with normal leading-edge	Fixed	2.9	0.60, 0.80, 0.90, 1.20, 1.30, 1.50, 1.70, 1.90	XI(a)
	Free	2.9	0.60, 0.80, 0.90, 1.20, 1.30, 1.50, 1.70, 1.90	XI(b)
Plane sweptback wing, 5 percent thick, with modified leading-edge	Fixed	3.0	0.22	XII(a)
		6.0	0.22	
		8.0	0.22	
	Free	2.9	0.60, 0.80, 0.90, 1.20, 1.30, 1.50, 1.70, 1.90	XII(b)
		3.0	0.22	
		3.8	0.60, 0.80, 0.90, 1.30	
Sweptback wing, 5 percent thick with modified lead- ing edge, cambered for $C_{L_d} = 0.225$ at $M = 1.0$	Fixed	2.9	0.60, 0.80, 0.90, 1.20, 1.30, 1.50, 1.70, 1.90	XIII(a)
		3.0	0.22	
		6.0	0.22	
	Free	2.9	0.60, 0.80, 0.90, 1.20, 1.30, 1.50, 1.70, 1.90	XIII(b)
		3.0	0.22	
		6.0	0.22	
Sweptback wing, 5 percent thick with normal lead- ing edge, cambered for $C_{L_d} = 0.292$ at $M = 1.0$	Fixed	2.9	0.60, 0.80, 0.90, 1.20, 1.30, 1.50, 1.70, 1.90	XIV(a)
	Free	2.9	0.60, 0.80, 0.90, 1.20, 1.30, 1.50, 1.70, 1.90	XIV(b)
Sweptback wing, 5 percent thick with modified lead- ing edge, cambered for $C_{L_d} = 0.292$ at $M = 1.0$	Fixed	2.9	0.60, 0.80, 0.90, 1.20, 1.30, 1.50, 1.70, 1.90	XV(a)
		3.0	0.22	
		6.0	0.22	
	Free	2.9	0.60, 0.80, 0.90, 1.20, 1.30, 1.50, 1.70, 1.90	XV(b)
		3.0	0.22	
		5.7	0.80, 0.90	
		6.0	0.22	
		8.0	0.22	

TABLE IX.- DATA FOR PLANE TRIANGULAR WING OF ASPECT RATIO 2, 5 PERCENT THICK
(a) Fixed transition

α	C_L	C_D	C_m	α	C_L	C_D	C_m	α	C_L	C_D	C_m	α	C_L	C_D	C_m
M = 0.81; R = 2.8x10 ⁶				M = 0.90; R = 2.8x10 ⁶				M = 1.30; R = 2.8x10 ⁶				M = 0.81; R = 5.6x10 ⁶			
-6.47	-0.316	0.0375	0.050	-6.50	-0.320	0.0392	0.053	-4.12	-0.189	0.0262	0.046	-6.69	-0.318	0.0376	0.051
-5.94	-.287	.0323	.046	-5.95	-.295	.0341	.050	-3.60	-.160	.0227	.038	-6.12	-.290	.0322	.046
-5.40	-.265	.0282	.042	-5.42	-.270	.0296	.046	-3.08	-.138	.0205	.033	-5.61	-.261	.0277	.041
-4.85	-.238	.0243	.038	-4.86	-.241	.0251	.041	-2.05	-.094	.0171	.021	-5.01	-.234	.0235	.036
-4.32	-.210	.0205	.033	-4.33	-.212	.0211	.035	-1.01	-.049	.0153	.010	-4.44	-.205	.0198	.032
-3.77	-.180	.0174	.028	-3.78	-.180	.0175	.029	-.49	-.027	.0149	.005	-3.89	-.181	.0171	.028
-3.22	-.156	.0150	.023	-3.23	-.156	.0150	.025	.56	.017	.0150	-.006	-3.33	-.153	.0147	.022
-2.16	-.103	.0117	.015	-2.17	-.105	.0116	.016	.99	.035	.0153	-.011	-2.22	-.105	.0117	.015
-1.05	-.054	.0102	.007	-1.07	-.054	.0098	.007	2.05	.089	.0173	-.023	-1.11	-.055	.0102	.007
-.56	-.032	.0098	.003	-.56	-.031	.0095	.003	3.08	.136	.0205	-.035	-.59	-.031	.0099	.003
.48	-.016	.0100	-.004	.48	-.017	.0096	-.005	3.59	.159	.0230	-.041	.50	.018	.0099	-.005
1.05	.051	.0103	-.008	1.03	.044	.0099	-.010	4.11	.183	.0257	-.047	1.07	.045	.0100	-.009
2.11	.091	.0118	-.016	2.14	.098	.0118	-.019	4.62	.205	.0288	-.053	2.19	.098	.0117	-.018
3.20	.143	.0151	-.025	3.23	.149	.0151	-.028	5.14	.230	.0325	-.059	3.31	.149	.0147	-.026
3.72	.167	.0172	-.029	3.76	.176	.0176	-.034	5.65	.253	.0365	-.064	3.87	.174	.0169	-.030
4.29	.195	.0198	-.034	4.31	.208	.0210	-.040	6.17	.277	.0409	-.070	4.42	.203	.0196	-.036
4.82	.222	.0232	-.039	4.86	.234	.0246	-.044	7.20	.324	.0514	-.082	4.98	.239	.0228	-.040
5.36	.248	.0269	-.043	5.40	.261	.0288	-.049					5.54	.258	.0268	-.045
5.91	.279	.0317	-.048	5.94	.288	.0335	-.054					6.09	.281	.0309	-.048
6.46	.308	.0370	-.053	6.49	.321	.0396	-.060					6.68	.317	.0372	-.055
7.55	.364	.0488	-.062	7.59	.381	.0533	-.071					7.80	.377	.0503	-.065
M = 0.90; R = 5.6x10 ⁶				M = 1.30; R = 5.6x10 ⁶				M = 1.30; R = 7.7x10 ⁶				M = 0.81; R = 8.5x10 ⁶			
-6.73	-.328	.0408	.054	-4.25	-.193	.0260	.047	-4.36	-.195	.0264	.047	-6.93	-.312	.0367	.049
-6.17	-.302	.0350	.050	-3.72	-.168	.0232	.040	-3.81	-.171	.0237	.041	-6.31	-.287	.0315	.045
-5.61	-.276	.0300	.047	-3.19	-.146	.0209	.035	-3.27	-.135	.0213	.035	-5.73	-.261	.0271	.041
-5.05	-.244	.0253	.042	-2.12	-.097	.0172	.022	-2.19	-.099	.0176	.023	-5.16	-.231	.0228	.037
-4.48	-.217	.0215	.036	-1.06	-.050	.0154	.011	-1.09	-.051	.0156	.011	-4.57	-.205	.0193	.031
-3.91	-.186	.0180	.031	-.52	-.027	.0149	.005	-.52	-.028	.0152	.005	-3.99	-.177	.0142	.026
-3.36	-.162	.0156	.026	.49	.020	.0150	-.006	.51	.020	.0152	-.006	-3.42	-.152	.0141	.022
-2.24	-.108	.0119	.016	1.05	.044	.0153	-.012	1.07	.046	.0157	-.012	-2.30	-.105	.0112	.015
-1.12	-.056	.0099	.007	2.11	.091	.0172	-.024	2.16	.095	.0176	-.024	-1.16	-.056	.0098	.007
-.59	-.031	.0096	.003	3.17	.140	.0206	-.036	3.25	.143	.0211	-.036	-.63	-.032	.0094	.003
.51	.019	.0096	-.005	3.70	.163	.0228	-.042	3.79	.167	.0234	-.042	.53	.020	.0095	-.005
1.09	.049	.0099	-.010	4.23	.187	.0256	-.048	4.35	.193	.0254	-.049	1.13	.049	.0098	-.009
2.32	.103	.0120	-.020	4.77	.212	.0289	-.054	4.89	.217	.0297	-.054	2.26	.099	.0114	-.017
3.33	.155	.0153	-.029	5.30	.236	.0326	-.060	5.44	.241	.0335	-.060	3.40	.148	.0142	-.025
3.69	.185	.0173	-.035	5.83	.260	.0367	-.066	5.99	.265	.0378	-.066	3.97	.174	.0164	-.030
4.46	.215	.0212	-.040	6.37	.285	.0415	-.072	6.53	.280	.0425	-.072	4.56	.202	.0192	-.035
5.02	.240	.0247	-.044	7.43	.331	.0518	-.083	7.62	.338	.0535	-.084	5.12	.228	.0225	-.039
5.59	.270	.0293	-.050									5.71	.256	.0263	-.044
6.15	.296	.0340	-.053									6.28	.281	.0306	-.047
6.73	.333	.0409	-.062									6.86	.311	.0363	-.052
7.67	.397	.0577	-.074									8.02	.369	.0496	-.059
α	C_L	C_D	C_m	α	C_L	C_D	C_m	α	C_L	C_D	C_m	α	C_L	C_D	C_m
M = 0.90; R = 8.5x10 ⁶				M = 0.81; R = 11.3x10 ⁶				M = 0.90; R = 11.3x10 ⁶							
-6.94	-0.326	0.0400	0.054	-7.13	-0.330	0.0403	0.052	-6.05	-0.288	0.0314	0.048				
-6.37	-.297	.0340	.048	-6.48	-.304	.0339	.049	-5.48	-.270	.0282	.047				
-5.78	-.270	.0288	.045	-5.93	-.272	.0267	.043	-4.86	-.241	.0233	.042				
-5.21	-.247	.0250	.042	-5.34	-.249	.0248	.039	-4.19	-.189	.0178	.032				
-4.62	-.216	.0208	.036	-4.77	-.223	.0266	.035	-3.63	-.173	.0154	.028				
-4.05	-.189	.0176	.031	-4.13	-.184	.0167	.028	-2.43	-.120	.0113	.019				
-3.46	-.160	.0147	.025	-3.55	-.164	.0147	.024	-1.24	-.065	.0092	.009				
-2.32	-.110	.0114	.017	-2.40	-.118	.0119	.017	-.65	-.039	.0086	.005				
-1.16	-.057	.0096	.008	-1.22	-.062	.0099	.008	.57	.027	.0089	-.007				
-.63	-.032	.0092	.004	-.66	-.036	.0095	.004	1.18	.056	.0093	-.012				
.54	.022	.0093	-.005	.54	.019	.0094	-.004	2.38	.112	.0114	-.022				
1.13	.051	.0096	-.010	1.16	.051	.0096	-.009	3.60	.172	.0156	-.032				
2.29	.103	.0115	-.019	2.34	.103	.0114	-.018	4.21	.204	.0187	-.038				
3.44	.156	.0149	-.029	3.52	.156	.0146	-.027	4.82	.232	.0225	-.044				
4.01	.185	.0175	-.034	4.11	.185	.0171	-.032	5.42	.262	.0269	-.049				
4.59	.212	.0204	-.039	4.71	.213	.0200	-.036	6.03	.290	.0320	-.053				
5.18	.241	.0244	-.044	5.26	.248	.0220	-.039	6.64	.321	.0377	-.059				
5.76	.270	.0290	-.049	5.90	.269	.0277	-.046								
6.34	.300	.0343	-.055	6.51	.302	.0333	-.051								
6.94	.328	.0402	-.059	7.13	.337	.0406	-.057								
8.11	.391	.0532	-.070	8.33	.391	.0551	-.064								

TABLE IX.- DATA FOR PLANE TRIANGULAR WING OF ASPECT RATIO 2, 5 PERCENT THICK - Concluded (b) Free transition

α	C_L	C_D	C_m	α	C_L	C_D	C_m	α	C_L	C_D	C_m	α	C_L	C_D	C_m
M = 0.81; R = 2.8x10 ⁶				M = 0.90; R = 2.8x10 ⁶				M = 1.30; R = 2.8x10 ⁶				M = 0.81; R = 5.6x10 ⁶			
-6.44	-0.310	0.0358	0.048	-6.47	-0.330	0.0392	0.056	-4.12	-0.188	0.0292	0.046	-6.62	-0.319	0.0364	0.050
-5.90	-.282	.0307	.044	-5.94	-.305	.0343	.052	-3.60	-.160	.0216	.039	-6.07	-.290	.0310	.045
-5.35	-.250	.0260	.038	-5.39	-.276	.0289	.047	-3.09	-.139	.0196	.033	-5.51	-.260	.0261	.040
-4.82	-.226	.0221	.034	-4.84	-.243	.0237	.040	-2.05	-.092	.0157	.021	-4.95	-.233	.0222	.035
-4.27	-.200	.0184	.030	-4.30	-.210	.0194	.034	-1.01	-.048	.0136	.010	-4.40	-.206	.0189	.031
-3.74	-.174	.0154	.026	-3.77	-.186	.0165	.030	-.50	-.026	.0132	.005	-3.85	-.180	.0160	.027
-3.20	-.148	.0129	.021	-3.22	-.159	.0136	.025	.48	.019	.0132	-.006	-3.30	-.154	.0136	.022
-2.13	-.098	.0094	.013	-2.14	-.103	.0095	.014	1.00	.044	.0141	-.012	-2.19	-.103	.0103	.014
-1.09	-.052	.0077	.006	-1.10	-.054	.0076	.006	2.04	.090	.0162	-.023	-1.10	-.053	.0080	.007
-.54	-.026	.0071	.002	-.56	-.031	.0071	.003	3.08	.137	.0201	-.035	-.57	-.029	.0074	.003
.47	.014	.0070	-.003	.48	.011	.0069	-.003	3.59	.161	.0225	-.041	.51	.018	.0073	-.004
1.02	.037	.0075	-.007	1.02	.038	.0072	-.007	4.11	.184	.0253	-.047	1.06	.044	.0078	-.008
2.09	.086	.0092	-.015	2.10	.088	.0091	-.016	4.62	.208	.0287	-.053	2.18	.094	-.004	-.016
3.18	.136	.0124	-.023	3.10	.144	.0130	-.026	5.14	.232	.0324	-.059	3.27	.147	.0132	-.025
3.71	.158	.0144	-.027	3.74	.172	.0157	-.032	5.66	.257	.0367	-.065	3.83	.173	.0155	-.029
4.26	.187	.0173	-.032	4.27	.201	.0188	-.037	6.18	.281	.0414	-.071	4.38	.200	.0189	-.034
4.79	.214	.0207	-.037	4.82	.225	.0224	-.041	7.21	.330	.0522	-.083	4.94	.227	.0215	-.039
5.33	.237	.0240	-.041	5.36	.255	.0269	-.047					5.49	.254	.0253	-.042
5.86	.267	.0289	-.046	5.91	.285	.0321	-.053					6.05	.281	.0298	-.047
6.41	.294	.0341	-.050	6.45	.319	.0383	-.060					6.61	.312	.0356	-.053
7.50	.358	.0468	-.061	7.53	.375	.0512	-.069					7.73	.372	.0489	-.062
M = 0.90; R = 5.6x10 ⁶				M = 1.30; R = 5.6x10 ⁶				M = 1.30; R = 7.7x10 ⁶				M = 0.81; R = 8.7x10 ⁶			
-6.66	-.332	.0396	.055	-4.26	-.194	.0261	.047	-4.37	-.198	.0259	.048	-6.82	-.325	.0378	.050
-6.11	-.303	.0337	.051	-3.72	-.169	.0232	.040	-3.81	-.173	.0229	.041	-6.24	-.298	.0317	.046
-5.54	-.275	.0287	.046	-3.19	-.145	.0206	.034	-3.28	-.149	.0205	.035	-5.66	-.264	.0266	.040
-4.98	-.239	.0232	.040	-2.13	-.098	.0170	.022	-2.19	-.101	.0169	.023	-5.10	-.238	.0226	.036
-4.42	-.214	.0198	.035	-1.06	-.051	.0146	.011	-1.10	-.051	.0146	.011	-4.52	-.210	.0200	.032
-3.87	-.187	.0168	.031	-.52	-.028	.0140	.005	-.55	-.029	.0141	.006	-3.96	-.184	.0158	.027
-3.32	-.160	.0142	.026	.49	.019	.0142	-.006	.51	.020	.0143	-.006	-3.39	-.156	.0136	.023
-2.21	-.107	.0101	.016	1.05	.045	.0149	-.012	1.07	.046	.0149	-.012	-2.27	-.107	.0105	.015
-1.11	-.056	.0077	.008	2.12	.094	.0171	-.024	2.17	.095	.0171	-.024	-1.14	-.055	.0087	.007
-.59	-.030	.0072	.004	3.17	.140	.0206	-.036	3.26	.145	.0207	-.037	-.55	-.028	.0082	.003
.50	.018	.0071	-.005	3.70	.164	.0231	-.042	3.80	.170	.0231	-.043	.53	.023	.0083	-.005
1.08	.045	.0076	-.009	4.24	.189	.0260	-.048	4.35	.194	.0261	-.049	1.12	.051	.0086	-.009
2.19	.100	.0100	-.019	4.77	.214	.0294	-.054	4.89	.220	.0295	-.055	2.24	.103	.0106	-.017
3.29	.154	.0139	-.028	5.31	.238	.0332	-.060	5.44	.243	.0334	-.061	3.37	.154	.0137	-.025
3.85	.181	.0165	-.033	5.84	.263	.0374	-.066	5.98	.267	.0377	-.067	3.94	.182	.0160	-.030
4.41	.212	.0199	-.039	6.38	.289	.0424	-.072	6.53	.292	.0426	-.073	4.51	.209	.0189	-.035
4.97	.240	.0234	-.044	7.44	.335	.0530	-.084	7.62	.339	.0535	-.084	5.09	.238	.0224	-.040
5.53	.267	.0280	-.048									5.65	.265	.0262	-.044
6.08	.298	.0328	-.054									6.23	.293	.0309	-.050
6.66	.330	.0397	-.060									6.79	.321	.0368	-.054
7.77	.390	.0531	-.070									7.95	.384	.0518	-.063
α	C_L	C_D	C_m	α	C_L	C_D	C_m	α	C_L	C_D	C_m	α	C_L	C_D	C_m
M = 0.90; R = 8.7x10 ⁶				M = 0.81; R = 11.3x10 ⁶				M = 0.90; R = 11.3x10 ⁶							
-6.88	-0.342	0.0411	0.057	-7.04	-0.339	0.0407	0.053	-7.18	-0.356	0.0439	0.059				
-6.30	-.310	.0346	.053	-6.42	-.294	.0324	.046	-6.55	-.316	.0353	.053				
-5.73	-.286	.0297	.048	-5.84	-.272	.0274	.042	-5.94	-.281	.0290	.046				
-5.15	-.255	.0249	.043	-5.27	-.250	.0238	.039	-5.33	-.252	.0245	.042				
-4.57	-.223	.0207	.036	-4.65	-.214	.0189	.032	-4.75	-.227	.0208	.037				
-4.01	-.195	.0173	.032	-4.08	-.186	.0156	.028	-4.16	-.200	.0172	.032				
-3.43	-.167	.0143	.027	-3.50	-.160	.0133	.024	-3.55	-.167	.0139	.026				
-2.88	-.112	.0105	.017	-2.35	-.111	.0103	.016	-2.38	-.114	.0103	.017				
-1.15	-.059	.0086	.008	-1.18	-.059	.0086	.007	-1.19	-.059	.0083	.006				
-.62	-.031	.0080	.003	-.63	-.031	.0082	.003	-.65	-.032	.0079	.003				
.53	.024	.0079	-.005	.57	.027	.0081	-.006	.58	.028	.0080	-.006				
1.12	.053	.0083	-.010	1.15	.055	.0086	-.010	1.18	.057	.0085	-.011				
2.26	.106	.0104	-.020	2.31	.106	.0103	-.018	2.35	.111	.0103	-.020				
3.41	.163	.0142	-.029	3.48	.161	.0136	-.028	3.53	.168	.0139	-.030				
3.98	.191	.0170	-.034	4.06	.187	.0159	-.032	4.14	.202	.0174	-.037				
4.56	.222	.0203	-.040	4.65	.217	.0191	-.037	4.74	.233	.0209	-.043				
5.15	.252	.0244	-.045	5.25	.250	.0232	-.043	5.34	.262	.0252	-.048				
5.71	.280	.0287	-.050	5.82	.272	.0267	-.046	5.94	.290	.0300	-.052				
6.29	.306	.0336	-.055	6.42	.304	.0329	-.052	6.53	.313	.0346	-.055				
6.87	.337	.0399	-.060	7.01	.332	.0392	-.056	7.16	.356	.0436	-.063				
8.03	.400	.0549	-.070	8.20	.392	.0532	-.064	8.38	.421	.0600	-.085				

TABLE X.- DATA FOR TRIANGULAR WING OF ASPECT RATIO 2, 3 PERCENT THICK,
CONICALLY CAMBERED FOR $C_{Ld} = 0.215$ AT $M = 1.0$
(a) Fixed transition

α	C_L	C_D	C_m	α	C_L	C_D	C_m	α	C_L	C_D	C_m	α	C_L	C_D	C_m
M = 0.61; R = 5.6x10 ⁶				M = 0.81; R = 5.6x10 ⁶				M = 0.90; R = 5.6x10 ⁶				M = 1.30; R = 5.6x10 ⁶			
-6.65	-0.345	0.0563	0.051	-6.80	-0.383	0.0631	0.065	-6.89	-0.417	0.0695	0.083	-6.42	-0.330	0.0567	0.085
-6.10	-.319	.0502	.047	-6.23	-.352	.0557	.061	-6.31	-.383	.0610	.075	-5.88	-.304	.0507	.078
-5.54	-.291	.0444	.044	-5.66	-.321	.0491	.055	-5.73	-.346	.0531	.068	-5.35	-.280	.0454	.072
-4.99	-.265	.0392	.040	-5.10	-.292	.0430	.051	-5.16	-.312	.0462	.061	-4.81	-.253	.0403	.065
-4.44	-.239	.0345	.036	-4.53	-.263	.0376	.045	-4.59	-.284	.0405	.056	-4.28	-.230	.0360	.059
-3.88	-.213	.0303	.032	-3.97	-.232	.0325	.041	-4.02	-.249	.0347	.049	-3.75	-.205	.0319	.053
-3.33	-.185	.0263	.029	-3.40	-.201	.0281	.036	-3.44	-.216	.0298	.042	-3.21	-.180	.0282	.046
-2.78	-.160	.0231	.026	-2.85	-.177	.0245	.031	-2.88	-.186	.0256	.037	-2.68	-.154	.0249	.040
-2.23	-.136	.0202	.022	-2.28	-.147	.0211	.027	-2.31	-.156	.0219	.031	-2.14	-.130	.0223	.034
-1.13	-.085	.0155	.014	-1.16	-.089	.0157	.017	-1.17	-.093	.0160	.019	-1.06	-.074	.0175	.020
-.58	-.059	.0138	.011	-.60	-.062	.0138	.013	-.60	-.062	.0138	.014	-.53	-.049	.0160	.014
-.29	-.044	.0130	.009	-.31	-.048	.0131	.011	-.31	-.045	.0130	.011	-.26	-.034	.0153	.010
-.01	-.032	.0124	.007	-.03	-.036	.0124	.008	-.02	-.033	.0124	.008	.02	-.023	.0148	.008
.20	-.023	.0120	.006	.20	-.021	.0119	.007	.21	-.018	.0118	.006	.23	-.012	.0145	.005
.48	-.010	.0114	.004	.49	-.006	.0113	.004	.50	-.004	.0113	.003	.51	.003	.0142	.001
1.03	.010	.0110	.001	1.05	.016	.0110	0	1.06	.017	.0110	-.001	.98	.016	.0139	-.002
2.15	.061	.0107	-.007	2.13	.070	.0107	-.009	2.14	.072	.0110	-.009	2.07	.066	.0142	-.015
2.65	.089	.0110	-.011	2.69	.096	.0112	-.013	2.71	.101	.0116	-.015	2.60	.091	.0150	-.021
3.19	.111	.0114	-.014	3.24	.123	.0119	-.017	3.26	.127	.0123	-.019	3.13	.116	.0161	-.028
3.73	.132	.0120	-.017	3.80	.147	.0127	-.022	3.82	.153	.0132	-.024	3.67	.139	.0173	-.033
4.28	.156	.0131	-.021	4.35	.171	.0137	-.025	4.38	.180	.0146	-.029	4.20	.165	.0192	-.040
4.82	.177	.0146	-.023	4.89	.192	.0158	-.029	4.94	.205	.0165	-.033	4.74	.191	.0214	-.047
5.36	.198	.0166	-.027	5.44	.215	.0174	-.032	5.50	.233	.0186	-.038	5.27	.217	.0240	-.052
5.91	.223	.0184	-.030	6.01	.243	.0199	-.037	6.06	.260	.0212	-.043	5.81	.242	.0269	-.059
6.45	.243	.0203	-.033	6.56	.266	.0222	-.040	6.63	.288	.0243	-.048	6.34	.267	.0305	-.065
7.00	.262	.0263	-.040	7.07	.320	.0297	-.049	7.15	.344	.0325	-.058	7.41	.316	.0321	-.078
8.65	.345	.0358	-.048	8.81	.384	.0427	-.060	8.91	.414	.0470	-.070	8.48	.371	.0506	-.092
10.89	.464	.0681	-.064	13.36	.617	.1276	-.088	11.28	.598	.1018	-.121	10.81	.468	.0809	-.117
13.14	.580	.1117	-.075	15.65	.747	.1877	-.112					13.00	.566	.1196	-.142
15.37	.691	.1629	-.085												
17.64	.816	.2278	-.102												
18.76	.871	.2617	-.108												
α	C_L	C_D	C_m	α	C_L	C_D	C_m	α	C_L	C_D	C_m	α	C_L	C_D	C_m
M = 1.70; R = 5.6x10 ⁶				M = 1.90; R = 5.6x10 ⁶											
-6.36	-.264	.0478	.066	-6.30	-.232	.0430	.056								
-5.83	-.244	.0431	.062	-5.78	-.215	.0390	.052								
-5.29	-.224	.0388	.057	-5.25	-.198	.0355	.049								
-4.77	-.205	.0351	.053	-4.73	-.181	.0322	.044								
-4.24	-.186	.0316	.048	-4.20	-.164	.0290	.041								
-3.71	-.166	.0284	.042	-3.68	-.146	.0262	.037								
-3.17	-.144	.0253	.037	-3.15	-.128	.0236	.032								
-2.64	-.123	.0228	.032	-2.62	-.111	.0214	.028								
-2.11	-.103	.0205	.027	-2.10	-.093	.0194	.024								
-1.05	-.059	.0168	.017	-1.04	-.074	.0161	.015								
-.52	-.038	.0156	.011	-.51	-.055	.0149	.010								
-.25	-.028	.0150	.008	-.24	-.027	.0145	.007								
-.004	-.031	.0152	.009	0	-.029	.0145	.006								
.02	-.019	.0147	.007	.03	-.018	.0142	.006								
.24	-.007	.0145	.003	.24	-.009	.0140	.004								
.49	-.006	.0145	.003	.51	0	.0138	.001								
.98	.014	.0143	-.002	1.03	.010	.0137	-.002								
2.05	.054	.0148	-.012	2.04	.048	.0144	-.010								
2.59	.076	.0156	-.017	2.57	.066	.0151	-.015								
3.11	.096	.0167	-.023	3.09	.083	.0161	-.019								
3.64	.117	.0181	-.029	3.62	.102	.0175	-.024								
4.17	.137	.0199	-.033	4.14	.118	.0190	-.027								
4.70	.157	.0219	-.039	4.67	.136	.0207	-.032								
5.23	.179	.0245	-.043	5.19	.153	.0229	-.036								
5.76	.199	.0273	-.049	5.72	.172	.0254	-.040								
6.30	.221	.0305	-.054	6.25	.191	.0282	-.045								
7.36	.261	.0378	-.064	7.30	.226	.0347	-.053								
8.42	.303	.0470	-.075	8.36	.263	.0428	-.062								
10.70	.381	.0704	-.093	10.47	.334	.0626	-.078								
12.85	.455	.0989	-.110	12.57	.400	.0867	-.093								
				16.97	.530	.1543	-.113								

TABLE XI.- DATA FOR PLANE WING OF ASPECT RATIO 3 WITH 45° SWEEPBACK,
5 PERCENT THICK WITH NORMAL LEADING EDGE
(a) Fixed transition

α	C_L	C_D	C_m	α	C_L	C_D	C_m	α	C_L	C_D	C_m	α	C_L	C_D	C_m
K = 0.60; R = 2.9x10 ⁶				K = 0.80; R = 2.9x10 ⁶				K = 0.90; R = 2.9x10 ⁶				K = 1.20; R = 2.9x10 ⁶			
-6.74	-0.429	0.0514	0.013	-6.90	-0.480	0.0588	0.023	-5.90	-0.468	0.0495	0.045	-6.60	-0.475	0.0663	0.098
-6.20	-0.396	0.0438	0.011	-6.34	-0.443	0.0500	0.022	-5.33	-0.422	0.0405	0.036	-6.06	-0.437	0.0587	0.089
-5.65	-0.356	0.0360	0.008	-5.79	-0.406	0.0421	0.019	-4.75	-0.371	0.0327	0.028	-5.52	-0.394	0.0515	0.079
-5.10	-0.319	0.0293	0.006	-5.22	-0.361	0.0341	0.015	-4.18	-0.321	0.0267	0.020	-4.98	-0.355	0.0457	0.070
-4.55	-0.281	0.0240	0.004	-4.66	-0.316	0.0273	0.010	-3.61	-0.271	0.0219	0.014	-4.44	-0.315	0.0400	0.061
-4.01	-0.250	0.0202	0.004	-4.10	-0.276	0.0224	0.007	-3.04	-0.228	0.0186	0.011	-3.90	-0.278	0.0356	0.053
-3.46	-0.211	0.0173	0.002	-3.54	-0.236	0.0188	0.006	-2.47	-0.183	0.0157	0.008	-3.36	-0.241	0.0315	0.045
-2.91	-0.177	0.0156	0.001	-2.98	-0.198	0.0164	0.004	-1.93	-0.103	0.0124	0.004	-2.82	-0.166	0.0254	0.031
-2.37	-0.147	0.0143	0.001	-2.43	-0.163	0.0144	0.003	-1.38	-0.058	0.0115	0.002	-1.20	-0.092	0.0217	0.016
-1.82	-0.083	0.0121	0	-1.33	-0.095	0.0120	0.002	-0.86	-0.027	0.0111	-0.001	-0.65	-0.052	0.0208	0.009
-0.72	-0.046	0.0114	-0.001	-0.75	-0.055	0.0112	0	-0.33	0.004	0.0112	-0.003	-0.37	-0.035	0.0205	0.006
-0.45	-0.028	0.0113	-0.002	-0.46	-0.031	0.0110	-0.001	0.11	0.032	0.0112	-0.004	0.02	0.002	0.0203	0.002
0.02	0.002	0.0112	-0.003	0.02	0.001	0.0109	-0.003	0.99	0.075	0.0123	-0.007	0.31	0.025	0.0204	-0.006
0.30	0.022	0.0112	-0.003	0.96	0.063	0.0120	-0.004	2.13	0.164	0.0150	-0.012	0.86	0.061	0.0213	-0.013
0.93	0.093	0.0114	-0.003	2.09	0.144	0.0141	-0.007	2.70	0.207	0.0171	-0.015	1.99	0.137	0.0238	-0.027
2.04	0.121	0.0136	-0.005	2.65	0.180	0.0155	-0.008	3.27	0.251	0.0202	-0.019	2.49	0.174	0.0258	-0.034
2.58	0.154	0.0148	-0.006	3.20	0.215	0.0177	-0.010	3.85	0.302	0.0246	-0.027	3.03	0.212	0.0284	-0.042
3.12	0.187	0.0163	-0.006	3.76	0.256	0.0207	-0.012	4.41	0.350	0.0295	-0.033	3.57	0.249	0.0316	-0.049
3.67	0.224	0.0188	-0.008	4.32	0.297	0.0250	-0.015	4.99	0.397	0.0361	-0.040	4.11	0.287	0.0356	-0.057
4.22	0.258	0.0220	-0.009	4.89	0.341	0.0307	-0.019	5.56	0.447	0.0449	-0.051	4.65	0.325	0.0399	-0.066
4.77	0.295	0.0264	-0.011	5.45	0.381	0.0374	-0.022	6.12	0.485	0.0539	-0.055	5.19	0.363	0.0452	-0.074
5.31	0.332	0.0321	-0.012	6.00	0.420	0.0450	-0.025	6.67	0.521	0.0640	-0.060	5.73	0.403	0.0514	-0.084
5.87	0.373	0.0383	-0.015	6.56	0.455	0.0521	-0.027	7.77	0.584	0.0745	-0.065	6.27	0.443	0.0583	-0.093
6.42	0.411	0.0457	-0.018	7.66	0.523	0.0702	-0.028	8.85	0.630	0.1049	-0.065	7.36	0.527	0.0753	-0.112
7.51	0.479	0.0611	-0.020	8.74	0.586	0.0886	-0.026	11.02	0.735	0.1518	-0.074	8.44	0.605	0.0945	-0.129
8.59	0.544	0.0790	-0.019	10.89	0.670	0.1319	-0.035	12.11	0.797	0.1815	-0.082				
10.72	0.630	0.1162	-0.015	13.01	0.747	0.1777	-0.037								
12.85	0.732	0.1640	-0.020	15.10	0.800	0.2239	-0.044								
14.95	0.803	0.2123	-0.021	17.18	0.851	0.2737	-0.058								
17.01	0.842	0.2594	-0.032	18.21	0.875	0.3005	-0.068								
18.02	0.854	0.2840	-0.045												
K = 1.30; R = 2.9x10 ⁶				K = 1.50; R = 2.9x10 ⁶				K = 1.70; R = 2.9x10 ⁶				K = 1.90; R = 2.9x10 ⁶			
-6.02	-0.389	0.0577	0.081	-6.46	-0.347	0.0575	0.075	-6.45	-0.303	0.0537	0.063	-6.42	-0.266	0.0498	0.054
-5.49	-0.354	0.0516	0.074	-5.93	-0.321	0.0520	0.069	-5.92	-0.279	0.0488	0.058	-5.89	-0.244	0.0454	0.050
-4.95	-0.318	0.0457	0.066	-5.40	-0.293	0.0469	0.062	-5.40	-0.257	0.0444	0.053	-5.37	-0.223	0.0414	0.045
-4.41	-0.286	0.0409	0.058	-4.87	-0.265	0.0422	0.056	-4.87	-0.232	0.0402	0.048	-4.85	-0.204	0.0379	0.041
-3.88	-0.252	0.0365	0.051	-4.34	-0.237	0.0379	0.049	-4.34	-0.209	0.0366	0.043	-4.32	-0.183	0.0347	0.037
-3.34	-0.217	0.0328	0.043	-3.82	-0.211	0.0345	0.044	-3.81	-0.182	0.0332	0.037	-3.80	-0.162	0.0319	0.033
-2.26	-0.149	0.0270	0.029	-3.28	-0.183	0.0313	0.038	-3.28	-0.159	0.0304	0.032	-3.27	-0.140	0.0293	0.028
-1.19	-0.081	0.0235	0.015	-2.22	-0.126	0.0263	0.025	-2.23	-0.109	0.0260	0.022	-2.23	-0.096	0.0254	0.019
-0.65	-0.048	0.0225	0.008	-1.16	-0.067	0.0232	0.013	-1.16	-0.058	0.0232	0.014	-1.17	-0.053	0.0230	0.010
-0.37	-0.029	0.0222	0.005	-0.60	-0.037	0.0222	0.007	-0.62	-0.033	0.0225	0.006	-0.64	-0.031	0.0224	0.006
0.02	0.003	0.0221	-0.002	-0.39	-0.021	0.0219	0.003	-0.34	-0.018	0.0224	0.003	-0.37	-0.020	0.0222	0.003
0.30	0.022	0.0221	-0.005	0.07	0.003	0.0219	-0.002	0.02	0.002	0.0224	-0.001	0.04	0.002	0.0221	-0.001
0.86	0.057	0.0231	-0.013	0.34	0.020	0.0220	-0.005	0.30	0.018	0.0226	-0.005	0.30	0.012	0.0222	-0.003
1.93	0.124	0.0258	-0.026	0.88	0.051	0.0231	-0.012	0.84	0.043	0.0235	-0.010	0.85	0.033	0.0231	-0.007
2.47	0.159	0.0278	-0.033	1.96	0.108	0.0257	-0.024	1.91	0.093	0.0257	-0.021	1.91	0.076	0.0249	-0.022
3.01	0.193	0.0303	-0.041	2.49	0.137	0.0276	-0.030	2.43	0.118	0.0274	-0.026	2.44	0.099	0.0265	-0.020
3.54	0.225	0.0333	-0.047	3.02	0.164	0.0298	-0.036	2.96	0.141	0.0292	-0.030	2.95	0.122	0.0283	-0.025
4.08	0.260	0.0373	-0.055	3.62	0.193	0.0328	-0.042	3.49	0.167	0.0318	-0.036	3.47	0.142	0.0305	-0.029
4.62	0.293	0.0413	-0.062	4.09	0.221	0.0358	-0.048	4.02	0.190	0.0345	-0.041	4.00	0.162	0.0329	-0.033
5.15	0.326	0.0462	-0.070	4.61	0.247	0.0394	-0.054	4.55	0.215	0.0378	-0.046	4.52	0.184	0.0359	-0.038
5.69	0.359	0.0516	-0.078	5.14	0.276	0.0436	-0.060	5.07	0.239	0.0415	-0.051	5.05	0.205	0.0392	-0.042
6.23	0.393	0.0579	-0.085	5.67	0.304	0.0484	-0.067	5.60	0.264	0.0456	-0.056	5.57	0.225	0.0426	-0.046
7.30	0.458	0.0720	-0.100	6.20	0.333	0.0539	-0.073	6.13	0.286	0.0500	-0.061	6.10	0.247	0.0469	-0.051
8.36	0.519	0.0875	-0.113	7.25	0.386	0.0634	-0.085	7.18	0.333	0.0602	-0.071	7.14	0.288	0.0557	-0.060
10.50	0.639	0.1297	-0.139	8.31	0.439	0.0791	-0.097	8.24	0.379	0.0721	-0.081	8.18	0.330	0.0662	-0.068
12.63	0.751	0.1715	-0.161	10.42	0.543	0.1118	-0.119	10.35	0.470	0.1004	-0.100	10.28	0.410	0.0912	-0.085
				12.54	0.640	0.1509	-0.140	12.45	0.558	0.1349	-0.118	12.38	0.489	0.1223	-0.101
				14.65	0.735	0.1968	-0.160	14.56	0.642	0.1753	-0.136	14.46	0.566	0.1580	-0.116
				16.02	0.795	0.2302	-0.171	16.07	0.726	0.2226	-0.152	16.07	0.641	0.2005	-0.128
												17.62	0.676	0.2231	-0.134

TABLE XI.- DATA FOR PLANE WING OF ASPECT RATIO 3 WITH 45° SWEEPBACK,
5 PERCENT THICK WITH NORMAL LEADING EDGE
(b) Free transition

α	C_L	C_D	C_m	α	C_L	C_D	C_m	α	C_L	C_D	C_m	α	C_L	C_D	C_m
M = 0.60; R = 2.9×10^6				M = 0.80; R = 2.9×10^6				M = 0.90; R = 2.9×10^6				M = 1.20; R = 2.9×10^6			
-6.74	-0.430	0.0497	0.013	-6.89	-0.478	0.0583	0.023	-7.01	-0.545	0.0687	0.055	-6.61	-0.472	0.0547	0.100
-6.20	-0.399	0.0428	0.012	-6.34	-0.445	0.0500	0.022	-6.45	-0.511	0.0588	0.051	-6.07	-0.432	0.0569	0.090
-5.64	-0.355	0.0347	0.008	-5.78	-0.405	0.0417	0.019	-5.90	-0.471	0.0488	0.044	-5.53	-0.394	0.0499	0.080
-5.10	-0.319	0.0290	0.007	-5.22	-0.363	0.0341	0.015	-5.33	-0.426	0.0400	0.036	-4.96	-0.349	0.0434	0.070
-4.55	-0.282	0.0231	0.005	-4.66	-0.320	0.0271	0.011	-4.76	-0.374	0.0323	0.027	-4.44	-0.313	0.0382	0.061
-4.00	-0.245	0.0186	0.003	-4.10	-0.281	0.0219	0.008	-4.17	-0.319	0.0250	0.018	-3.90	-0.272	0.0332	0.052
-3.46	-0.216	0.0159	0.003	-3.54	-0.239	0.0177	0.006	-3.60	-0.272	0.0202	0.014	-3.36	-0.234	0.0289	0.044
-2.92	-0.179	0.0137	0.001	-2.98	-0.200	0.0147	0.004	-3.03	-0.223	0.0163	0.009	-2.82	-0.196	0.0254	0.036
-2.37	-0.145	0.0117	0	-2.42	-0.160	0.0122	0.002	-2.46	-0.177	0.0130	0.005	-2.28	-0.161	0.0222	0.030
-1.83	-0.079	0.0085	-0.002	-1.31	-0.084	0.0061	-0.002	-1.34	-0.100	0.0085	0.001	-1.19	-0.084	0.0176	0.014
-1.72	-0.044	0.0072	-0.002	-0.75	-0.053	0.0058	-0.001	-0.77	-0.060	0.0070	0.001	-0.72	-0.046	0.0164	0.006
-1.50	-0.043	0.0067	-0.003	-0.47	-0.036	0.0066	-0.001	-0.46	-0.030	0.0066	-0.001	-0.45	-0.028	0.0161	0.003
-1.45	-0.032	0.0070	-0.001	0.02	-0.002	0.0062	-0.002	0.02	0	0.0065	-0.002	0.02	0	0.0158	-0.001
0.02	-0.001	0.0067	-0.003	0.38	0.019	0.0062	-0.002	0.40	0.028	0.0066	-0.003	0.30	0.022	0.0160	-0.005
0.38	0.018	0.0067	-0.002	0.96	0.062	0.0073	-0.003	0.99	0.075	0.0078	-0.005	0.86	0.058	0.0172	-0.012
0.94	0.056	0.0068	-0.002	2.08	0.133	0.0105	-0.005	2.12	0.156	0.0116	-0.009	1.95	0.138	0.0202	-0.028
2.03	0.116	0.0101	-0.003	2.64	0.174	0.0127	-0.007	2.70	0.207	0.0148	-0.014	2.49	0.172	0.0231	-0.035
2.58	0.153	0.0119	-0.005	3.20	0.214	0.0153	-0.010	3.27	0.251	0.0181	-0.019	3.03	0.208	0.0263	-0.042
3.12	0.183	0.0136	-0.006	3.75	0.252	0.0184	-0.011	3.83	0.295	0.0221	-0.024	3.57	0.245	0.0301	-0.049
3.66	0.218	0.0162	-0.007	4.32	0.297	0.0236	-0.015	4.40	0.344	0.0280	-0.030	4.11	0.283	0.0344	-0.058
4.21	0.257	0.0200	-0.009	4.88	0.337	0.0287	-0.018	4.98	0.396	0.0346	-0.039	4.65	0.321	0.0390	-0.066
4.76	0.293	0.0243	-0.010	5.44	0.378	0.0355	-0.022	5.56	0.453	0.0411	-0.052	5.19	0.362	0.0448	-0.076
5.31	0.334	0.0303	-0.012	6.00	0.424	0.0436	-0.026	6.11	0.487	0.0524	-0.055	5.73	0.401	0.0512	-0.085
5.85	0.374	0.0369	-0.015	6.56	0.460	0.0517	-0.027	6.67	0.526	0.0630	-0.059	6.28	0.443	0.0585	-0.095
6.41	0.411	0.0439	-0.018	7.12	0.506	0.0609	-0.028	7.24	0.584	0.0733	-0.062	7.36	0.526	0.0758	-0.115
7.51	0.485	0.0601	-0.021	8.74	0.581	0.0881	-0.028	8.85	0.657	0.1049	-0.066	8.45	0.607	0.0955	-0.132
8.59	0.547	0.0774	-0.021	10.89	0.680	0.1319	-0.037	11.02	0.744	0.1529	-0.076				
10.71	0.636	0.1152	-0.015	13.01	0.751	0.1770	-0.037	13.18	0.853	0.2098	-0.091				
12.86	0.746	0.1652	-0.021	15.09	0.805	0.2234	-0.044								
14.95	0.809	0.2125	-0.022	17.17	0.857	0.2742	-0.059								
17.01	0.854	0.2617	-0.034												
18.02	0.861	0.2855	-0.047												
M = 1.30; R = 2.9×10^6				M = 1.50; R = 2.9×10^6				M = 1.70; R = 2.9×10^6				M = 1.90; R = 2.9×10^6			
-6.57	-0.415	0.0527	0.090	-6.50	-0.346	0.0558	0.075	-6.45	-0.299	0.0519	0.062	-6.40	-0.262	0.0480	0.054
-6.03	-0.382	0.0559	0.082	-5.97	-0.318	0.0501	0.068	-5.92	-0.275	0.0469	0.057	-5.88	-0.243	0.0437	0.050
-5.49	-0.347	0.0496	0.074	-5.44	-0.293	0.0449	0.062	-5.39	-0.251	0.0422	0.052	-5.35	-0.221	0.0395	0.045
-4.95	-0.313	0.0438	0.066	-4.91	-0.263	0.0399	0.056	-4.87	-0.228	0.0380	0.047	-4.83	-0.201	0.0359	0.041
-4.42	-0.279	0.0386	0.058	-4.38	-0.235	0.0354	0.049	-4.34	-0.204	0.0342	0.042	-4.30	-0.178	0.0324	0.036
-3.88	-0.247	0.0342	0.050	-3.85	-0.208	0.0314	0.043	-3.81	-0.179	0.0306	0.037	-3.78	-0.159	0.0297	0.032
-3.34	-0.214	0.0302	0.043	-3.31	-0.180	0.0279	0.037	-3.28	-0.156	0.0277	0.032	-3.25	-0.136	0.0269	0.028
-2.81	-0.180	0.0264	0.035	-2.78	-0.152	0.0248	0.031	-2.76	-0.133	0.0251	0.027	-2.73	-0.116	0.0247	0.023
-2.27	-0.146	0.0230	0.028	-2.25	0	0	0.013	-2.23	-0.108	0.0229	0.022	-2.21	-0.094	0.0229	0.019
-1.79	-0.077	0.0188	0.013	-1.18	-0.066	0.0184	0.012	-1.16	-0.056	0.0196	0.011	-1.15	-0.049	0.0201	0.010
-1.72	-0.041	0.0177	0.006	-0.63	-0.036	0.0173	0.006	-0.62	-0.030	0.0186	0.006	-0.61	-0.026	0.0193	0.005
-1.44	-0.025	0.0173	0.003	-0.43	-0.020	0.0170	0.003	-0.42	-0.009	0.0183	0.001	-0.34	-0.015	0.0191	0.003
0.02	0.001	0.0171	-0.001	0.03	0.004	0.0173	-0.002	0.02	0.003	0.0182	-0.002	0.02	0.001	0.0190	-0.001
0.30	0.021	0.0172	-0.005	0.30	0.018	0.0174	-0.005	0.30	0.017	0.0183	-0.005	0.29	0.014	0.0190	-0.004
0.85	0.053	0.0185	-0.011	0.85	0.047	0.0185	-0.011	0.84	0.043	0.0194	-0.010	0.82	0.034	0.0200	-0.008
1.94	0.125	0.0217	-0.026	1.92	0.107	0.0212	-0.023	1.91	0.094	0.0220	-0.021	1.89	0.081	0.0221	-0.018
2.47	0.158	0.0242	-0.033	2.46	0.136	0.0234	-0.029	2.44	0.118	0.0238	-0.026	2.42	0.102	0.0238	-0.022
3.01	0.191	0.0276	-0.041	2.99	0.162	0.0258	-0.035	2.97	0.143	0.0262	-0.031	2.94	0.123	0.0257	-0.026
3.55	0.223	0.0311	-0.048	3.52	0.191	0.0289	-0.041	3.49	0.167	0.0287	-0.036	3.46	0.144	0.0280	-0.031
4.09	0.257	0.0353	-0.055	4.06	0.219	0.0325	-0.047	4.02	0.190	0.0317	-0.040	3.99	0.165	0.0306	-0.035
5.16	0.325	0.0451	-0.071	4.59	0.245	0.0364	-0.054	4.55	0.212	0.0351	-0.045	4.51	0.186	0.0337	-0.039
5.70	0.359	0.0509	-0.079	5.12	0.275	0.0412	-0.060	5.08	0.237	0.0390	-0.051	5.04	0.207	0.0370	-0.044
6.24	0.392	0.0573	-0.087	5.65	0.302	0.0458	-0.066	5.61	0.261	0.0433	-0.056	5.56	0.228	0.0407	-0.048
7.31	0.456	0.0715	-0.102	6.18	0.330	0.0513	-0.073	6.13	0.286	0.0480	-0.061	6.08	0.250	0.0448	-0.053
8.38	0.519	0.0878	-0.116	7.25	0.386	0.0636	-0.085	7.19	0.330	0.0582	-0.070	7.13	0.292	0.0445	-0.052
10.52	0.638	0.1267	-0.143	8.31	0.438	0.0772	-0.097	8.24	0.377	0.0703	-0.080	8.18	0.334	0.0533	-0.070
12.65	0.750	0.1729	-0.166	10.44	0.542	0.1104	-0.121	10.36	0.469	0.0995	-0.100	10.28	0.415	0.0908	-0.087
				12.56	0.638	0.1496	-0.142	12.46	0.554	0.1338	-0.119	12.38	0.493	0.1218	-0.102
				14.68	0.734	0.1962	-0.162	14.57	0.639	0.1747	-0.136	14.48	0.568	0.1582	-0.116
								16.68	0.718	0.2210	-0.149	16.58	0.641	0.2001	-0.127
												17.62	0.677	0.2233	-0.134

TABLE XII.- DATA FOR PLANE WING OF ASPECT RATIO 3 WITH 45° SWEEPBACK,
5 PERCENT THICK WITH MODIFIED LEADING EDGE
(a) Fixed transition

α	C_L	C_D	C_m	α	C_L	C_D	C_m	α	C_L	C_D	C_m
M = 0.22; R = 3.0×10^6				M = 0.22; R = 6.0×10^6				M = 0.22; R = 8.0×10^6			
-3.84	-0.212	0.0158	0.001	-3.66	-0.197	0.0156	0.002	-3.91	-0.224	0.0150	0.003
-3.52	-.186	.0156	.001	-3.10	-.167	.0141	.001	-3.71	-.201	.0157	.003
-2.98	-.157	.0138	0	-2.49	-.138	.0132	.001	-3.10	-.171	.0140	.002
-2.41	-.130	.0121	-.001	-1.95	-.108	.0117	0	-2.58	-.140	.0127	.001
-1.90	-.099	.0115	-.001	-1.46	-.079	.0111	0	-1.98	-.110	.0114	.001
-1.42	-.070	.0121	-.002	-.95	-.050	.0108	-.001	-1.46	-.082	.0108	.001
-.88	-.045	.0111	-.001	.37	-.021	.0102	-.001	-1.11	-.053	.0106	0
-.37	-.014	.0108	-.002	.17	-.004	.0100	-.001	-.34	-.025	.0099	0
.14	.011	.0106	-.001	.72	.037	.0103	-.001	.17	.001	.0098	-.001
.55	.042	.0114	-.001	1.16	.062	.0107	-.002	.21	.007	.0101	-.001
1.15	.068	.0110	-.001	1.75	.096	.0113	-.002	.72	.038	.0099	-.001
1.63	.101	.0116	-.002	2.41	.131	.0124	-.002	1.23	.065	.0103	-.002
2.11	.129	.0124	-.003	2.96	.166	.0136	-.003	1.87	.099	.0111	-.002
2.65	.162	.0139	-.003	3.60	.194	.0149	-.004	2.51	.134	.0120	-.002
3.35	.194	.0152	-.004	4.18	.224	.0163	-.004	3.03	.165	.0132	-.003
3.76	.225	.0168	-.005	4.66	.253	.0178	-.005	3.66	.196	.0145	-.004
4.43	.225	.0188	-.006	5.23	.284	.0196	-.006	4.25	.226	.0158	-.004
5.06	.286	.0220	-.006	5.70	.311	.0216	-.007	4.76	.255	.0173	-.005
5.57	.319	.0264	-.006	6.32	.340	.0239	-.008	5.30	.284	.0191	-.006
6.00	.349	.0304	-.007	6.84	.369	.0266	-.009	5.85	.312	.0214	-.007
6.63	.377	.0351	-.008	7.87	.428	.0336	-.011	6.35	.341	.0233	-.008
7.59	.450	.0505	-.011	8.83	.485	.0434	-.014	6.97	.371	.0260	-.009
8.51	.507	.0645	-.013	9.99	.553	.0611	-.016	7.93	.432	.0313	-.012
9.62	.571	.0836	-.014	11.01	.618	.0899	-.016	8.99	.490	.0387	-.014
10.65	.618	.1002	-.014	12.11	.681	.1167	-.017	10.11	.556	.0541	-.017
11.67	.674	.1210	-.016	13.16	.732	.1411	-.017	11.14	.616	.0755	-.019
12.68	.716	.1433	-.011	15.11	.803	.1885	-.008	12.23	.680	.1131	-.016
14.66	.794	.1890	-.011	17.19	.859	.2403	-.014	13.32	.718	.1384	-.012
16.74	.865	.2413	-.015	19.20	.908	.2926	-.018	15.63	.786	.1889	-.008
18.75	.904	.2913	-.019	21.05	.938	.3490	-.047	17.32	.858	.2388	-.014
20.66	.922	.3431	-.048	23.08	.950	.3948	-.054	19.39	.913	.2949	-.018
22.64	.946	.3918	-.054					21.14	.934	.3510	-.050
24.65	.948	.4320	-.055								

TABLE XII.- DATA FOR PLANE WING OF ASPECT RATIO 3 WITH 45° SWEEPBACK,
5 PERCENT THICK WITH MODIFIED LEADING EDGE - Continued
(b) Free transition

M = 0.60; R = 2.9x10 ⁶				M = 0.80; R = 2.9x10 ⁶				M = 0.90; R = 2.9x10 ⁶				M = 1.20; R = 2.9x10 ⁶				M = 1.30; R = 2.9x10 ⁶			
α	C_L	C_D	C_m	α	C_L	C_D	C_m	α	C_L	C_D	C_m	α	C_L	C_D	C_m	α	C_L	C_D	C_m
-4.58	-0.275	0.0208	0.003	-4.67	-0.314	0.0256	0.010	-4.74	-0.359	0.0321	0.026	-4.86	-0.319	0.0398	0.063	-4.43	-0.289	0.0399	0.054
-3.50	-0.208	0.0144	0.002	-3.56	-0.234	0.0172	0.005	-3.60	-0.266	0.0205	0.012	-3.77	-0.239	0.0305	0.045	-3.36	-0.218	0.0307	0.043
-2.41	-0.138	0.0111	0.001	-2.45	-0.155	0.0117	0.001	-2.45	-0.173	0.0131	0.005	-2.30	-0.165	0.0237	0.030	-2.29	-0.149	0.0243	0.028
-1.32	-0.071	0.0083	0.000	-1.33	-0.090	0.0086	0.000	-1.32	-0.099	0.0093	0.001	-1.23	-0.090	0.0185	0.015	-1.22	-0.082	0.0198	0.014
-0.77	-0.041	0.0072	0.002	-0.78	-0.046	0.0073	0.002	-0.76	-0.054	0.0079	0.001	-0.72	-0.049	0.0173	0.006	-0.72	-0.043	0.0188	0.006
-0.49	-0.024	0.0067	0.003	-0.49	-0.030	0.0069	0.002	-0.47	-0.033	0.0076	0.001	-0.44	-0.029	0.0169	0.003	-0.44	-0.026	0.0184	0.003
0	0.005	0.0053	0.003	0.09	0.011	0.0055	0.001	0.07	0.011	0.0074	0.002	0.05	0.005	0.0168	0.002	0.05	0.005	0.0183	0.002
0.34	0.024	0.0055	0.003	0.37	0.030	0.0068	0.001	0.41	0.036	0.0075	0.003	0.34	0.025	0.0170	0.005	0.33	0.023	0.0184	0.005
0.89	0.056	0.0072	0.003	0.92	0.058	0.0074	0.001	1.04	0.062	0.0082	0.004	0.90	0.050	0.0179	0.013	0.89	0.058	0.0192	0.012
1.99	0.121	0.0097	0.001	2.06	0.140	0.0105	0.003	2.13	0.161	0.0120	0.006	1.97	0.145	0.0216	0.029	1.96	0.131	0.0228	0.027
3.08	0.193	0.0138	0.007	3.17	0.220	0.0155	0.008	3.27	0.260	0.0191	0.019	3.05	0.219	0.0280	0.044	3.04	0.199	0.0292	0.042
4.16	0.261	0.0187	0.007	4.29	0.301	0.0233	0.010	4.42	0.359	0.0305	0.033	4.14	0.298	0.0368	0.051	4.10	0.267	0.0373	0.057
5.27	0.336	0.0299	0.011	5.41	0.397	0.0363	0.027	5.57	0.462	0.0470	0.052	5.21	0.377	0.0478	0.079	5.18	0.346	0.0477	0.073
6.36	0.415	0.0448	0.016	6.53	0.467	0.0527	0.036	6.68	0.535	0.0597	0.060	6.29	0.460	0.0626	0.098	6.24	0.409	0.0620	0.093
8.54	0.525	0.0813	0.019	8.70	0.560	0.0835	0.046	8.89	0.646	0.1077	0.066	8.46	0.525	0.1012	0.136	8.37	0.514	0.0930	0.119
10.69	0.659	0.1225	0.018	10.85	0.678	0.1331	0.033	11.01	0.747	0.1553	0.073	10.63	0.762	0.1459	0.144	10.51	0.653	0.1331	0.146
12.79	0.742	0.1678	0.019	12.95	0.748	0.1770	0.034									12.63	0.763	0.1804	0.168
14.89	0.810	0.2147	0.021	15.04	0.802	0.2232	0.041												
16.94	0.851	0.2622	0.021	17.12	0.855	0.2724	0.056												
17.94	0.851	0.2829	0.044	18.14	0.876	0.2983	0.066												

M = 1.50; R = 2.9x10 ⁶				M = 1.70; R = 2.9x10 ⁶				M = 1.90; R = 2.9x10 ⁶				M = 0.22; R = 3.0x10 ⁶			
α	C_L	C_D	C_m	α	C_L	C_D	C_m	α	C_L	C_D	C_m	α	C_L	C_D	C_m
-4.33	-0.241	0.0369	0.050	-4.33	-0.269	0.0353	0.043	-4.33	-0.186	0.0345	0.037	-3.92	-0.216	0.0136	0.022
-3.29	-0.184	0.0293	0.037	-3.27	-0.199	0.0288	0.032	-3.28	-0.142	0.0286	0.029	-3.55	-0.186	0.0131	0.001
-2.24	-0.129	0.0236	0.024	-2.22	-0.111	0.0238	0.022	-2.24	-0.099	0.0242	0.019	-3.07	-0.159	0.0115	0.001
-1.18	-0.069	0.0199	0.012	-1.16	-0.058	0.0203	0.011	-1.18	-0.054	0.0211	0.010	-2.52	-0.127	0.0098	0.002
-0.68	-0.036	0.0188	0.005	-0.62	-0.032	0.0193	0.006	-0.65	-0.031	0.0203	0.006	-1.89	-0.097	0.0080	0.004
-0.40	-0.020	0.0184	0.002	-0.35	-0.017	0.0189	0.003	-0.38	-0.018	0.0200	0.003	-1.49	-0.073	0.0076	0.003
0.09	0.008	0.0183	0.002	0.09	0.007	0.0189	0.002	0.09	0.002	0.0199	0.001	-0.99	-0.049	0.0076	0.002
0.36	0.022	0.0184	0.005	0.36	0.020	0.0191	0.003	0.33	0.014	0.0200	0.004	-0.34	-0.017	0.0067	0.002
0.91	0.054	0.0191	0.012	0.90	0.046	0.0196	0.010	0.86	0.036	0.0204	0.008	0.14	0.006	0.0064	0.001
1.97	0.115	0.0225	0.025	1.96	0.100	0.0226	0.022	1.92	0.085	0.0227	0.018	0.61	0.033	0.0063	0.001
3.04	0.173	0.0277	0.037	3.02	0.150	0.0272	0.032	2.97	0.128	0.0264	0.027	1.07	0.055	0.0070	0.002
4.10	0.229	0.0390	0.050	4.07	0.198	0.0318	0.042	4.02	0.172	0.0315	0.036	1.67	0.089	0.0080	0.002
5.15	0.289	0.0440	0.063	5.13	0.247	0.0412	0.052	5.06	0.212	0.0378	0.044	2.26	0.116	0.0088	0.002
6.22	0.341	0.0590	0.079	6.18	0.296	0.0507	0.063	6.11	0.254	0.0459	0.053	2.70	0.150	0.0107	0.004
8.33	0.419	0.0821	0.100	8.28	0.390	0.0745	0.083	8.20	0.337	0.0667	0.071	3.25	0.184	0.0124	0.005
10.44	0.525	0.1167	0.123	10.38	0.480	0.1042	0.108	10.29	0.416	0.0920	0.087	3.85	0.214	0.0145	0.006
12.56	0.650	0.1567	0.144	12.49	0.567	0.1399	0.121	12.38	0.521	0.1223	0.101	4.44	0.246	0.0169	0.006
14.66	0.746	0.2045	0.164	14.58	0.649	0.1809	0.137	14.47	0.566	0.1688	0.115	5.04	0.276	0.0190	0.006
16.77	0.832	0.2575	0.180	16.79	0.728	0.2277	0.151	16.57	0.637	0.2003	0.126	5.62	0.308	0.0241	0.007
				17.73	0.765	0.2529	0.156	17.61	0.674	0.2240	0.133	6.04	0.341	0.0287	0.008
												6.59	0.373	0.0337	0.016
												7.61	0.440	0.0457	0.012
												8.98	0.498	0.0582	0.014
												9.70	0.566	0.0819	0.015
												10.70	0.618	0.0996	0.016
												11.79	0.670	0.1205	0.017
												12.77	0.713	0.1431	0.011
												14.83	0.791	0.1897	0.011
												16.81	0.890	0.2392	0.014
												18.87	0.900	0.2915	0.019
												20.76	0.945	0.3475	0.039
												22.83	0.959	0.3977	0.051

TABLE XII.- DATA FOR PLANE WING OF ASPECT RATIO 3 WITH 45° SWEEPBACK,
5 PERCENT THICK WITH MODIFIED LEADING EDGE
(b) Free transition - Concluded

α	C_L	C_D	C_m	α	C_L	C_D	C_m	α	C_L	C_D	C_m	α	C_L	C_D	C_m
M = 0.60; R = 3.8x10 ⁶				M = 0.80; R = 3.8x10 ⁶				M = 0.90; R = 3.8x10 ⁶				M = 1.30; R = 3.8x10 ⁶			
-4.65	-0.279	0.0221	0.004	-4.79	-0.325	0.0272	0.012	-4.89	-0.379	0.0326	0.026	-4.53	-0.287	0.0394	0.058
-3.56	-.215	.0146	.002	-3.66	-.247	.0172	.006	-3.71	-.277	.0206	.013	-3.44	-.219	.0311	.042
-2.46	-.147	.0117	0	-2.50	-.166	.0116	.002	-2.53	-.184	.0134	.006	-2.34	-.150	.0245	.028
-1.34	-.076	.0087	-.002	-1.38	-.087	.0083	-.002	-1.42	-.096	.0093	0	-1.25	-.082	.0198	.014
-.79	-.043	.0076	-.003	-.80	-.052	.0070	-.002	-.78	-.054	.0077	-.001	-.75	-.048	.0187	.007
-.50	-.028	.0072	-.002	-.50	-.032	.0065	-.002	-.49	-.033	.0072	-.002	-.46	-.028	.0184	.003
0	.003	.0068	-.001	.03	.008	.0062	-.002	.09	.020	.0073	-.003	.06	.006	.0182	-.003
.29	.024	.0069	-.001	.35	.035	.0063	-.002	.44	.044	.0075	-.004	.36	.029	.0184	-.007
.91	.058	.0075	-.001	.98	.069	.0069	-.002	1.04	.084	.0083	-.005	.92	.063	.0192	-.014
2.02	.128	.0103	-.003	2.11	.147	.0109	-.006	2.20	.171	.0123	-.010	2.02	.134	.0231	-.028
3.13	.198	.0135	-.006	3.25	.226	.0160	-.010	3.38	.264	.0191	-.019	3.12	.202	.0293	-.042
4.24	.266	.0188	-.008	4.40	.308	.0244	-.014	4.57	.372	.0308	-.037	4.21	.270	.0372	-.058
5.35	.338	.0298	-.010	5.54	.394	.0376	-.021	5.73	.470	.0478	-.055	5.30	.337	.0482	-.073
6.46	.417	.0468	-.015	6.68	.472	.0545	-.025	6.87	.542	.0665	-.063	6.40	.405	.0610	-.088
8.68	.558	.0829	-.020	8.91	.598	.0934	-.028	9.08	.654	.1102	-.067	8.57	.533	.0934	-.118
10.83	.649	.1222	-.016	11.07	.684	.1360	-.033	11.27	.751	.1567	-.075	10.14	.624	.1223	-.137
12.98	.746	.1693	-.019	13.19	.748	.1801	-.033								
15.09	.818	.2180	-.021	15.30	.804	.2276	-.041								
17.17	.858	.2637	-.032												
18.15	.856	.3475	-.045												
M = 0.80; R = 5.7x10 ⁶				M = 0.90; R = 5.7x10 ⁶				M = 0.22; R = 6.0x10 ⁶				M = 0.22; R = 8.0x10 ⁶			
-5.01	-.332	.0282	.009	-5.23	-.418	.0392	.038	-3.94	-.220	.0147	.003	-3.94	-.225	.0143	.004
-3.83	-.254	.0178	.006	-3.94	-.298	.0227	.017	-3.61	-.192	.0142	.002	-3.64	-.196	.0143	.003
-2.64	-.174	.0125	.003	-2.70	-.202	.0145	.009	-3.10	-.164	.0128	.002	-3.14	-.170	.0129	.002
-1.44	-.098	.0095	.001	-1.47	-.110	.0101	.003	-2.52	-.134	.0110	.001	-2.55	-.140	.0113	.001
-.85	-.057	.0084	-.001	-.86	-.065	.0088	.001	-2.01	-.105	.0100	0	-2.04	-.111	.0103	.001
-.54	-.037	.0081	-.001	-.38	-.043	.0083	0	-1.49	-.076	.0088	-.001	-1.46	-.079	.0091	0
.12	.016	.0078	-.002	.04	-.012	.0079	-.001	-.99	-.047	.0081	-.001	-.99	-.049	.0085	-.001
.44	.040	.0080	-.003	.51	.048	.0082	-.004	-.37	-.018	.0075	-.001	-.40	-.020	.0085	-.001
1.03	.078	.0086	-.004	1.11	.091	.0091	-.007	.11	.009	.0073	-.001	.14	.009	.0081	-.001
2.23	.158	.0113	-.007	2.35	.186	.0129	-.014	.66	.035	.0079	0	.72	.040	.0082	-.001
3.41	.236	.0160	-.010	3.60	.285	.0204	-.024	1.23	.066	.0084	0	1.26	.068	.0087	-.001
4.60	.315	.0231	-.013	4.86	.392	.0336	-.040	1.75	.097	.0095	-.001	1.87	.102	.0096	-.001
5.80	.399	.0381	-.018	6.10	.491	.0524	-.058	2.41	.131	.0108	-.002	2.51	.136	.0109	-.002
7.00	.484	.0562	-.024					2.96	.165	.0123	-.003	3.03	.167	.0120	-.001
8.18	.554	.0754	-.028					3.60	.196	.0136	-.004	3.66	.198	.0134	-.004
								4.18	.226	.0153	-.005	4.28	.229	.0150	-.004
								4.66	.255	.0170	-.005	4.72	.259	.0162	-.005
								5.24	.287	.0188	-.006	5.27	.288	.0181	-.006
								5.81	.315	.0209	-.007	5.88	.319	.0205	-.007
								6.29	.343	.0232	-.008	6.40	.347	.0227	-.008
								6.84	.371	.0261	-.009	6.97	.376	.0253	-.009
								7.87	.439	.0409	-.010	8.00	.438	.0315	-.012
								8.90	.493	.0513	-.012	9.02	.496	.0389	-.014
								9.80	.564	.0725	-.016	10.11	.566	.0572	-.020
								10.98	.622	.0947	-.015	11.17	.629	.0788	-.022
								12.11	.683	.1212	-.015	12.30	.690	.1138	-.020
								13.10	.734	.1455	-.017	13.32	.730	.1410	-.013
								14.95	.797	.1872	-.005	15.30	.796	.1879	-.010
								17.19	.860	.2419	-.014	17.38	.868	.2428	-.015
								19.23	.911	.2960	-.018	19.46	.919	.2981	-.018
								21.05	.950	.3496	-.032	21.11	.942	.3495	-.048
								22.95	.955	.3965	-.051				

TABLE XIII.- DATA FOR WING OF ASPECT RATIO 3 WITH 45° SWEEPBACK, 5 PERCENT THICK WITH MODIFIED LEADING EDGE, CONICALLY CAMBERED FOR $C_{Ld} = 0.225$ AT $M = 1.0$

(a) Fixed Transition

α	C_L	C_D	C_m	α	C_L	C_D	C_m	α	C_L	C_D	C_m	α	C_L	C_D	C_m
$M = 0.60; R = 2.9 \times 10^6$				$M = 0.80; R = 2.9 \times 10^6$				$M = 0.90; R = 2.9 \times 10^6$				$M = 1.20; R = 2.9 \times 10^6$			
-6.77	-0.449	0.0646	0.011	-6.90	-0.489	0.0710	0.021	-6.99	-0.534	0.0851	0.045	-6.69	-0.517	0.0837	0.109
-6.23	-0.419	0.0570	0.011	-6.37	-0.466	0.0660	0.022	-6.44	-0.502	0.0794	0.044	-6.10	-0.475	0.0745	0.099
-5.69	-0.390	0.0504	0.011	-5.81	-0.428	0.0573	0.021	-5.89	-0.468	0.0660	0.040	-5.56	-0.432	0.0558	0.088
-5.13	-0.348	0.0431	0.008	-5.26	-0.394	0.0497	0.020	-5.33	-0.433	0.0576	0.037	-5.01	-0.385	0.0477	0.077
-4.59	-0.317	0.0376	0.007	-4.71	-0.357	0.0428	0.017	-4.78	-0.398	0.0497	0.035	-4.47	-0.344	0.0508	0.067
-4.04	-0.276	0.0318	0.005	-4.15	-0.316	0.0363	0.014	-4.22	-0.356	0.0420	0.030	-3.93	-0.304	0.0449	0.057
-3.49	-0.238	0.0273	0.003	-3.59	-0.274	0.0304	0.011	-3.65	-0.312	0.0351	0.025	-3.39	-0.262	0.0396	0.048
-2.94	-0.201	0.0232	0.001	-3.02	-0.230	0.0254	0.007	-3.08	-0.262	0.0286	0.018	-2.84	-0.218	0.0346	0.038
-2.40	-0.164	0.0199	-0.001	-2.46	-0.187	0.0211	0.004	-2.50	-0.212	0.0233	0.011	-2.30	-0.175	0.0305	0.029
-1.80	-0.092	0.0152	-0.003	-1.84	-0.106	0.0154	-0.001	-1.85	-0.108	0.0161	0.001	-1.29	-0.096	0.0249	0.014
-1.74	-0.057	0.0136	-0.003	-1.77	-0.063	0.0135	-0.003	-1.77	-0.060	0.0138	-0.002	-1.74	-0.054	0.0231	0.006
-1.45	-0.030	0.0127	-0.005	-1.48	-0.041	0.0128	-0.004	-1.48	-0.039	0.0131	-0.003	-1.46	-0.037	0.0225	0.002
0.03	-0.001	0.0120	-0.006	0.03	0	0.0120	-0.007	0.03	0.001	0.0124	-0.007	0.01	-0.008	0.0220	-0.003
0.31	0.022	0.0117	-0.007	0.32	0.025	0.0116	-0.007	0.32	0.025	0.0120	-0.008	0.30	0.016	0.0218	-0.008
0.95	0.067	0.0112	-0.007	0.96	0.063	0.0114	-0.009	0.98	0.070	0.0119	-0.011	0.99	0.051	0.0212	-0.014
2.04	0.127	0.0123	-0.009	2.09	0.146	0.0126	-0.012	2.12	0.162	0.0137	-0.017	1.94	0.132	0.0239	-0.031
2.59	0.163	0.0132	-0.010	2.65	0.188	0.0138	-0.014	2.70	0.212	0.0156	-0.021	2.48	0.172	0.0260	-0.040
3.14	0.200	0.0147	-0.011	3.21	0.227	0.0152	-0.016	3.26	0.255	0.0178	-0.024	3.02	0.210	0.0285	-0.048
3.68	0.230	0.0156	-0.012	3.77	0.264	0.0171	-0.018	3.83	0.304	0.0212	-0.031	3.56	0.248	0.0318	-0.056
4.22	0.264	0.0178	-0.014	4.32	0.305	0.0196	-0.019	4.40	0.353	0.0253	-0.036	4.10	0.288	0.0358	-0.065
4.76	0.298	0.0197	-0.015	4.88	0.343	0.0227	-0.021	4.98	0.401	0.0300	-0.042	4.64	0.330	0.0405	-0.074
5.31	0.332	0.0219	-0.016	5.43	0.380	0.0259	-0.022	5.55	0.456	0.0371	-0.052	5.18	0.368	0.0456	-0.083
5.85	0.368	0.0250	-0.018	5.99	0.419	0.0297	-0.023	6.13	0.512	0.0454	-0.063	5.73	0.410	0.0517	-0.093
6.39	0.396	0.0277	-0.018	6.53	0.461	0.0332	-0.026	6.71	0.568	0.0522	-0.076	6.27	0.457	0.0582	-0.103
7.48	0.465	0.0404	-0.019	7.69	0.552	0.0539	-0.034	7.84	0.660	0.0600	-0.092	7.36	0.542	0.0759	-0.123
8.59	0.549	0.0647	-0.025	8.78	0.616	0.0800	-0.039	8.88	0.672	0.0986	-0.075	8.45	0.625	0.0958	-0.139
10.75	0.664	0.1068	-0.023	10.90	0.690	0.1225	-0.041	11.04	0.772	0.1465	-0.082	10.64	0.789	0.1436	-0.161
12.88	0.764	0.1594	-0.028	13.05	0.794	0.1748	-0.048					11.70	0.824	0.1637	-0.148
15.00	0.848	0.2088	-0.030	15.13	0.836	0.2194	-0.050								
17.07	0.904	0.2647	-0.036	17.23	0.904	0.2761	-0.066								
$M = 1.30; R = 2.9 \times 10^6$				$M = 1.50; R = 2.9 \times 10^6$				$M = 1.70; R = 2.9 \times 10^6$				$M = 1.90; R = 2.9 \times 10^6$			
-6.59	-0.449	0.0783	0.097	-6.54	-0.375	0.0693	0.083	-6.47	-0.320	0.0632	0.068	-6.43	-0.279	0.0580	0.057
-6.05	-0.413	0.0701	0.088	-6.00	-0.344	0.0624	0.074	-5.94	-0.295	0.0574	0.062	-5.90	-0.260	0.0532	0.053
-5.51	-0.376	0.0626	0.080	-5.47	-0.314	0.0561	0.067	-5.41	-0.269	0.0521	0.056	-5.38	-0.236	0.0484	0.047
-4.98	-0.340	0.0557	0.071	-4.94	-0.284	0.0504	0.060	-4.88	-0.242	0.0471	0.050	-4.85	-0.216	0.0444	0.043
-4.44	-0.306	0.0498	0.062	-4.40	-0.252	0.0451	0.052	-4.35	-0.217	0.0428	0.044	-4.66	-0.191	0.0415	0.037
-3.90	-0.270	0.0443	0.053	-3.87	-0.223	0.0406	0.045	-3.83	-0.191	0.0388	0.038	-3.80	-0.168	0.0370	0.032
-3.36	-0.233	0.0395	0.044	-3.33	-0.192	0.0365	0.037	-3.30	-0.167	0.0355	0.032	-3.28	-0.146	0.0339	0.027
-2.83	-0.196	0.0352	0.036	-2.80	-0.162	0.0330	0.030	-2.77	-0.142	0.0324	0.026	-2.75	-0.125	0.0313	0.022
-2.28	-0.084	0.0265	0.012	-2.27	-0.133	0.0300	0.023	-2.24	-0.115	0.0299	0.020	-2.23	-0.103	0.0291	0.017
-1.73	-0.050	0.0248	0.005	-1.72	-0.071	0.0256	0.010	-1.29	-0.062	0.0261	0.008	-1.25	-0.058	0.0258	0.007
-1.45	-0.031	0.0241	0.001	-1.72	-0.041	0.0241	0.003	-1.71	-0.036	0.0247	0.003	-1.71	-0.035	0.0247	0.002
0.04	0.010	0.0234	-0.007	-1.45	-0.027	0.0236	0	-1.44	-0.023	0.0243	0	-1.45	-0.026	0.0244	0
0.30	0.016	0.0235	-0.008	0.02	-0.004	0.0232	-0.004	0.02	-0.005	0.0240	-0.004				
0.85	0.052	0.0236	-0.016	0.29	0.012	0.0231	-0.008	0.29	0.007	0.0239	-0.007	0.28	0.003	0.0240	-0.006
1.93	0.120	0.0259	-0.030	0.85	0.045	0.0233	-0.015	0.83	0.036	0.0242	-0.013	0.82	0.027	0.0241	-0.011
2.47	0.157	0.0280	-0.038	1.92	0.104	0.0255	-0.028	1.90	0.088	0.0262	-0.024	1.88	0.071	0.0255	-0.020
3.01	0.191	0.0305	-0.046	2.45	0.132	0.0273	-0.034	2.96	0.137	0.0296	-0.034	2.41	0.092	0.0267	-0.024
3.54	0.226	0.0336	-0.054	2.99	0.162	0.0297	-0.040	3.48	0.161	0.0318	-0.039	2.93	0.114	0.0284	-0.029
4.08	0.261	0.0373	-0.062	3.52	0.191	0.0324	-0.047	4.01	0.187	0.0346	-0.044	3.46	0.136	0.0304	-0.033
4.62	0.294	0.0415	-0.069	4.05	0.220	0.0355	-0.053	4.54	0.211	0.0378	-0.049	3.98	0.156	0.0327	-0.037
5.15	0.328	0.0462	-0.077	4.59	0.251	0.0396	-0.059	5.07	0.236	0.0414	-0.054	4.51	0.180	0.0357	-0.042
5.69	0.364	0.0517	-0.085	5.12	0.278	0.0436	-0.065	5.60	0.261	0.0455	-0.060	5.03	0.201	0.0386	-0.046
6.23	0.399	0.0579	-0.093	5.65	0.305	0.0481	-0.071	6.12	0.285	0.0498	-0.064	5.55	0.222	0.0421	-0.050
7.30	0.470	0.0723	-0.109	6.18	0.334	0.0532	-0.078	7.18	0.334	0.0600	-0.075	6.06	0.245	0.0460	-0.055
8.38	0.535	0.0889	-0.122	7.25	0.394	0.0654	-0.091	8.24	0.387	0.0727	-0.086	7.13	0.287	0.0548	-0.064
10.51	0.659	0.1274	-0.149	8.32	0.452	0.0796	-0.103	10.35	0.482	0.1013	-0.105	8.18	0.329	0.0651	-0.072
12.65	0.777	0.1749	-0.172	10.45	0.558	0.1126	-0.126	12.46	0.574	0.1367	-0.125	10.28	0.419	0.0915	-0.090
				12.57	0.661	0.1529	-0.148	14.57	0.665	0.1792	-0.144	12.38	0.501	0.1230	-0.106
				13.71	-0.013	-0.0019	-0.043	16.68	0.751	0.2277	-0.160	14.47	0.578	0.1591	-0.121
												16.58	0.656	0.2021	-0.134

TABLE XIII.- DATA FOR WING OF ASPECT RATIO 3 WITH 45° SWEEPBACK, 5 PERCENT THICK WITH MODIFIED LEADING EDGE, CONICALLY CAMBERED FOR $C_{Ld} = 0.225$ AT $M = 1.0$

(b) Free transition - Concluded

α	C_L	C_D	C_m	α	C_L	C_D	C_m	α	C_L	C_D	C_m	α	C_L	C_D	C_m
$M = 1.30; R = 2.9 \times 10^6$				$M = 1.50; R = 2.9 \times 10^6$				$M = 1.70; R = 2.9 \times 10^6$				$M = 1.90; R = 2.9 \times 10^6$			
-6.59	-0.452	0.0783	0.099	-6.53	-0.376	0.0682	0.082	-6.47	-0.322	0.0625	0.069	-6.42	-0.285	0.0573	0.059
-6.06	-0.417	0.0702	0.090	-6.00	-0.346	0.0614	0.075	-5.94	-0.296	0.0566	0.063	-5.90	-0.263	0.0523	0.054
-5.52	-0.379	0.0624	0.081	-5.47	-0.318	0.0554	0.068	-5.41	-0.271	0.0513	0.057	-5.37	-0.242	0.0478	0.050
-4.98	-0.343	0.0555	0.072	-4.93	-0.287	0.0495	0.061	-4.88	-0.246	0.0464	0.051	-4.85	-0.220	0.0434	0.045
-4.44	-0.307	0.0493	0.063	-4.40	-0.254	0.0440	0.052	-4.36	-0.221	0.0420	0.045	-4.33	-0.197	0.0393	0.039
-3.90	-0.268	0.0434	0.053	-3.86	-0.223	0.0393	0.045	-3.83	-0.192	0.0377	0.038	-3.80	-0.175	0.0358	0.034
-3.36	-0.232	0.0385	0.044	-3.33	-0.193	0.0352	0.037	-3.30	-0.167	0.0341	0.032	-3.28	-0.153	0.0328	0.029
-2.82	-0.195	0.0342	0.036	-2.80	-0.164	0.0316	0.030	-2.77	-0.140	0.0309	0.026	-2.76	-0.132	0.0301	0.024
-2.28	-0.157	0.0305	0.027	-2.26	-0.133	0.0289	0.023	-2.24	-0.118	0.0284	0.021	-2.23	-0.110	0.0278	0.019
-1.72	-0.122	0.0250	0.012	-1.26	-0.070	0.0239	0.009	-1.25	-0.062	0.0243	0.008	-1.25	-0.062	0.0243	0.009
-1.17	-0.088	0.0210	0.005	-0.72	-0.041	0.0225	0.003	-0.71	-0.037	0.0229	0.003	-0.72	-0.041	0.0231	0.004
-0.65	-0.051	0.0175	0.001	-0.45	-0.025	0.0220	0	-0.44	-0.022	0.0225	0	-0.45	-0.031	0.0227	0.002
0.02	-0.014	0.0147	-0.004	0.02	-0.005	0.0210	-0.004	0.03	0.002	0.0221	-0.006	0.02	-0.007	0.0221	-0.004
0.30	0.015	0.0214	0.008	0.30	0.013	0.0214	-0.008	0.28	0.006	0.0220	-0.007	0.27	-0.004	0.0221	-0.004
0.86	0.054	0.0216	-0.016	0.85	0.045	0.0215	-0.015	0.83	0.036	0.0224	-0.013	0.81	0.021	0.0222	-0.009
1.54	0.126	0.0237	-0.031	1.52	0.105	0.0236	-0.028	1.50	0.087	0.0244	-0.024	1.48	0.065	0.0237	-0.019
2.47	0.160	0.0258	-0.039	2.58	0.161	0.0278	-0.040	2.43	0.112	0.0259	-0.029	2.40	0.085	0.0249	-0.023
3.01	0.190	0.0282	-0.046	3.52	0.193	0.0307	-0.047	2.96	0.138	0.0280	-0.034	2.92	0.108	0.0266	-0.028
3.55	0.227	0.0317	-0.054	4.05	0.223	0.0340	-0.054	3.48	0.163	0.0304	-0.040	3.45	0.131	0.0287	-0.032
4.08	0.263	0.0356	-0.063	4.58	0.249	0.0376	-0.060	4.01	0.189	0.0332	-0.045	3.97	0.121	0.0310	-0.036
4.62	0.297	0.0400	-0.070	5.11	0.279	0.0418	-0.066	4.54	0.213	0.0364	-0.050	4.49	0.173	0.0336	-0.040
5.16	0.333	0.0452	-0.079	5.65	0.310	0.0469	-0.073	5.07	0.236	0.0399	-0.055	5.02	0.195	0.0367	-0.045
5.70	0.370	0.0510	-0.087	6.18	0.337	0.0519	-0.080	5.59	0.261	0.0440	-0.061	5.54	0.217	0.0402	-0.050
6.23	0.402	0.0570	-0.095	7.24	0.392	0.0638	-0.092	6.12	0.285	0.0483	-0.066	6.06	0.238	0.0440	-0.054
7.31	0.475	0.0717	-0.111	8.31	0.455	0.0786	-0.106	7.18	0.335	0.0587	-0.076	7.11	0.283	0.0529	-0.063
8.38	0.540	0.0882	-0.126	10.43	0.561	0.1118	-0.128	8.23	0.388	0.0710	-0.087	8.16	0.326	0.0634	-0.072
10.22	0.667	0.1284	-0.153	12.55	0.661	0.1519	-0.150	10.34	0.481	0.0958	-0.107	10.26	0.416	0.0898	-0.081
12.65	0.781	0.1755	-0.175	14.68	0.763	0.2002	-0.170	12.45	0.569	0.1344	-0.125	12.35	0.496	0.1205	-0.107
								14.56	0.697	0.1760	-0.142	14.45	0.572	0.1564	-0.121
								16.67	0.743	0.2242	-0.157	16.54	0.648	0.1986	-0.131

α	C_L	C_D	C_m	α	C_L	C_D	C_m	α	C_L	C_D	C_m
$M = 0.22; R = 3.0 \times 10^6$				$M = 0.22; R = 6.0 \times 10^6$				$M = 0.22; R = 8.0 \times 10^6$			
-3.88	-0.242	0.0252	0.001	-3.94	-0.248	0.0255	0.002	-4.07	-0.254	0.0256	0.004
-3.65	-0.217	0.0238	0	-3.75	-0.223	0.0240	0.002	-3.78	-0.227	0.0236	0.003
-3.07	-0.187	0.0200	-0.001	-3.27	-0.190	0.0206	0	-3.26	-0.194	0.0199	0.002
-2.55	-0.154	0.0171	-0.001	-2.66	-0.156	0.0172	0	-2.69	-0.162	0.0168	0.001
-1.98	-0.119	0.0133	-0.003	-2.08	-0.126	0.0146	-0.001	-2.17	-0.132	0.0144	0.001
-1.53	-0.089	0.0124	-0.004	-1.57	-0.095	0.0126	-0.001	-1.66	-0.097	0.0126	0
-0.99	-0.058	0.0106	-0.004	-1.05	-0.067	0.0113	-0.001	-1.05	-0.066	0.0107	-0.001
-0.43	-0.026	0.0094	-0.005	-0.47	-0.034	0.0098	-0.002	-0.48	-0.037	0.0097	-0.001
-0.02	0	0.0090	-0.005	-0.05	-0.004	0.0092	-0.003	-0.05	-0.005	0.0091	-0.002
0.58	0.030	0.0087	-0.006	0.58	0.027	0.0085	-0.004	0.74	0.026	0.0086	-0.003
1.10	0.053	0.0082	-0.005	1.07	0.055	0.0085	-0.005	1.16	0.053	0.0084	-0.004
1.58	0.084	0.0084	-0.006	1.64	0.086	0.0086	-0.005	1.83	0.093	0.0088	-0.005
2.10	0.113	0.0089	-0.006	2.32	0.124	0.0093	-0.006	2.45	0.131	0.0099	-0.005
2.70	0.142	0.0096	-0.006	2.87	0.160	0.0110	-0.006	3.06	0.162	0.0112	-0.006
3.25	0.180	0.0113	-0.007	3.56	0.190	0.0124	-0.007	3.60	0.193	0.0125	-0.006
3.82	0.208	0.0128	-0.008	4.15	0.219	0.0139	-0.008	4.18	0.223	0.0140	-0.007
4.44	0.242	0.0150	-0.010	4.63	0.249	0.0158	-0.009	4.69	0.253	0.0156	-0.008
5.01	0.270	0.0170	-0.010	5.20	0.280	0.0177	-0.009	5.20	0.283	0.0174	-0.009
5.59	0.302	0.0196	-0.011	5.72	0.307	0.0198	-0.010	5.78	0.312	0.0200	-0.010
6.04	0.329	0.0218	-0.012	6.20	0.335	0.0220	-0.011	6.29	0.339	0.0222	-0.011
6.59	0.360	0.0245	-0.013	6.78	0.367	0.0248	-0.012	6.87	0.370	0.0249	-0.012
7.61	0.420	0.0303	-0.015	7.80	0.426	0.0304	-0.015	7.90	0.432	0.0306	-0.015
8.55	0.474	0.0363	-0.017	8.83	0.470	0.0348	-0.015	8.90	0.459	0.0373	-0.018
9.70	0.544	0.0581	-0.017	9.92	0.545	0.0446	-0.020	10.08	0.549	0.0458	-0.020
10.76	0.605	0.0823	-0.017	10.95	0.602	0.0534	-0.023	11.05	0.609	0.0538	-0.023
11.72	0.666	0.1051	-0.020	12.01	0.668	0.0754	-0.025	12.17	0.667	0.0675	-0.024
12.77	0.713	0.1281	-0.019	13.07	0.733	0.1023	-0.030	13.26	0.732	0.0973	-0.028
14.83	0.805	0.1789	-0.018	15.15	0.843	0.1762	-0.029	15.30	0.831	0.1733	-0.025
16.87	0.880	0.2322	-0.018	17.16	0.896	0.2347	-0.024	17.35	0.896	0.2356	-0.024
18.88	0.939	0.2910	-0.019	19.23	0.946	0.2975	-0.020	19.42	0.945	0.2983	-0.020
20.74	0.977	0.3465	-0.035	21.02	0.978	0.3526	-0.062	21.22	0.976	0.3567	-0.042
22.74	1.004	0.4043	-0.056	23.06	0.991	0.4044	-0.054	23.15	0.995	0.4071	-0.053
24.68	1.004	0.4451	-0.057	24.71	0.993	0.4409	-0.054	24.78	1.004	0.4458	-0.054

TABLE XIV.- DATA FOR WING OF ASPECT RATIO 3 WITH 45° SWEEPBACK, 5 PERCENT THICK WITH NORMAL LEADING EDGE, CONICALLY CAMBERED FOR $C_{Ld} = 0.292$ AT $M = 1.0$

(a) Fixed transition

α	C_L	C_D	C_m	α	C_L	C_D	C_m	α	C_L	C_D	C_m	α	C_L	C_D	C_m
$M = 0.60; R = 2.9 \times 10^6$				$M = 0.80; R = 2.9 \times 10^6$				$M = 0.90; R = 2.9 \times 10^6$				$M = 1.20; R = 2.9 \times 10^6$			
-6.80	-0.465	0.0693	0.015	-6.94	-0.500	0.0788	0.026	-7.03	-0.544	0.0903	0.051	-6.67	-0.532	0.0888	0.117
-6.26	-0.440	.0623	.016	-6.39	-0.472	.0699	.025	-6.48	-0.517	.0613	.050	-6.12	-0.487	.0792	.106
-5.72	-0.409	.0551	.017	-5.85	-0.447	.0624	.025	-5.93	-0.483	.0713	.046	-5.58	-0.443	.0701	.094
-5.18	-0.375	.0483	.016	-5.30	-0.415	.0549	.025	-5.38	-0.451	.0630	.043	-5.03	-0.398	.0617	.084
-4.63	-0.341	.0422	.015	-4.75	-0.380	.0478	.024	-4.82	-0.412	.0540	.040	-4.49	-0.360	.0546	.075
-4.08	-0.306	.0366	.013	-4.19	-0.341	.0411	.021	-4.27	-0.379	.0475	.038	-3.94	-0.320	.0482	.066
-3.53	-0.269	.0314	.012	-3.64	-0.305	.0353	.019	-3.71	-0.341	.0406	.035	-3.40	-0.281	.0428	.057
-2.98	-0.231	.0269	.010	-3.07	-0.263	.0299	.016	-3.14	-0.295	.0338	.029	-2.86	-0.242	.0377	.049
-2.44	-0.195	.0232	.008	-2.51	-0.222	.0252	.013	-2.57	-0.253	.0282	.024	-2.32	-0.204	.0333	.040
-1.94	-0.123	.0174	.005	-1.99	-0.140	.0182	.008	-1.42	-0.115	.0194	.013	-1.23	-0.122	.0268	.023
-0.79	-0.087	.0153	.003	-0.83	-0.099	.0158	.005	-0.85	-0.110	.0167	.009	-0.69	-0.083	.0248	.014
-0.51	-0.069	.0146	.003	-0.53	-0.068	.0144	.003	-0.55	-0.077	.0154	.005	-0.41	-0.063	.0241	.010
-0.03	-0.031	.0134	.001	-0.04	-0.033	.0135	.002	-0.05	-0.037	.0140	.002	-0.01	-0.019	.0229	.001
.25	-0.014	.0130	0	.24	-0.015	.0130	0	.24	-0.018	.0134	0	.25	-0.011	.0228	0
.89	.023	.0124	.001	.91	.033	.0123	.002	.93	.042	.0132	-.004	.82	.035	.0229	-.009
2.01	.099	.0131	-.002	2.06	.118	.0132	-.005	2.10	.137	.0142	-.010	1.92	.115	.0245	-.025
2.56	.135	.0137	-.003	2.62	.158	.0141	-.007	2.66	.180	.0155	-.012	2.47	.155	.0263	-.033
3.10	.166	.0145	-.004	3.18	.196	.0155	-.008	3.23	.224	.0176	-.016	3.01	.194	.0286	-.041
3.64	.199	.0157	-.005	3.73	.234	.0170	-.010	3.80	.268	.0201	-.020	3.55	.233	.0317	-.050
4.19	.235	.0172	-.006	4.29	.269	.0195	-.011	4.37	.315	.0242	-.026	4.09	.271	.0354	-.058
4.73	.267	.0193	-.007	4.85	.307	.0218	-.013	4.94	.365	.0290	-.034	4.63	.309	.0397	-.067
5.28	.304	.0216	-.009	5.40	.344	.0246	-.014	5.52	.415	.0347	-.042	5.17	.347	.0444	-.076
5.82	.333	.0240	-.010	5.96	.381	.0279	-.016	6.10	.468	.0424	-.053	5.71	.386	.0500	-.084
6.36	.364	.0268	-.011	6.52	.420	.0319	-.017	6.68	.526	.0522	-.066	6.26	.427	.0566	-.093
7.45	.431	.0342	-.012	7.64	.504	.0441	-.019	7.82	.623	.0733	-.085	7.34	.502	.0711	-.110
8.55	.505	.0506	-.014	8.77	.590	.0652	-.028	8.94	.699	.0969	-.093	8.43	.586	.0896	-.127
10.73	.641	.0979	-.018	10.99	.666	.1141	-.031					10.62	.752	.1352	-.153
12.86	.734	.1444	-.019	13.04	.762	.1640	-.040								
14.99	.826	.1986	-.023	15.13	.818	.2107	-.042								
17.08	.889	.2529	-.026	17.23	.880	.2654	-.057								
18.10	.902	.2779	-.033												
$M = 1.30; R = 2.9 \times 10^6$				$M = 1.50; R = 2.9 \times 10^6$				$M = 1.70; R = 2.9 \times 10^6$				$M = 1.90; R = 2.9 \times 10^6$			
-6.61	-0.457	.0630	.102	-6.54	-.381	.0724	.086	-6.48	-.327	.0664	.072	-6.43	-.289	.0611	.062
-6.07	-0.422	.0748	.094	-6.01	-.354	.0658	.079	-5.96	-.303	.0607	.066	-5.91	-.268	.0561	.057
-5.53	-0.387	.0671	.085	-5.48	-.325	.0595	.072	-5.43	-.278	.0552	.060	-5.38	-.247	.0513	.052
-4.99	-0.353	.0603	.076	-4.94	-.297	.0538	.065	-4.90	-.255	.0504	.055	-4.86	-.226	.0471	.047
-4.46	-0.318	.0541	.068	-4.41	-.268	.0486	.058	-4.37	-.229	.0459	.049	-4.33	-.205	.0433	.042
-3.92	-0.285	.0485	.059	-3.88	-.239	.0438	.051	-3.84	-.206	.0419	.043	-3.81	-.185	.0397	.037
-3.38	-0.248	.0433	.050	-3.34	-.209	.0395	.043	-3.31	-.182	.0383	.037	-3.29	-.165	.0366	.033
-2.84	-0.213	.0389	.042	-2.81	-.180	.0358	.036	-2.79	-.157	.0350	.031	-2.24	-.119	.0311	.022
-2.30	-0.180	.0349	.034	-2.28	-.149	.0325	.029	-2.26	-.131	.0321	.025	-1.27	-.074	.0275	.011
-1.22	-0.108	.0289	.019	-1.21	-.092	.0278	.015	-1.19	-.078	.0277	.013	-.74	-.051	.0261	.006
-.68	-0.071	.0267	.011	-.75	-.061	.0263	.009	-.73	-.049	.0262	.007	-.47	-.040	.0257	.004
-.48	-0.051	.0258	.008	-.47	-.043	.0255	.005	-.46	-.036	.0259	.004	.25	-.013	.0248	-.002
-.01	-0.016	.0247	0	-.01	-.013	.0247	-.001	-.02	-.021	.0255	.001	.78	.010	.0246	-.007
.25	-0.009	.0246	-.001	.26	-.005	.0246	-.003	.26	-.006	.0252	-.003	1.86	.057	.0260	-.017
.82	.031	.0242	-.010	.81	.027	.0243	-.010	.80	.020	.0251	-.009	2.38	.079	.0271	-.022
1.91	.105	.0265	-.025	1.90	.090	.0262	-.024	1.88	.073	.0269	-.020	2.91	.101	.0287	-.026
2.45	.141	.0282	-.033	2.43	.118	.0275	-.030	2.41	.100	.0282	-.026	3.44	.123	.0304	-.030
2.99	.176	.0305	-.041	2.97	.148	.0297	-.036	2.94	.124	.0299	-.031	3.96	.147	.0329	-.035
3.53	.212	.0335	-.049	3.50	.177	.0323	-.043	3.47	.149	.0320	-.036	4.49	.168	.0355	-.039
4.07	.245	.0370	-.057	4.03	.205	.0352	-.049	4.00	.175	.0345	-.041	5.01	.190	.0385	-.043
4.61	.279	.0410	-.064	4.57	.235	.0386	-.055	4.53	.199	.0374	-.046	5.54	.213	.0418	-.048
5.14	.313	.0455	-.072	5.10	.263	.0425	-.061	5.06	.223	.0395	-.048	6.07	.235	.0457	-.052
5.68	.346	.0506	-.079	5.63	.290	.0468	-.067	5.59	.247	.0442	-.056	7.11	.277	.0540	-.060
6.22	.378	.0564	-.086	6.16	.318	.0517	-.073	6.12	.273	.0488	-.061	8.16	.319	.0639	-.069
7.29	.443	.0655	-.100	7.23	.374	.0627	-.085	7.17	.320	.0582	-.071	10.26	.402	.0882	-.085
8.36	.507	.0848	-.114	8.29	.428	.0759	-.097	8.23	.366	.0693	-.080	12.36	.482	.1177	-.101
10.50	.629	.1213	-.138	10.42	.531	.1066	-.118	10.35	.461	.0970	-.099	14.46	.559	.1527	-.115
12.64	.746	.1667	-.162	12.54	.632	.1448	-.139	12.46	.550	.1303	-.117	16.56	.636	.1943	-.127
				14.67	.735	.1917	-.160	14.57	.639	.1706	-.135	17.61	.676	.2181	-.135
								16.69	.726	.2179	-.151				

TABLE XIV.- DATA FOR WING OF ASPECT RATIO 3 WITH 45° SWEEPBACK, 5 PERCENT THICK WITH NORMAL LEADING EDGE, CONICALLY CAMBERED FOR $C_{Ld} = 0.292$ AT $M = 1.0$ - Concluded

(b) Free transition

α	C_L	C_D	C_m	α	C_L	C_D	C_m	α	C_L	C_D	C_m	α	C_L	C_D	C_m
M = 0.60; R = 2.9×10^6				M = 0.80; R = 2.9×10^6				M = 0.90; R = 2.9×10^6				M = 1.20; R = 2.9×10^6			
-6.80	-0.470	0.0688	0.016	-6.93	-0.498	0.0778	0.026	-7.03	-0.550	0.0902	0.054	-6.67	-0.537	0.0890	0.119
-6.26	-.441	.0612	.017	-6.39	-.476	.0700	.026	-6.48	-.523	.0812	.052	-6.12	-.494	.0792	.107
-5.17	-.377	.0473	.016	-5.85	-.445	.0615	.025	-5.93	-.487	.0708	.048	-5.58	-.449	.0699	.096
-4.62	-.340	.0408	.014	-5.30	-.413	.0543	.024	-5.38	-.456	.0628	.047	-5.03	-.406	.0617	.085
-4.08	-.307	.0354	.013	-4.74	-.379	.0468	.023	-4.82	-.416	.0539	.042	-4.49	-.364	.0540	.078
-3.53	-.270	.0301	.011	-4.19	-.342	.0401	.021	-4.26	-.379	.0461	.039	-3.95	-.325	.0474	.066
-2.43	-.193	.0214	.007	-3.63	-.302	.0340	.018	-3.69	-.335	.0385	.032	-3.40	-.282	.0417	.056
-1.34	-.119	.0151	.003	-2.50	-.217	.0235	.012	-2.55	-.243	.0258	.021	-2.32	-.204	.0318	.039
-.78	-.060	.0129	.001	-1.38	-.134	.0162	.006	-1.41	-.150	.0172	.010	-1.23	-.123	.0252	.021
-.50	-.064	.0120	.001	-.81	-.088	.0135	.002	-.84	-.099	.0141	.005	-.77	-.082	.0231	.012
.25	-.010	.0106	-.002	-.52	-.066	.0123	.001	-.53	-.069	.0129	.002	-.49	-.059	.0222	.008
.90	.031	.0096	-.003	.25	-.009	.0106	-.003	.25	-.009	.0110	-.003	.25	-.010	.0208	-.003
2.01	.100	.0103	-.004	.92	.040	.0096	-.004	.94	.049	.0105	-.007	.82	.037	.0209	-.012
2.56	.137	.0111	-.005	2.07	.124	.0106	-.007	2.11	.146	.0114	-.013	1.92	.119	.0222	-.029
3.10	.169	.0120	-.006	2.62	.160	.0117	-.008	2.67	.187	.0128	-.016	2.46	.159	.0239	-.037
3.65	.204	.0130	-.007	3.17	.195	.0128	-.010	3.24	.230	.0148	-.019	3.00	.196	.0264	-.045
4.19	.237	.0150	-.008	3.73	.234	.0144	-.011	3.80	.273	.0176	-.023	3.54	.232	.0295	-.052
4.73	.268	.0168	-.009	4.29	.272	.0165	-.013	4.38	.324	.0220	-.031	4.08	.272	.0334	-.061
5.28	.304	.0191	-.011	4.84	.309	.0193	-.015	4.94	.367	.0264	-.036	4.62	.309	.0377	-.069
5.82	.337	.0220	-.012	5.40	.349	.0224	-.016	5.52	.418	.0327	-.045	5.16	.349	.0426	-.079
6.36	.370	.0249	-.013	5.96	.386	.0258	-.017	6.10	.478	.0418	-.059	5.71	.390	.0484	-.089
7.45	.434	.0322	-.014	6.52	.426	.0303	-.019	6.68	.533	.0514	-.070	6.25	.432	.0552	-.098
8.54	.502	.0484	-.015	7.63	.503	.0424	-.020	7.82	.630	.0731	-.089	7.33	.511	.0704	-.116
10.72	.642	.0967	-.019	8.77	.596	.0642	-.030	8.94	.705	.0967	-.098	8.42	.593	.0889	-.134
12.86	.741	.1442	-.021	10.88	.663	.1122	-.032					10.61	.736	.1343	-.156
14.98	.830	.1980	-.024	13.03	.764	.1626	-.041					12.75	.892	.1791	-.146
17.07	.896	.2533	-.028	15.13	.822	.2103	-.044								
18.09	.910	.2790	-.036	17.22	.884	.2651	-.059								
				18.26	.910	.2929	-.068								
M = 1.30; R = 2.9×10^6				M = 1.50; R = 2.9×10^6				M = 1.70; R = 2.9×10^6				M = 1.90; R = 2.9×10^6			
-6.61	-.462	.0829	.104	-6.55	-.388	.0727	.087	-6.49	-.333	.0663	.073	-6.43	-.293	.0607	.063
-6.07	-.429	.0747	.095	-6.01	-.397	.0656	.080	-5.96	-.308	.0603	.067	-5.91	-.272	.0555	.058
-5.54	-.394	.0669	.086	-5.48	-.328	.0591	.073	-5.43	-.283	.0547	.061	-5.38	-.249	.0506	.053
-5.00	-.358	.0598	.077	-4.95	-.300	.0532	.066	-4.90	-.260	.0498	.056	-4.86	-.227	.0462	.048
-4.46	-.323	.0532	.068	-4.42	-.271	.0478	.058	-4.37	-.234	.0451	.050	-4.33	-.207	.0422	.043
-3.92	-.289	.0474	.060	-3.88	-.242	.0430	.051	-3.85	-.210	.0409	.044	-3.81	-.185	.0386	.038
-3.38	-.252	.0421	.051	-3.35	-.212	.0385	.044	-3.32	-.186	.0372	.038	-3.29	-.164	.0353	.033
-2.30	-.179	.0333	.033	-2.82	-.182	.0345	.036	-2.79	-.159	.0337	.032	-2.76	-.143	.0324	.028
-1.22	-.106	.0269	.018	-2.28	-.152	.0311	.029	-2.26	-.136	.0309	.026	-2.24	-.120	.0299	.023
-.76	-.069	.0247	.010	-1.21	-.092	.0260	.015	-1.20	-.080	.0264	.013	-1.19	-.075	.0260	.013
-.49	-.053	.0238	.007	-.76	-.062	.0244	.008	-.74	-.053	.0248	.007	-.74	-.051	.0247	.007
.25	-.009	.0225	-.002	-.48	-.046	.0237	.005	-.47	-.040	.0242	.004	-.47	-.041	.0242	.004
.82	.032	.0221	-.011	-.03	-.025	.0230	0	.25	-.007	.0233	-.003	.25	-.013	.0232	-.002
1.91	.106	.0241	-.027	.26	-.005	.0226	-.004	.79	.018	.0232	-.009	.78	.009	.0229	-.007
2.45	.142	.0260	-.035	.81	.027	.0220	-.011	1.88	.075	.0250	-.021	1.86	.057	.0244	-.017
2.99	.178	.0286	-.042	1.90	.089	.0241	-.024	2.41	.100	.0264	-.026	2.39	.080	.0256	-.022
3.53	.213	.0316	-.050	2.43	.118	.0256	-.030	2.94	.124	.0281	-.031	2.91	.102	.0271	-.026
4.07	.247	.0351	-.058	2.97	.148	.0277	-.036	3.47	.149	.0302	-.036	3.44	.124	.0290	-.031
4.60	.279	.0390	-.066	3.50	.180	.0304	-.043	4.00	.175	.0328	-.041	3.96	.146	.0312	-.035
5.14	.316	.0439	-.074	4.04	.207	.0333	-.050	4.53	.200	.0359	-.046	4.48	.167	.0337	-.039
5.68	.348	.0491	-.082	4.57	.236	.0368	-.056	5.06	.226	.0393	-.052	5.01	.189	.0367	-.044
6.22	.384	.0552	-.090	5.10	.266	.0409	-.063	5.59	.250	.0431	-.057	5.53	.211	.0400	-.048
7.29	.448	.0683	-.104	5.64	.294	.0454	-.069	6.11	.274	.0473	-.062	6.06	.233	.0438	-.053
8.36	.512	.0838	-.117	6.17	.321	.0502	-.075	7.17	.322	.0570	-.072	7.11	.275	.0521	-.061
10.50	.635	.1212	-.143	7.24	.379	.0617	-.088	8.23	.369	.0683	-.082	8.16	.318	.0620	-.070
12.64	.750	.1666	-.165	8.30	.432	.0745	-.100	10.34	.463	.0958	-.102	10.26	.402	.0864	-.087
				10.42	.536	.1059	-.121	12.45	.551	.1292	-.119	12.35	.483	.1161	-.103
				12.55	.638	.1446	-.142	14.56	.639	.1695	-.136	14.45	.561	.1518	-.117
				14.68	.737	.1908	-.162	16.68	.724	.2165	-.150	16.55	.633	.1917	-.126
												17.60	.673	.2154	-.133

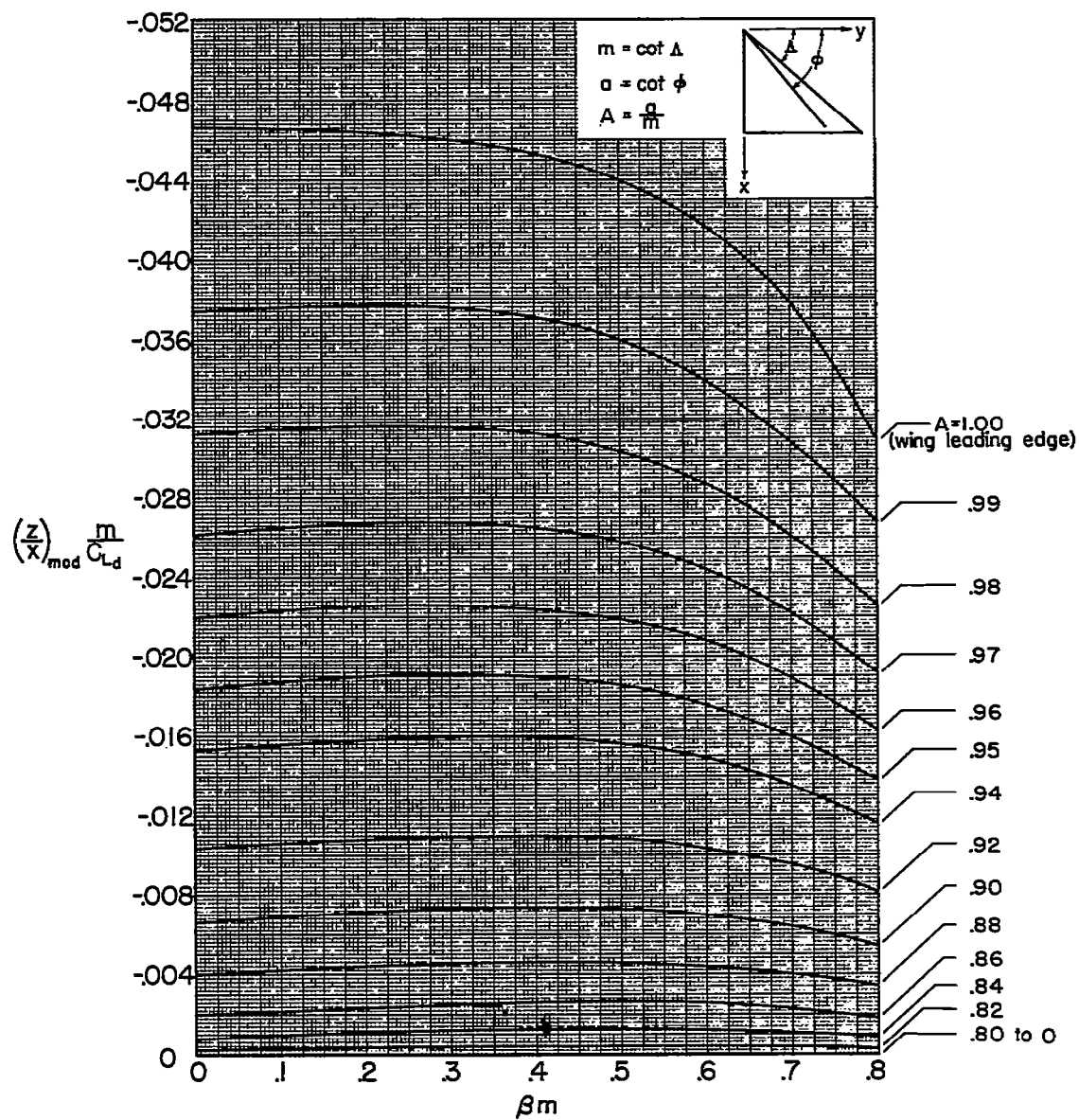
TABLE XV.- DATA FOR WING OF ASPECT RATIO 3 WITH 45° SWEEPBACK, 5 PERCENT THICK WITH MODIFIED LEADING EDGE, CONICALLY CAMBERED FOR $C_{Ld} = 0.292$ AT $M = 1.0$

(a) Fixed transition

α	C_L	C_D	C_m	α	C_L	C_D	C_m	α	C_L	C_D	C_m	α	C_L	C_D	C_m
M = 0.60; R = 2.9x10 ⁶				M = 0.80; R = 2.9x10 ⁶				M = 0.90; R = 2.9x10 ⁶				M = 1.20; R = 2.9x10 ⁶			
-6.84	-0.470	0.0683	0.018	-6.95	-0.507	0.0785	0.026	-7.00	-0.543	0.0895	0.049	-6.66	-0.532	0.0890	0.116
-6.29	-0.441	0.0607	0.018	-6.40	-0.474	0.0694	0.025	-6.47	-0.518	0.0809	0.050	-6.12	-0.490	0.0794	0.106
-5.76	-0.409	0.0515	0.018	-5.87	-0.446	0.0618	0.025	-5.92	-0.485	0.0717	0.047	-5.58	-0.446	0.0702	0.094
-5.21	-0.375	0.0468	0.016	-5.31	-0.414	0.0545	0.025	-5.36	-0.452	0.0631	0.044	-5.03	-0.403	0.0626	0.084
-4.66	-0.340	0.0408	0.015	-4.76	-0.380	0.0476	0.024	-4.80	-0.416	0.0549	0.041	-4.49	-0.365	0.0588	0.075
-4.12	-0.307	0.0354	0.014	-4.21	-0.346	0.0415	0.022	-4.25	-0.378	0.0474	0.037	-3.95	-0.325	0.0492	0.066
-3.58	-0.272	0.0306	0.012	-3.65	-0.309	0.0353	0.019	-3.70	-0.343	0.0408	0.036	-3.41	-0.285	0.0436	0.057
-2.48	-0.195	0.0223	0.008	-2.53	-0.221	0.0255	0.013	-2.56	-0.256	0.0290	0.025	-2.32	-0.207	0.0344	0.039
-1.39	-0.123	0.0166	0.005	-1.42	-0.141	0.0189	0.008	-1.42	-0.159	0.0200	0.013	-1.24	-0.128	0.0276	0.023
-0.81	-0.084	0.0148	0.003	-0.86	-0.103	0.0165	0.006	-0.85	-0.111	0.0172	0.009	-0.70	-0.088	0.0256	0.015
-0.24	-0.053	0.0140	0.002	-0.27	-0.079	0.0158	0.004	-0.27	-0.084	0.0159	0.006	-0.50	-0.064	0.0248	0.010
0.85	0.032	0.0130	0.002	0.88	0.038	0.0131	0.003	0.87	0.043	0.0138	0.004	0.82	0.038	0.0239	0.011
1.97	0.101	0.0140	-0.003	2.03	0.122	0.0143	-0.006	2.10	0.141	0.0150	-0.010	1.92	0.117	0.0258	-0.026
2.51	0.136	0.0147	-0.004	2.59	0.166	0.0153	-0.008	3.24	0.235	0.0190	-0.018	2.47	0.150	0.0277	-0.035
3.04	0.171	0.0157	-0.005	3.14	0.198	0.0164	-0.009	3.80	0.277	0.0217	-0.022	3.01	0.199	0.0304	-0.043
3.61	0.214	0.0170	-0.007	3.70	0.238	0.0179	-0.011	4.37	0.323	0.0257	-0.028	3.55	0.239	0.0334	-0.052
4.14	0.241	0.0180	-0.007	4.29	0.277	0.0205	-0.012	4.95	0.376	0.0316	-0.037	4.10	0.279	0.0376	-0.061
4.68	0.272	0.0203	-0.008	4.81	0.315	0.0230	-0.014	5.51	0.423	0.0375	-0.045	4.64	0.319	0.0418	-0.070
5.22	0.310	0.0227	-0.010	5.36	0.350	0.0258	-0.015	6.05	0.473	0.0431	-0.055	5.17	0.354	0.0464	-0.078
5.77	0.338	0.0251	-0.010	5.93	0.392	0.0291	-0.017	6.66	0.528	0.0535	-0.065	5.72	0.393	0.0522	-0.087
6.30	0.370	0.0278	-0.012	6.48	0.430	0.0334	-0.018	7.80	0.626	0.0767	-0.086	6.26	0.431	0.0587	-0.095
7.39	0.436	0.0344	-0.014	7.59	0.514	0.0476	-0.021					7.34	0.510	0.0737	-0.113
8.48	0.502	0.0440	-0.015	8.72	0.601	0.0689	-0.032					8.45	0.588	0.0918	-0.129
10.64	0.634	0.0866	-0.020	10.84	0.675	0.1158	-0.031								
12.81	0.755	0.1433	-0.023	12.97	0.765	0.1650	-0.042								
14.89	0.817	0.1952	-0.023	15.07	0.823	0.2124	-0.044								
17.00	0.890	0.2525	-0.028	17.16	0.876	0.2640	-0.056								
18.01	0.904	0.2769	-0.033	18.18	0.902	0.2911	-0.065								
M = 1.30; R = 2.9x10 ⁶				M = 1.50; R = 2.9x10 ⁶				M = 1.70; R = 2.9x10 ⁶				M = 1.90; R = 2.9x10 ⁶			
-6.58	-0.453	0.0822	0.102	-6.54	-0.381	0.0737	0.066	-6.48	-0.329	0.0677	0.072	-6.42	-0.293	0.0630	0.063
-5.52	-0.421	0.0745	0.094	-6.01	-0.356	0.0673	0.080	-5.96	-0.308	0.0622	0.067	-5.90	-0.271	0.0580	0.059
-4.98	-0.387	0.0672	0.085	-5.48	-0.327	0.0611	0.073	-5.43	-0.281	0.0566	0.061	-5.38	-0.250	0.0534	0.053
-4.44	-0.352	0.0603	0.076	-4.95	-0.300	0.0555	0.066	-4.90	-0.256	0.0518	0.055	-4.86	-0.229	0.0492	0.049
-3.91	-0.320	0.0544	0.068	-4.42	-0.271	0.0502	0.059	-4.37	-0.233	0.0473	0.049	-4.33	-0.208	0.0452	0.044
-3.37	-0.285	0.0487	0.060	-3.88	-0.241	0.0453	0.052	-3.84	-0.210	0.0434	0.044	-3.81	-0.186	0.0416	0.038
-2.80	-0.250	0.0436	0.051	-3.35	-0.214	0.0411	0.045	-3.32	-0.185	0.0398	0.038	-3.28	-0.165	0.0385	0.034
-2.30	-0.179	0.0353	0.034	-2.28	-0.153	0.0340	0.030	-2.26	-0.134	0.0336	0.026	-2.24	-0.121	0.0333	0.023
-1.22	-0.111	0.0295	0.019	-1.22	-0.095	0.0289	0.016	-1.20	-0.084	0.0293	0.014	-1.19	-0.077	0.0295	0.013
-0.76	-0.072	0.0276	0.011	-0.76	-0.062	0.0273	0.009	-0.74	-0.054	0.0278	0.008	-0.74	-0.053	0.0284	0.007
-0.49	-0.054	0.0268	0.006	-0.48	-0.045	0.0259	0.006	-0.47	-0.041	0.0273	0.004	-0.47	-0.041	0.0279	0.005
0.26	-0.004	0.0256	-0.003	0.26	-0.003	0.0259	-0.004	0.26	-0.003	0.0264	-0.004	0.26	-0.024	0.0273	0.001
0.82	0.035	0.0261	-0.011	0.81	0.030	0.0254	-0.011	0.80	0.022	0.0265	-0.010	0.84	-0.013	0.0271	-0.002
1.91	0.107	0.0278	-0.027	1.90	0.091	0.0277	-0.025	1.88	0.076	0.0286	-0.021	1.78	0.010	0.0269	-0.007
2.45	0.145	0.0298	-0.035	2.43	0.120	0.0294	-0.032	2.41	0.100	0.0299	-0.027	1.86	0.057	0.0282	-0.017
2.99	0.180	0.0322	-0.043	2.97	0.150	0.0314	-0.038	2.94	0.126	0.0316	-0.032	2.99	0.081	0.0292	-0.022
3.52	0.215	0.0353	-0.051	3.50	0.180	0.0340	-0.045	3.47	0.150	0.0336	-0.037	2.91	0.102	0.0307	-0.026
4.06	0.248	0.0387	-0.059	4.04	0.209	0.0369	-0.051	4.00	0.175	0.0361	-0.042	3.44	0.124	0.0325	-0.031
4.60	0.283	0.0429	-0.067	4.57	0.237	0.0402	-0.057	4.53	0.200	0.0390	-0.047	3.96	0.145	0.0346	-0.035
5.14	0.318	0.0478	-0.074	5.10	0.264	0.0441	-0.063	5.06	0.224	0.0423	-0.051	4.49	0.167	0.0371	-0.039
5.67	0.350	0.0528	-0.082	5.64	0.294	0.0487	-0.069	5.59	0.251	0.0463	-0.057	5.01	0.188	0.0400	-0.044
6.20	0.379	0.0581	-0.088	6.17	0.320	0.0534	-0.074	6.11	0.274	0.0503	-0.062	5.54	0.210	0.0433	-0.048
7.27	0.443	0.0712	-0.102	7.23	0.374	0.0644	-0.086	7.17	0.321	0.0599	-0.072	6.06	0.231	0.0468	-0.052
8.34	0.507	0.0865	-0.115	8.29	0.426	0.0774	-0.097	8.23	0.368	0.0712	-0.082	7.11	0.275	0.0557	-0.061
10.48	0.627	0.1231	-0.140	10.42	0.529	0.1083	-0.119	10.34	0.462	0.0986	-0.101	8.16	0.317	0.0654	-0.070
12.61	0.740	0.1677	-0.162	12.57	0.629	0.1469	-0.139	12.45	0.551	0.1323	-0.119	10.26	0.399	0.0890	-0.086
14.51	0.824	0.2114	-0.178	14.66	0.728	0.1924	-0.159	14.56	0.639	0.1725	-0.137	12.36	0.480	0.1192	-0.102
								16.68	0.725	0.2195	-0.152	14.45	0.556	0.1538	-0.116
												16.56	0.635	0.1956	-0.129
												17.61	0.673	0.2190	-0.136

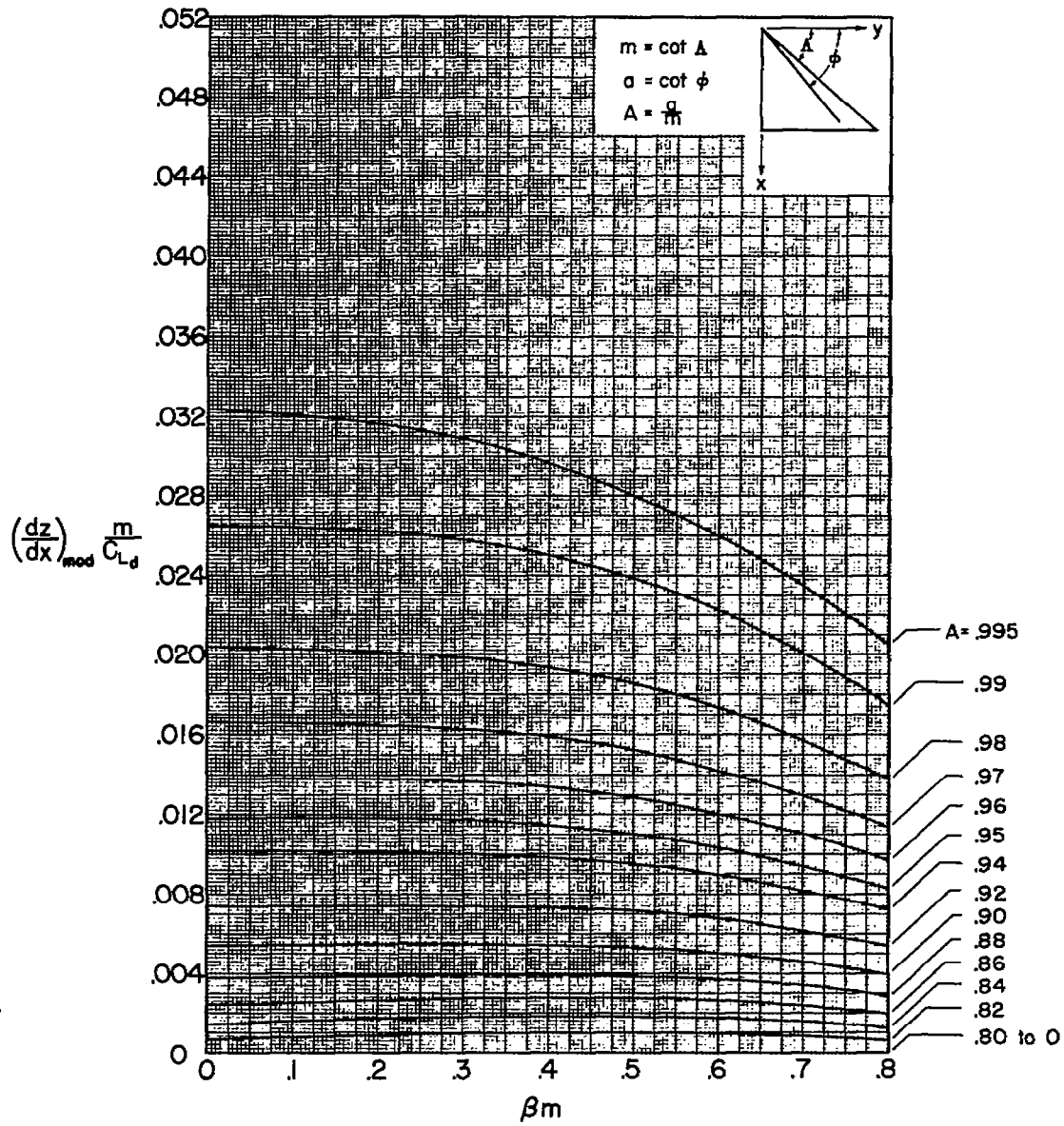
[REDACTED]

[REDACTED]



(a) Ordinates.

Figure 1.- Design charts for the determination of a modified conically cambered surface.



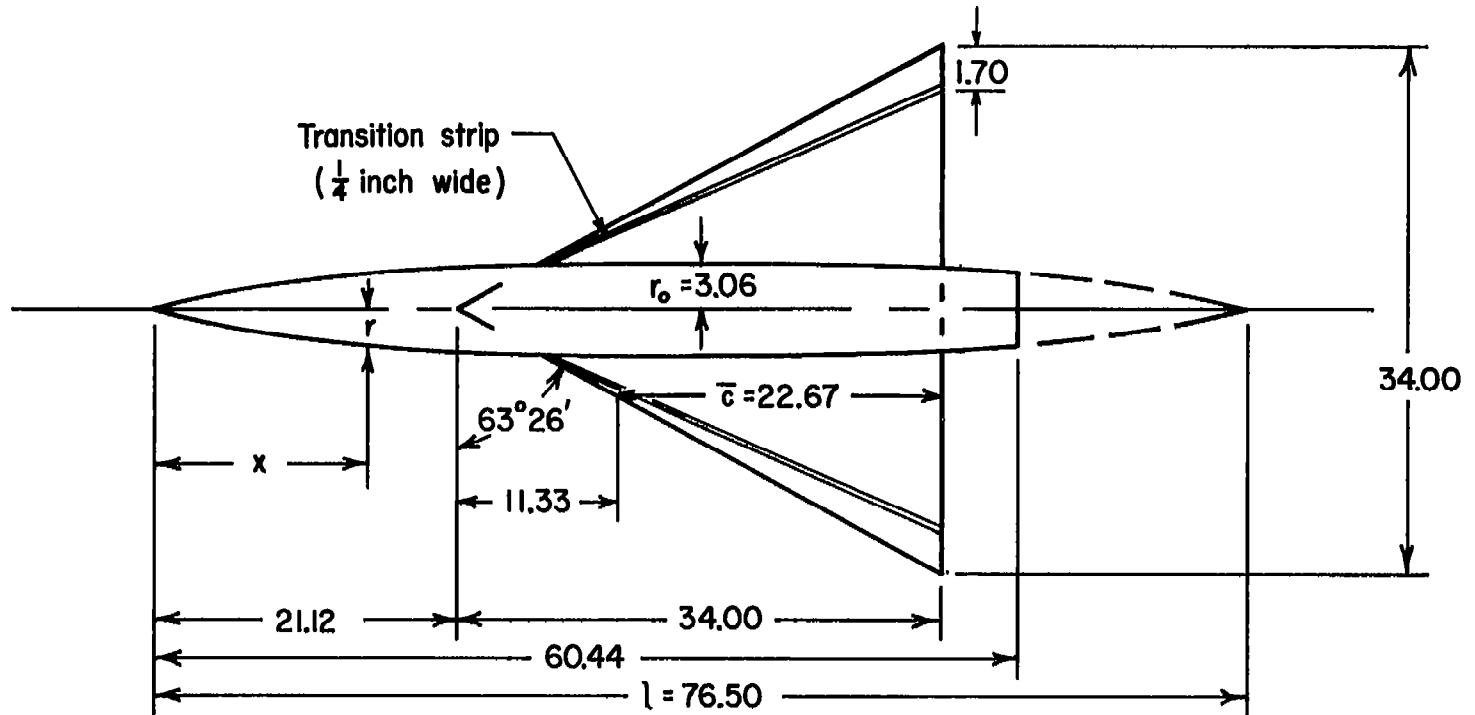
(b) Slopes.

Figure 1.- Concluded.

Equation of fuselage ordinates

$$\frac{r}{r_0} = \left[1 - \left(1 - \frac{2x}{l} \right)^2 \right]^{\frac{3}{4}}$$

All dimensions in inches
unless otherwise noted



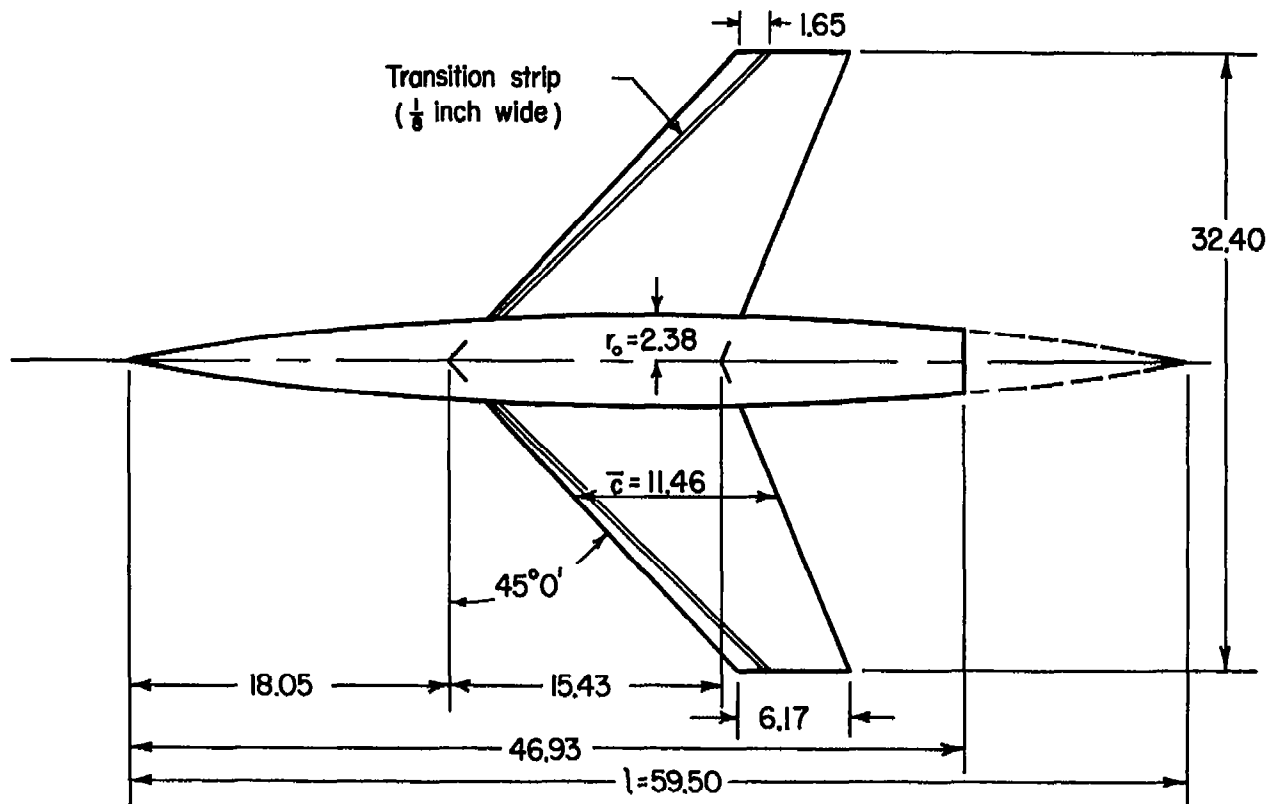
(a) Triangular wing.

Figure 2.- Dimensional sketches of models.

See figure 2 (a) for equation
of fuselage ordinates

All dimensions in inches
unless otherwise noted

60



(b) Sweptback wing.

Figure 2.- Concluded.

NACA RM A55G19

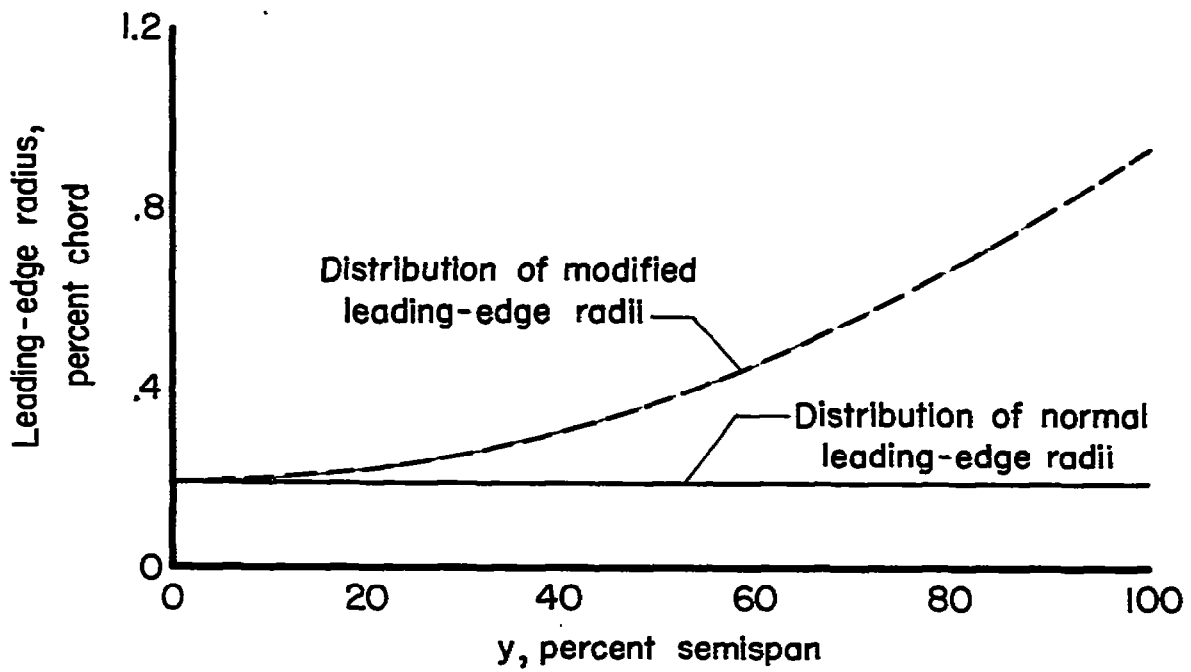
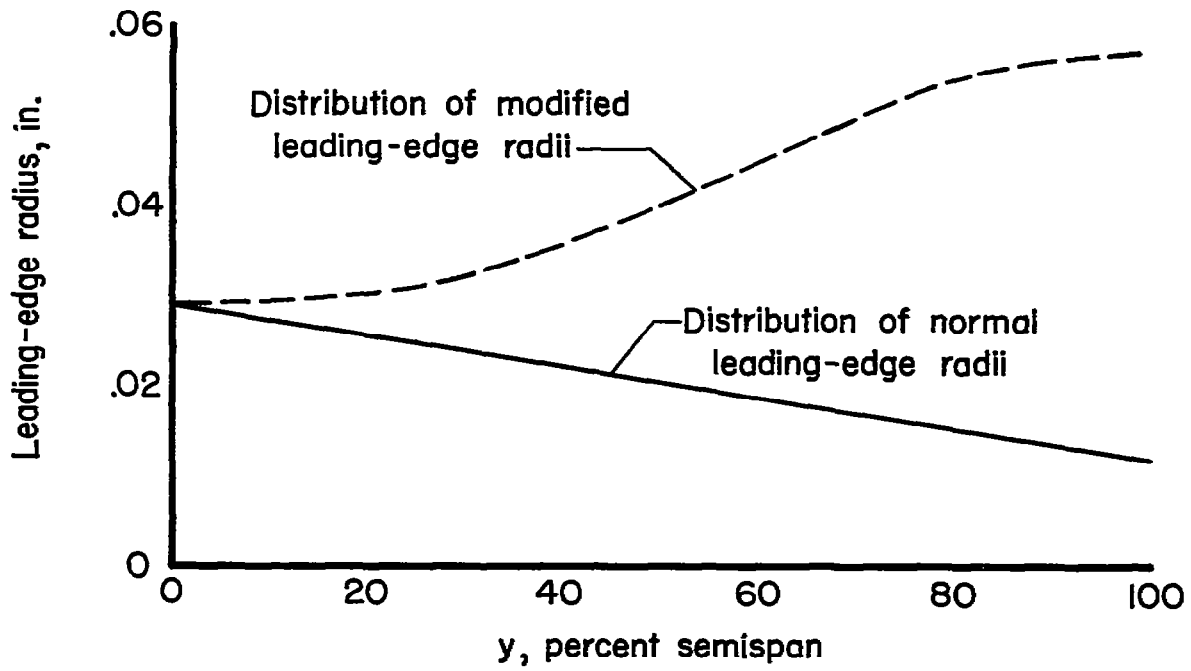
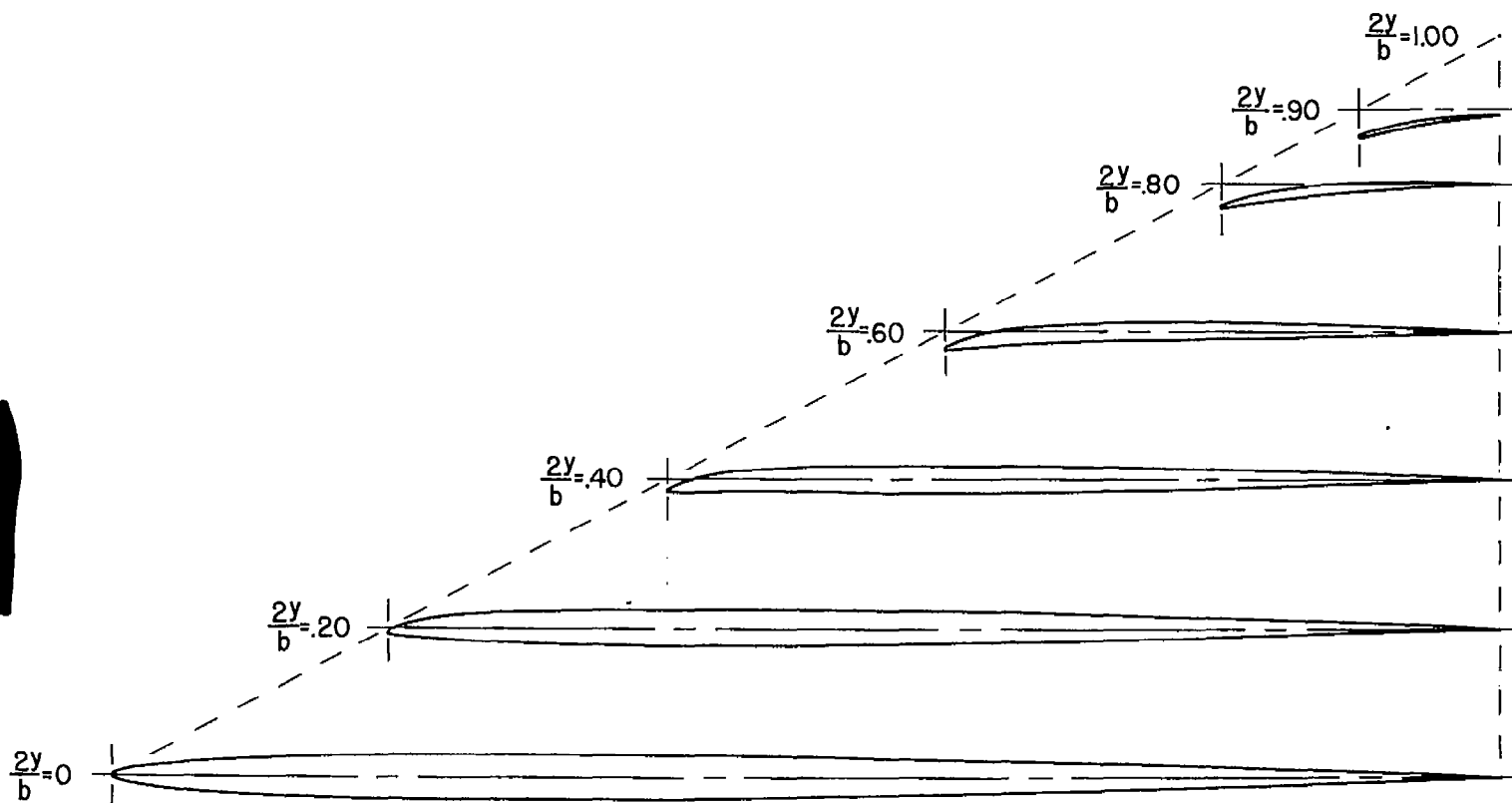
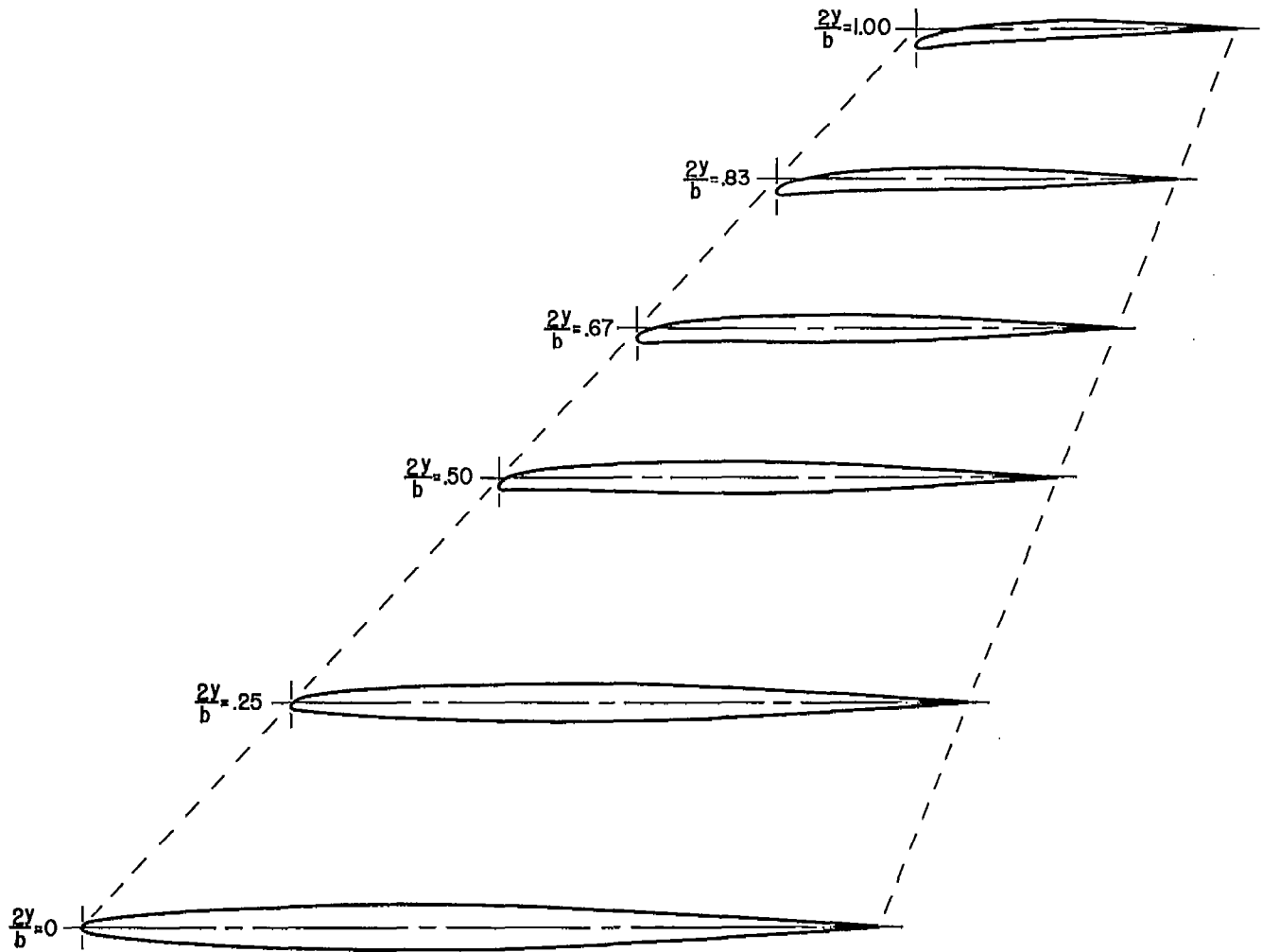


Figure 3.- Comparison of normal and modified leading-edge radii for sweptback wing.



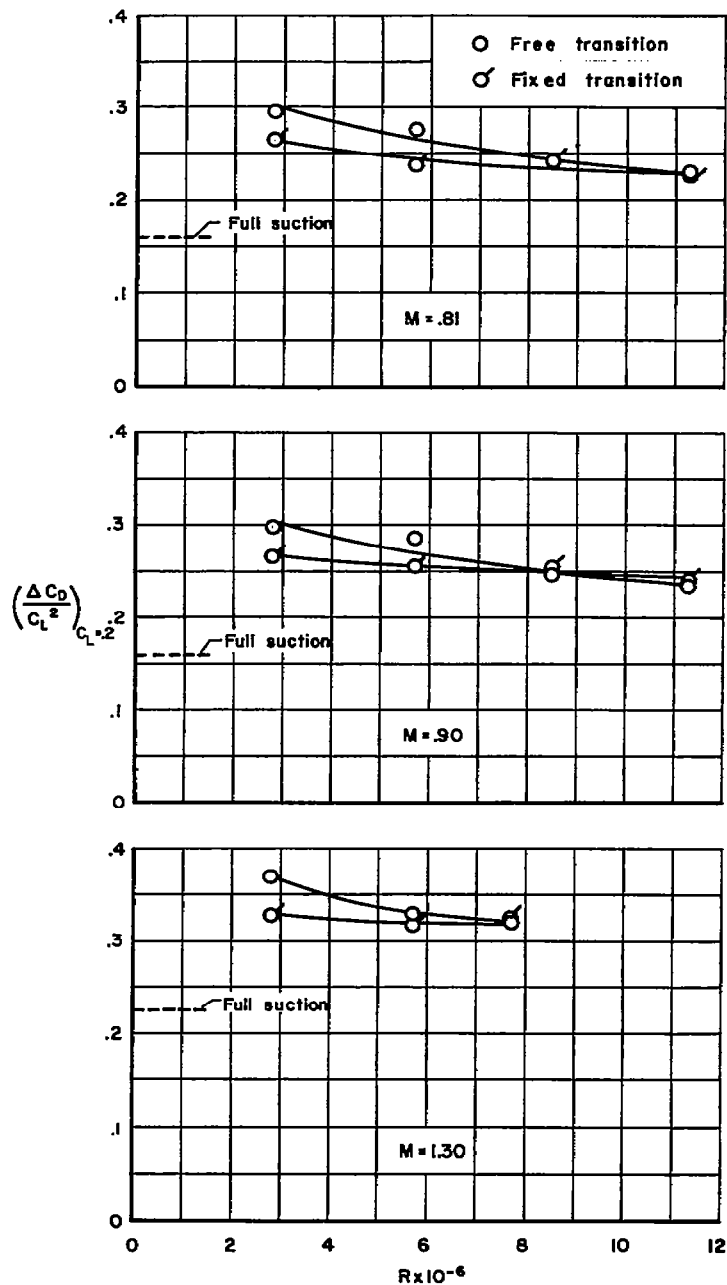
(a) Triangular wing; $C_{L_d} = 0.215$

Figure 4.- Representative airfoil sections for conically cambered wings.



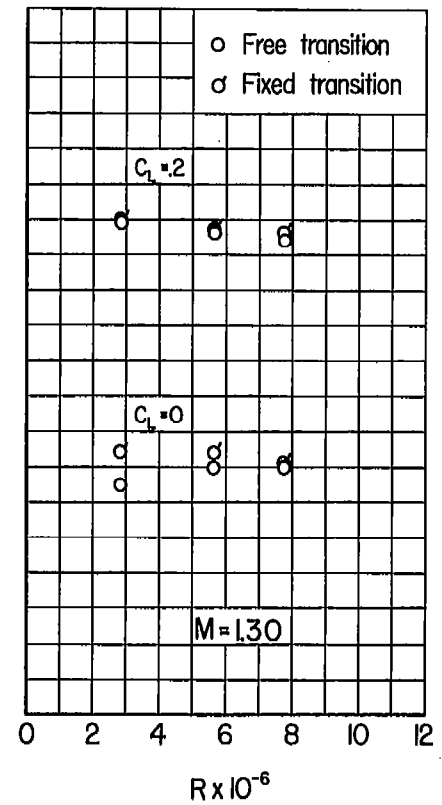
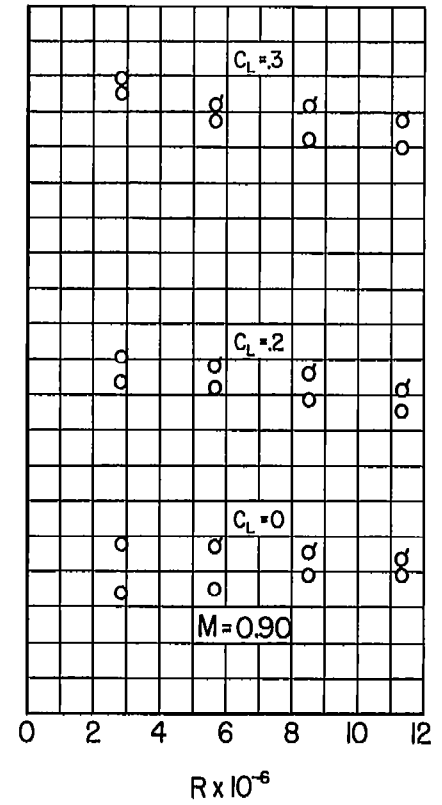
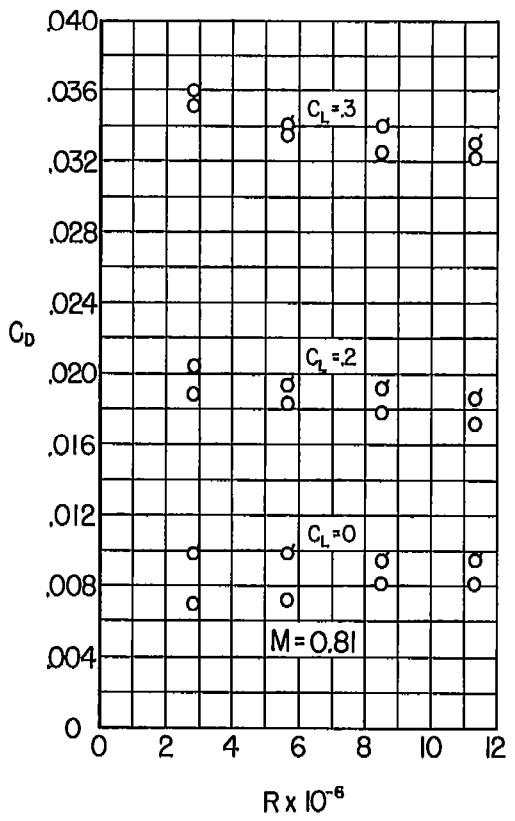
(b) Sweptback wing; $C_{L_d} = 0.292$

Figure 4.- Concluded.



(a) $\frac{\Delta C_D}{C_L^2}$ vs. Reynolds number.

Figure 5.- Effect of fixing transition on the variation of drag characteristics with Reynolds number for a 5-percent-thick plane triangular wing.



(b) C_D vs. Reynolds number.

Figure 5.- Concluded.

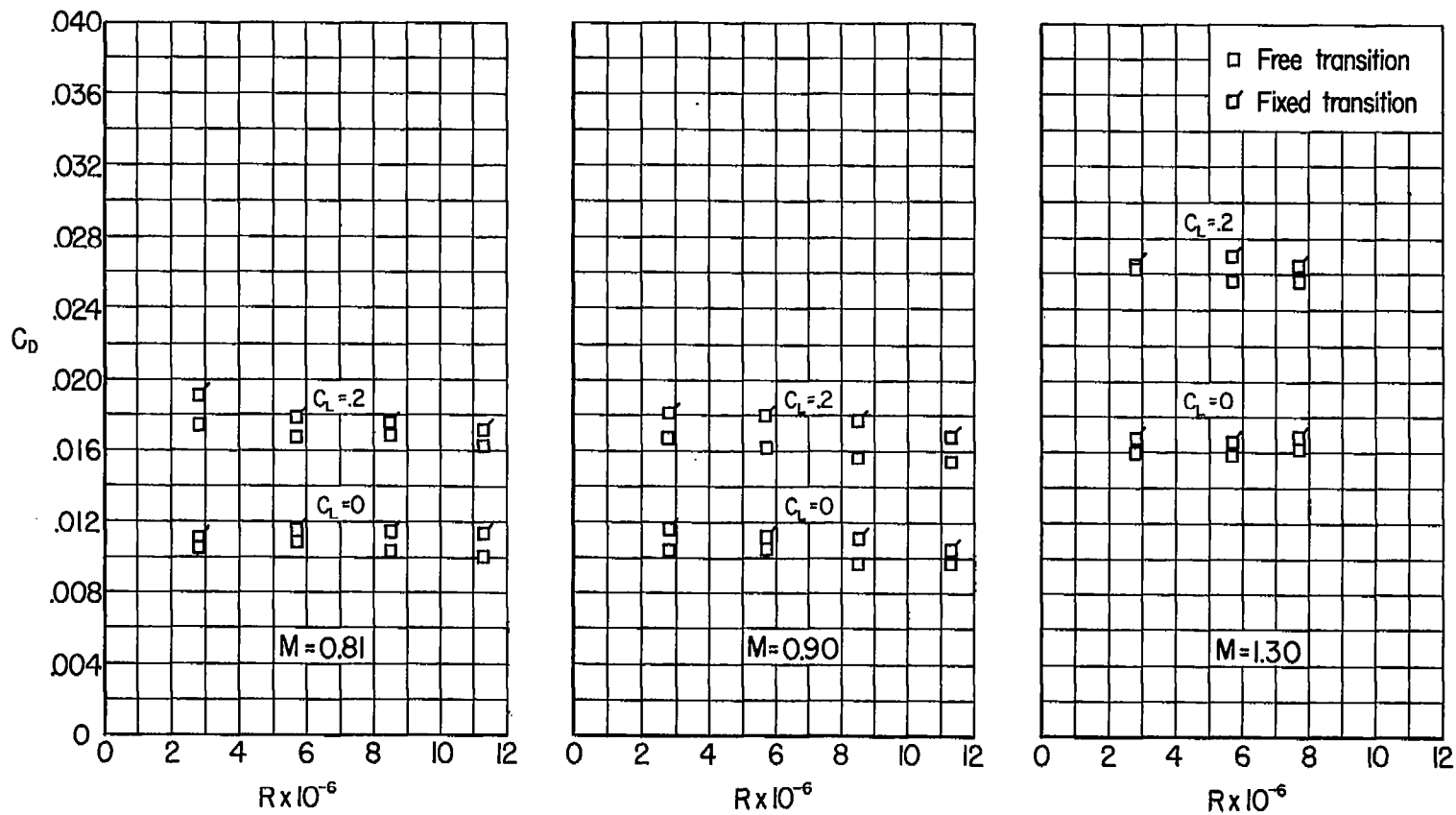


Figure 6.- Effect of fixing transition on the variation of drag coefficient with Reynolds number for a 5-percent-thick triangular wing with conical camber.

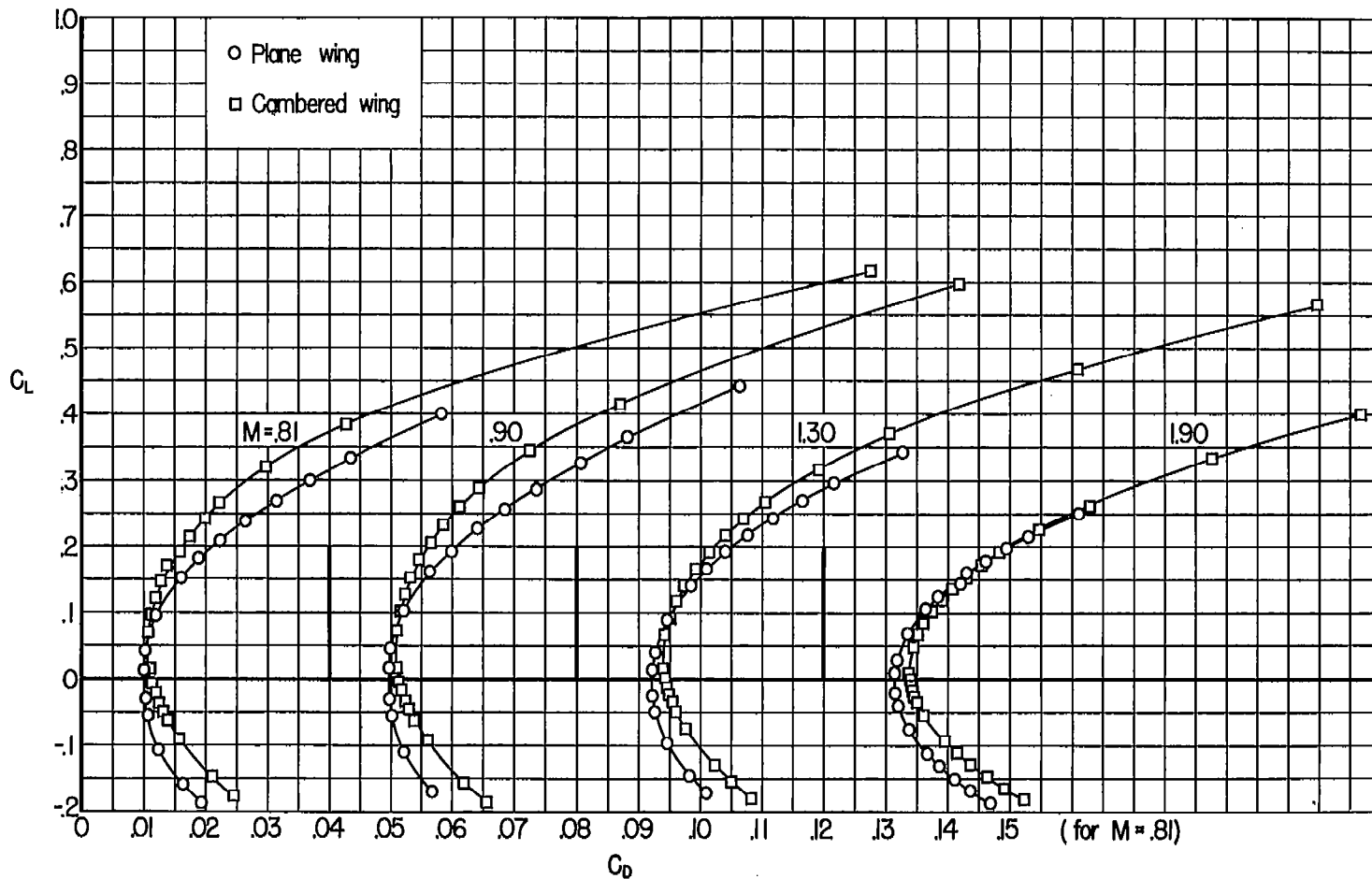


Figure 7.- Effect of conical camber on the variation of drag coefficient with lift coefficient for a 3-percent-thick triangular wing with fixed transition; $R = 5.6 \times 10^6$.

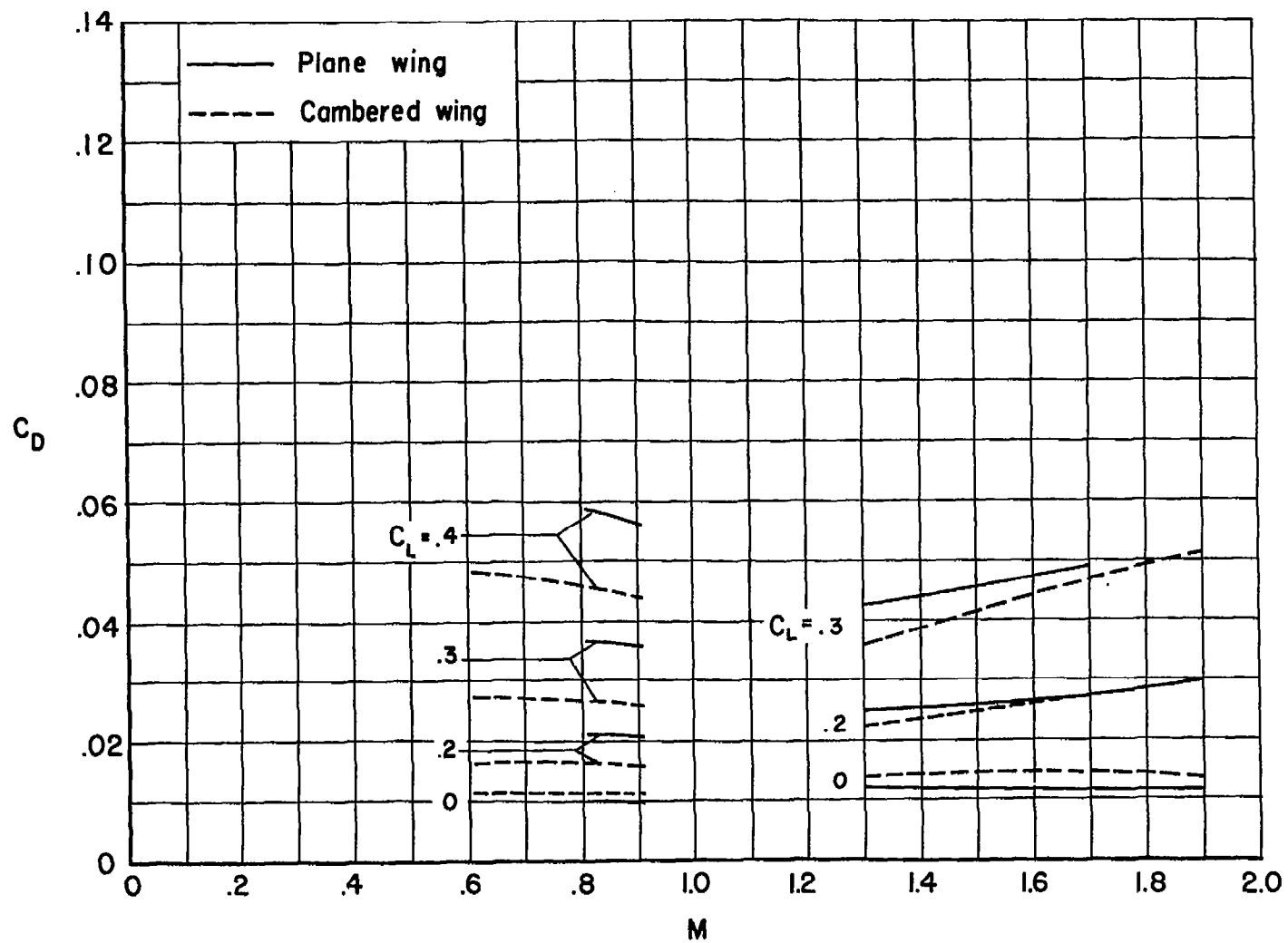


Figure 8.- Effect of conical camber on the variation of drag coefficient with Mach number for a 3-percent-thick triangular wing at several lift coefficients with fixed transition; $R = 5.6 \times 10^6$.

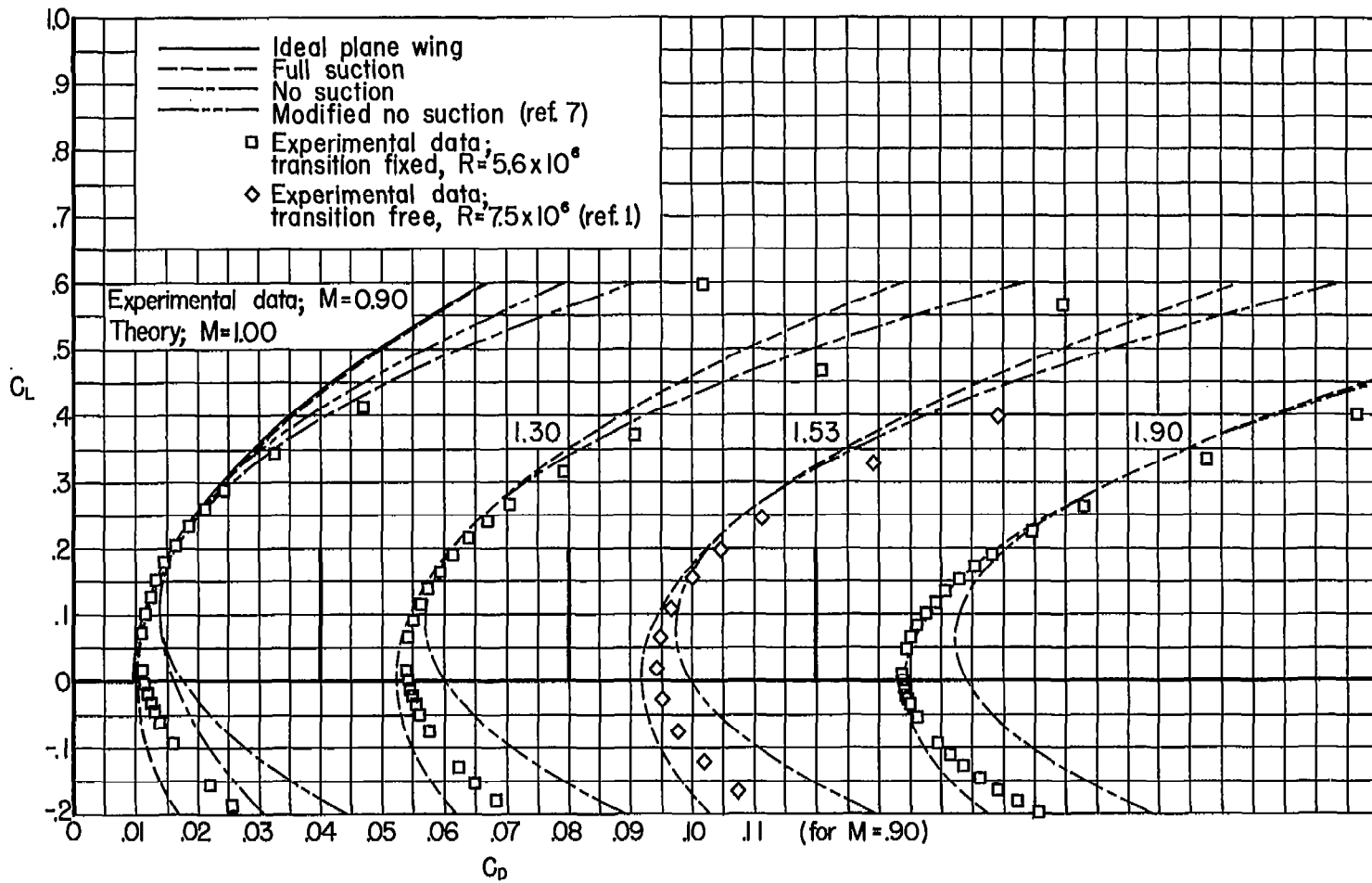
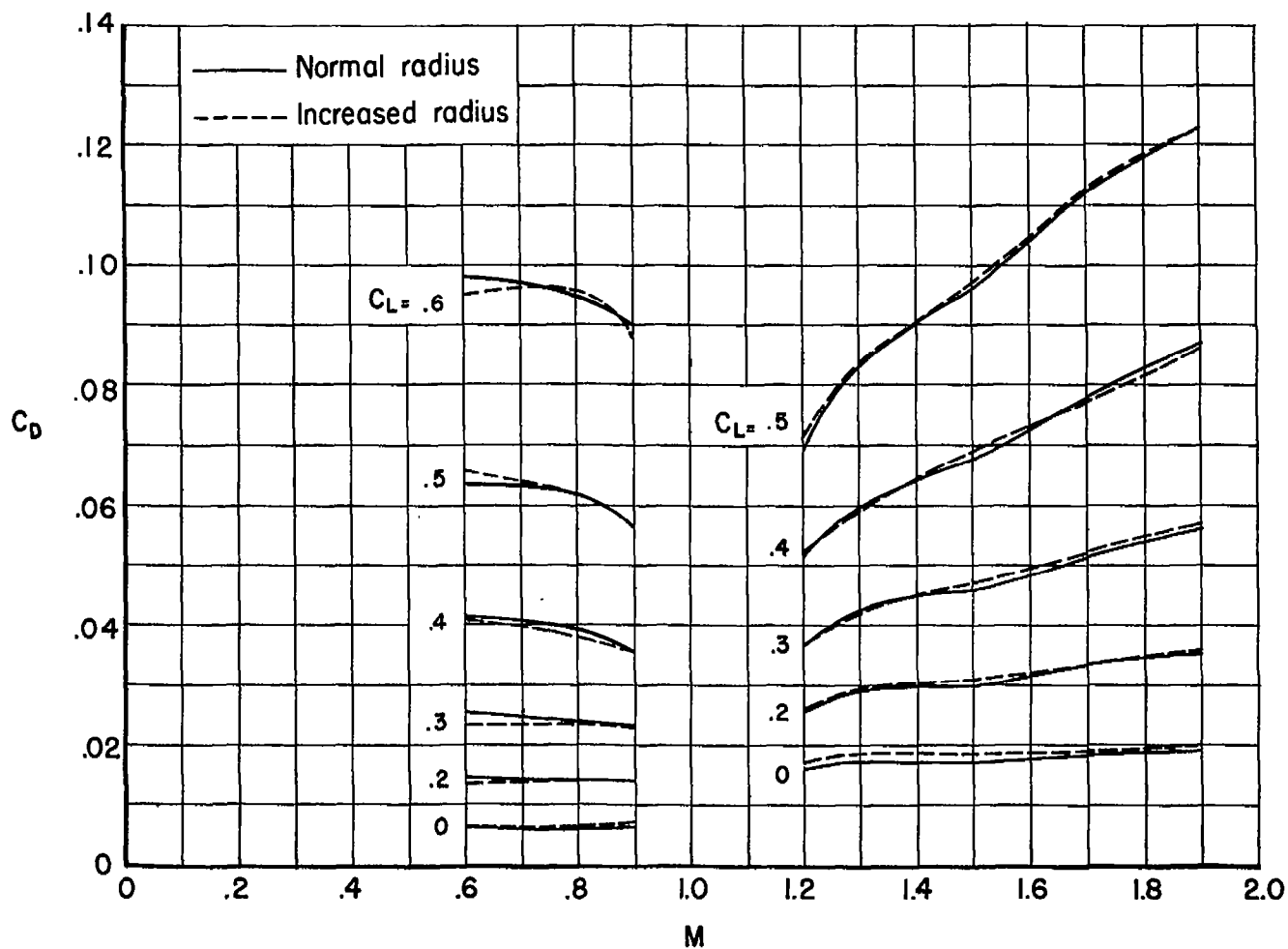
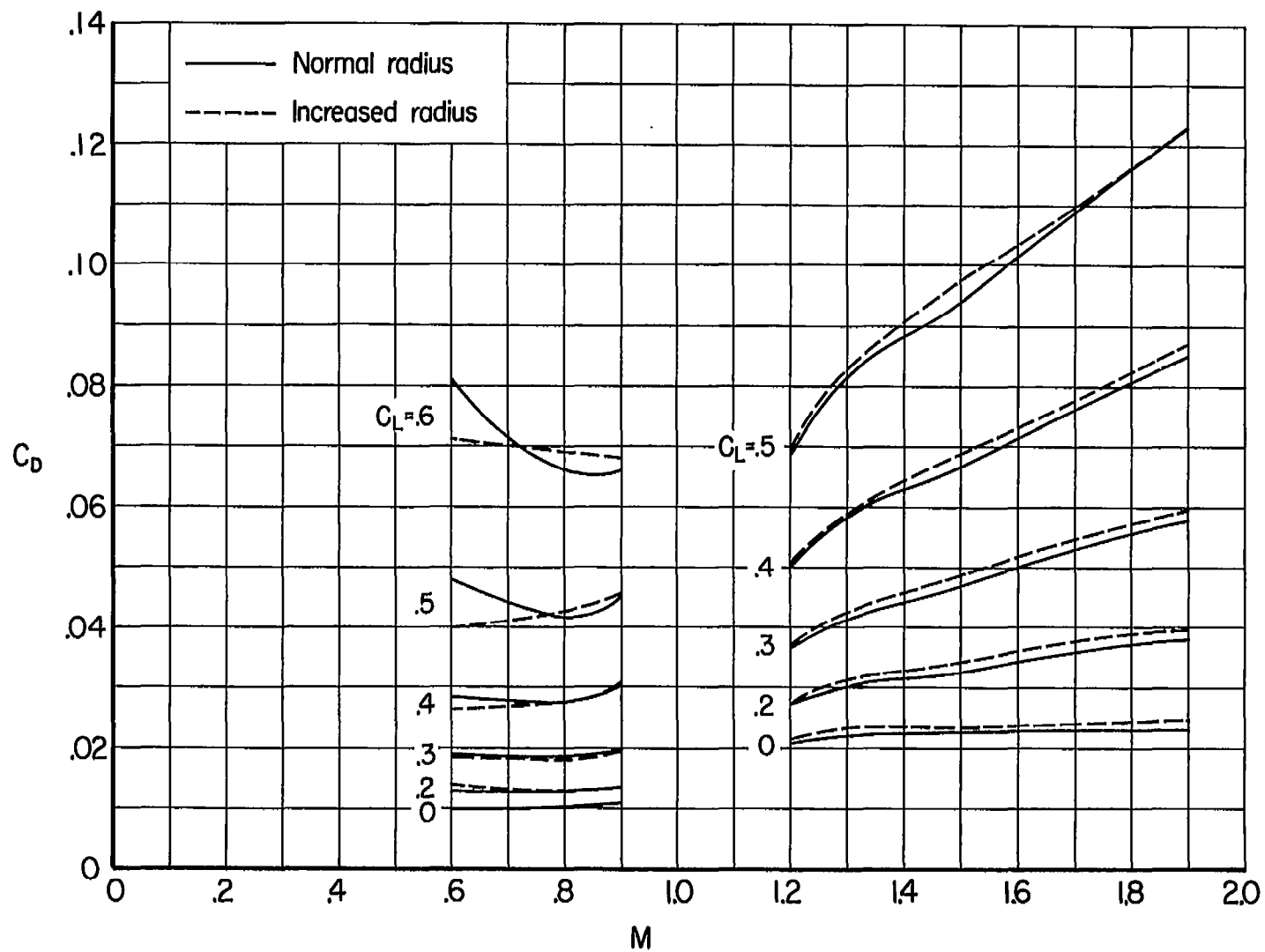


Figure 9.- Comparison of experimental drag polars with theoretical drag polars computed from lifting-surface theory for a triangular wing with conical camber.



(a) Plane wing.

Figure 10.- Effect of the leading-edge modification on the variation of drag coefficient with Mach number for a 5-percent-thick sweptback wing at several lift coefficients with free transition; $R = 2.9 \times 10^6$.



(b) Wing cambered for $C_{L_d} = 0.292$

Figure 10.- Concluded.

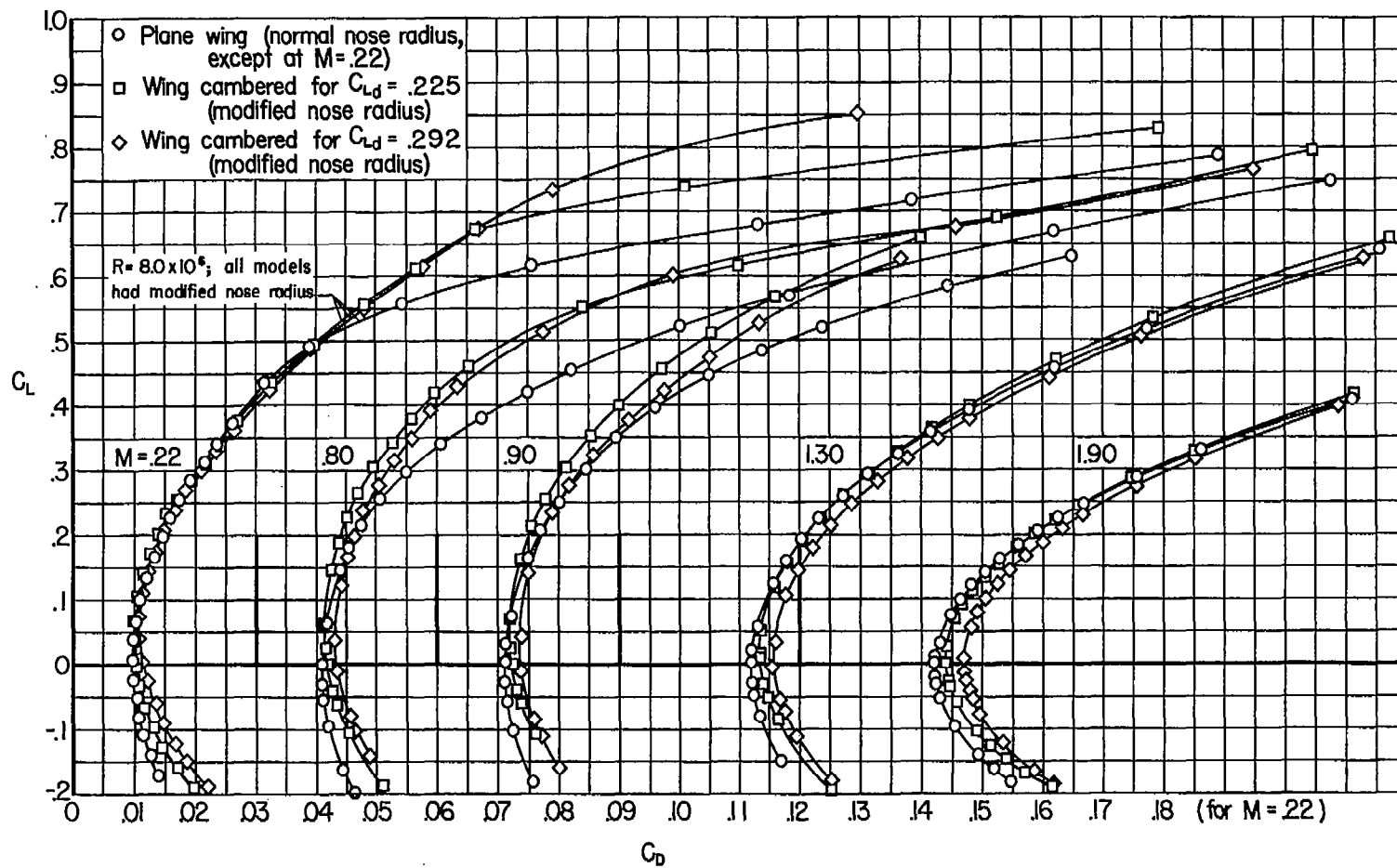


Figure 11.- Effect of conical camber on the variation of drag coefficient with lift coefficient for a 5-percent-thick sweptback wing with fixed transition; $R = 2.9 \times 10^8$ except as noted.

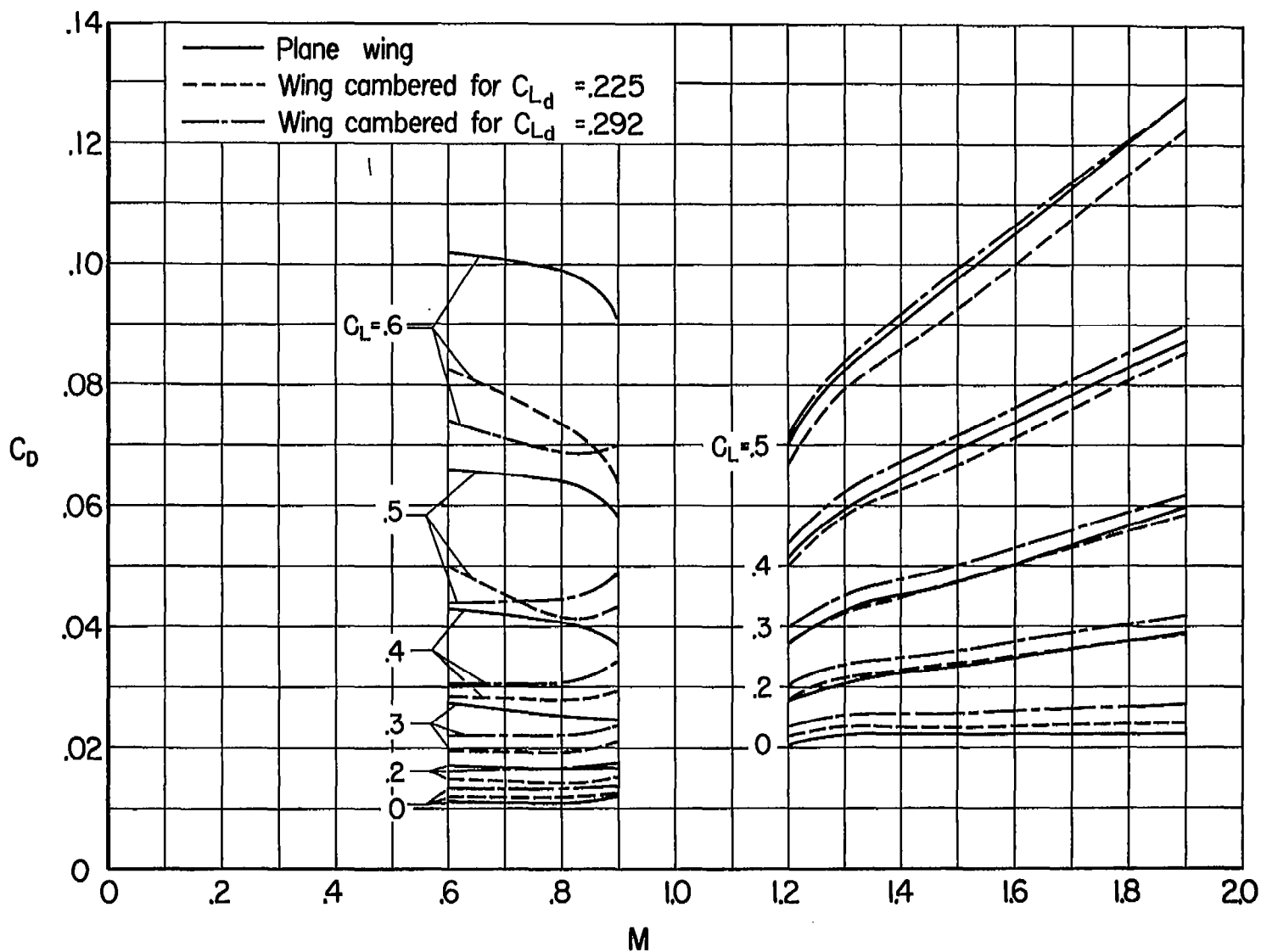
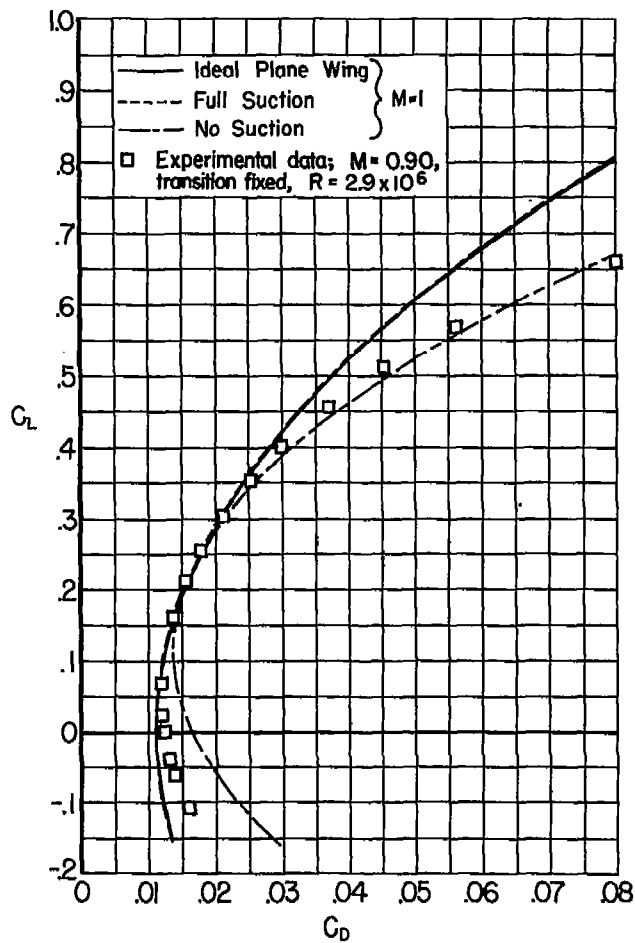
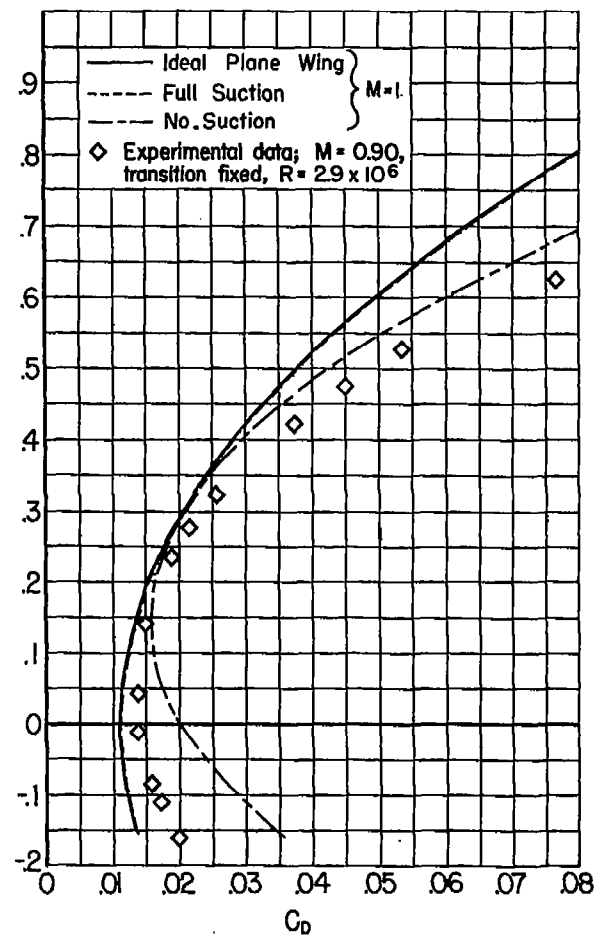


Figure 12.- Effect of conical camber on the variation of drag coefficient with Mach number for a 5-percent-thick sweptback wing at several lift coefficients with fixed transition; $R = 2.9 \times 10^6$.



(a) $C_{Ld} = 0.225$



(b) $C_{Ld} = 0.292$

Figure 13.- Comparison of experimental drag polars obtained at $M = 0.90$ with theoretical polars computed from lifting-surface theory at $M = 1.0$ for 5-percent-thick sweptback wings with conical camber.

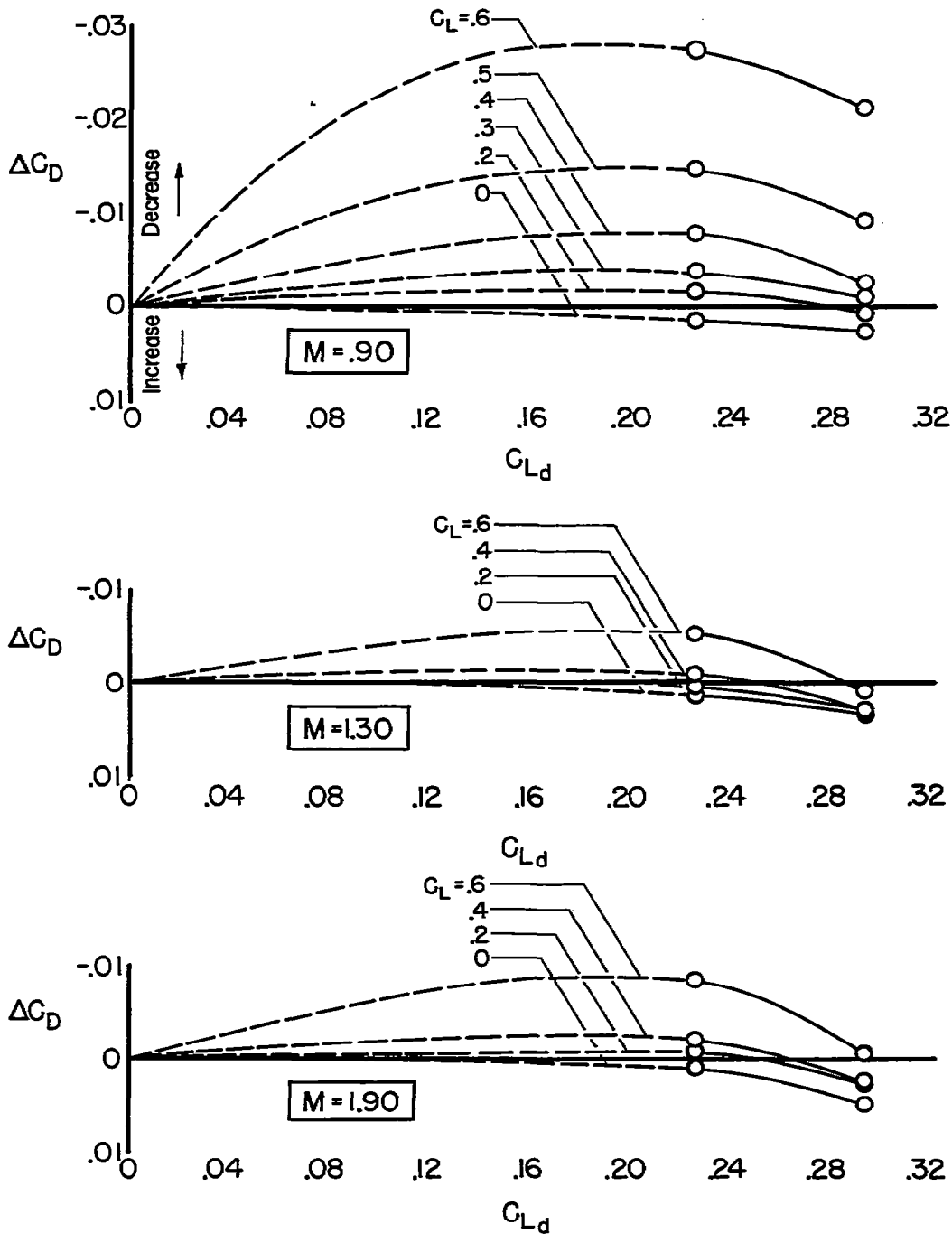


Figure 14.- Variation of incremental drag coefficient due to camber with design lift coefficient for a 5-percent-thick 45° sweptback wing with fixed transition; $R = 2.9 \times 10^6$.

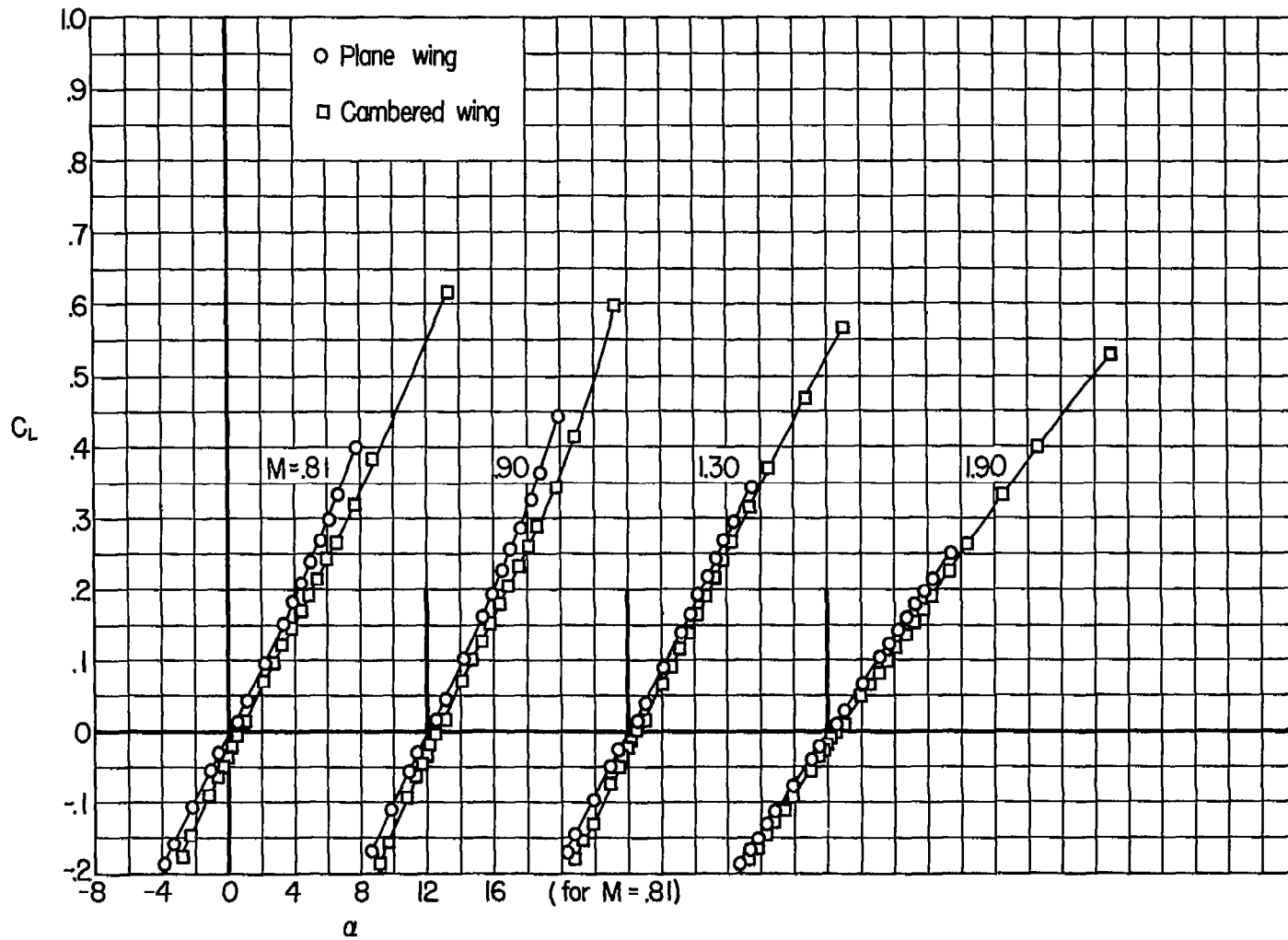
(a) C_L vs. α

Figure 15.- Effect of conical camber on the lift and pitching-moment characteristics of a 3-percent-thick triangular wing with fixed transition; $R = 5.6 \times 10^6$.

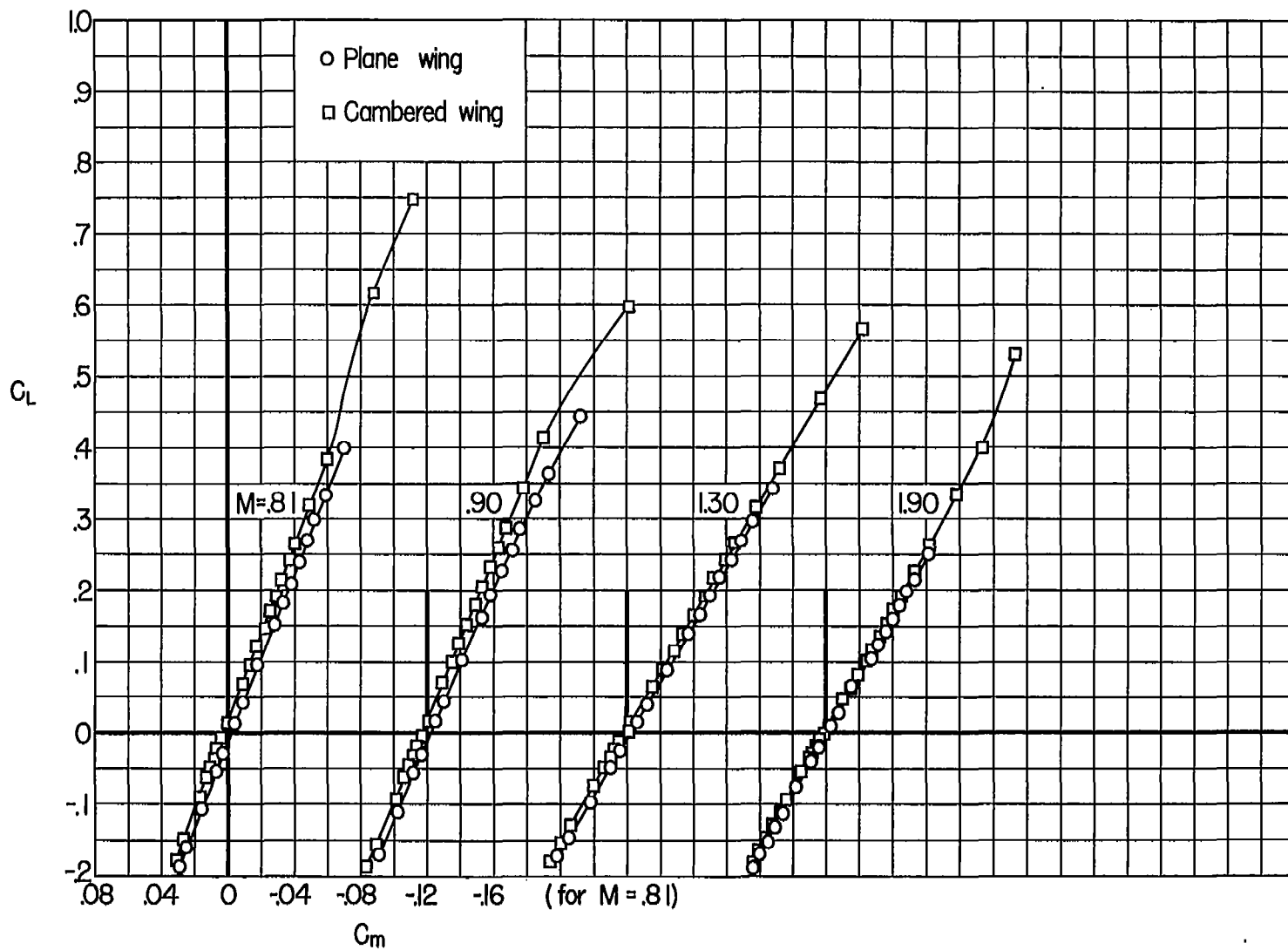
(b) C_L vs. C_m

Figure 15.- Concluded.

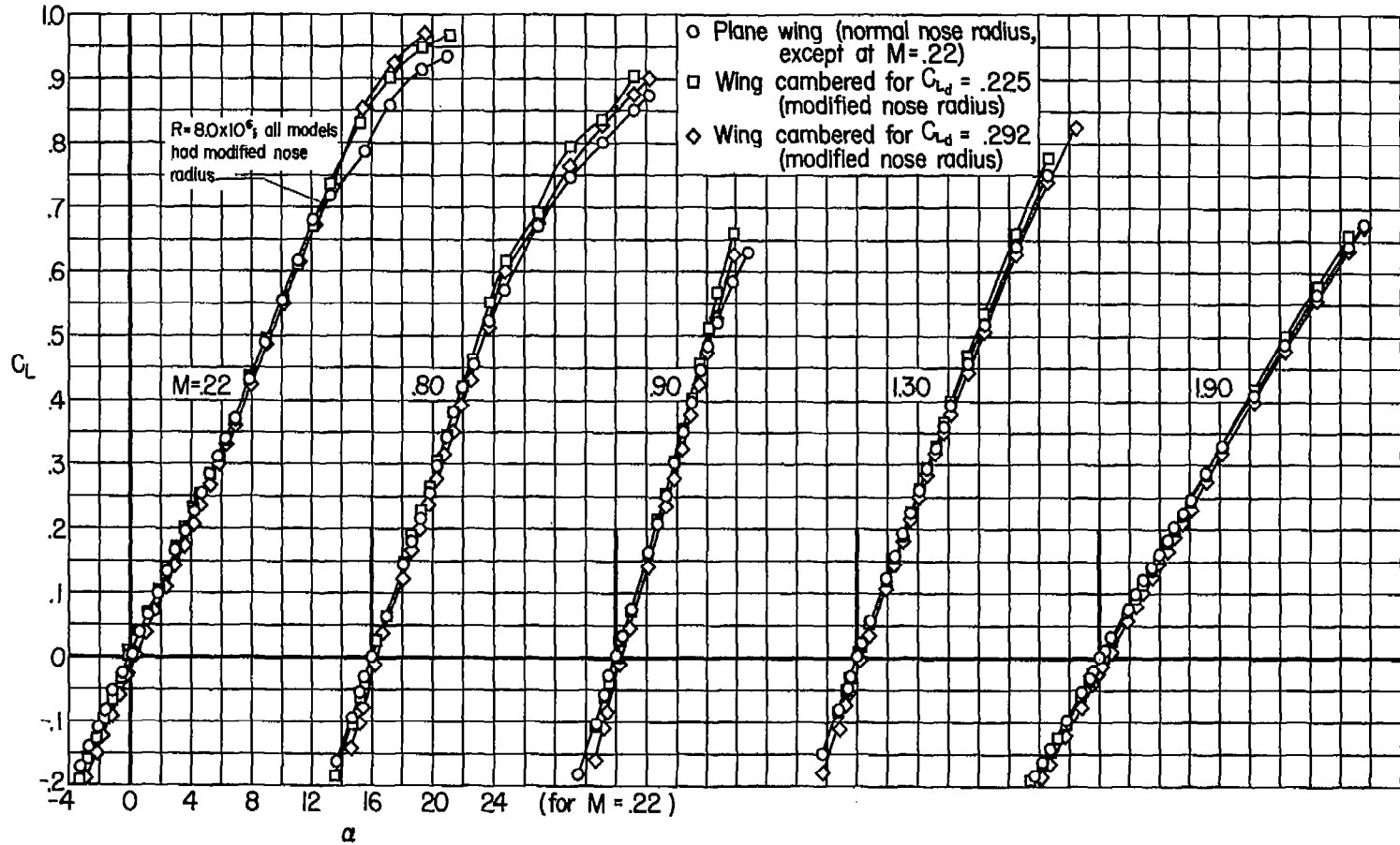
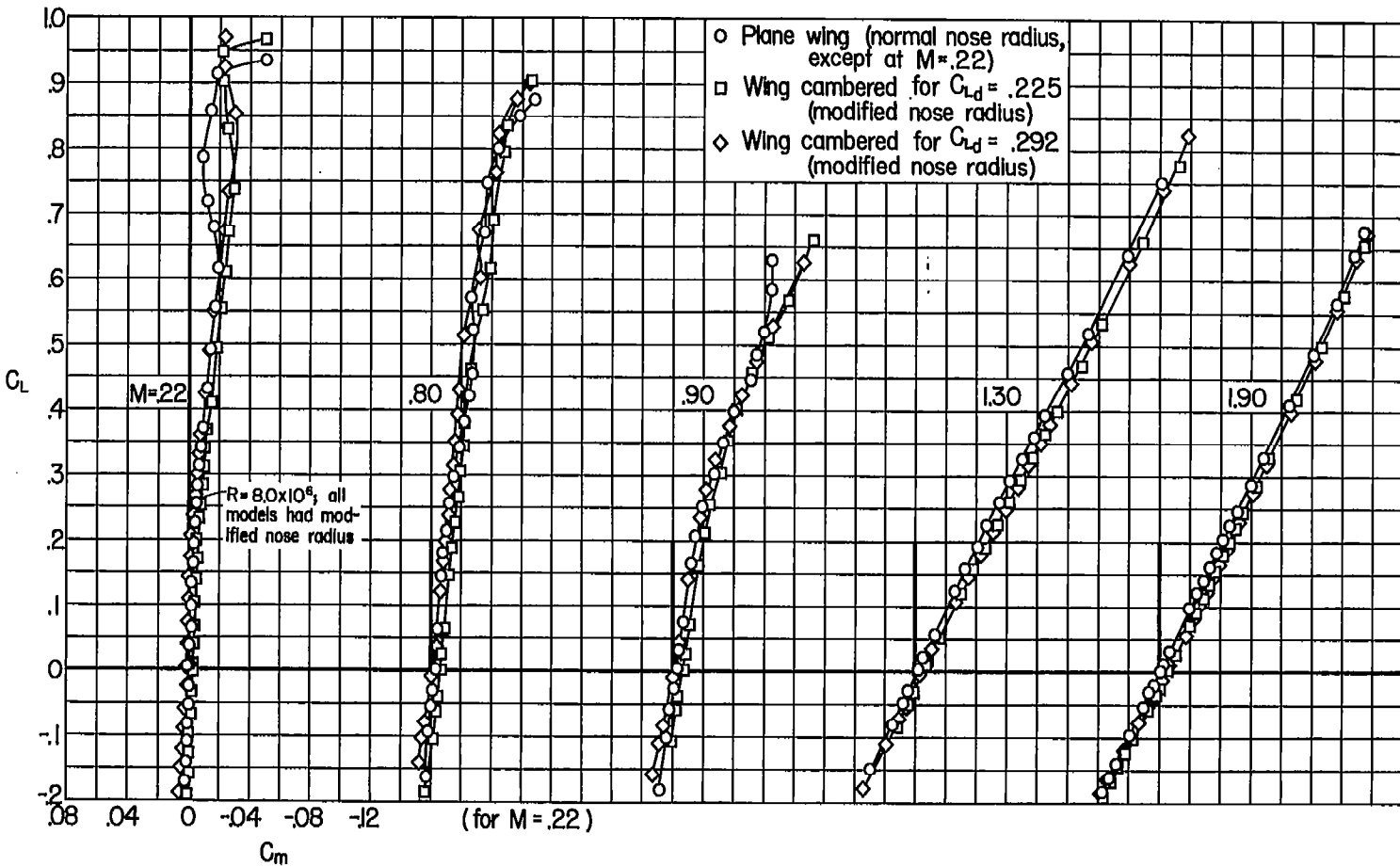
(a) C_L vs. α

Figure 16.- Effect of conical camber on the lift and pitching-moment characteristics for a 5-percent-thick sweptback wing with fixed transition; $R = 2.9 \times 10^6$ except as noted.



(b) C_L vs. C_m

Figure 16.- Concluded.

LANGLEY RESEARCH CENTER



3 1176 00520 7254

CONFIDENTIAL

CONFIDENTIAL